National Library of Canada
Acquisitions and Bibliographic Services Branch
395 Wellington Street
Ottawa, Ontario
K1A 0N4

Bibliothèque nationale du Canada
Direction des acquisitions et des services bibliographiques
395, rue Wellington
Ottawa (Ontario)
K1A 0N4

Your file Votre référence

Our file Notre référence

NOTICE

The quality of this microform is heavily dependent upon the quality of the original thesis submitted for microfilming. Every effort has been made to ensure the highest quality of reproduction possible.

If pages are missing, contact the university which granted the degree.

Some pages may have indistinct print especially if the original pages were typed with a poor typewriter ribbon or if the university sent us an inferior photocopy.

Reproduction in full or in part of this microform is governed by the Canadian Copyright Act, R.S.C. 1970, c. C-30, and subsequent amendments.

AVIS

La qualité de cette microforme dépend grandement de la qualité de la thèse soumise au microfilmage. Nous avons tout fait pour assurer une qualité supérieure de reproduction.

S'il manque des pages, veuillez communiquer avec l'université qui a conféré le grade.

La qualité d'impression de certaines pages peut laisser à désirer, surtout si les pages originales ont été dactylographiées à l'aide d'un ruban usé ou si l'université nous a fait parvenir une photocopie de qualité inférieure.

La reproduction, même partielle, de cette microforme est soumise à la Loi canadienne sur le droit d'auteur, SRC 1970, c. C-30, et ses amendements subséquents.

Canada

SYNTHESIS OF BRANCHED NUCLEOSIDES AND OLIGONUCLEOTIDES CONTAINING FLEXIBLE ALKYLAMINE LINKERS ON THE HETEROCYCLIC BASES

by

Miguel Angel Roman

A thesis submitted to the Faculty of Graduate Studies
and Research in partial fulfilment of the requirements of
the Degree of Master of Science

Department of Chemistry
McGill University
March 1995

ISBN 0-612-05621-X

To my parents and brother,

Miguel and Emilia Roman and Daniel Roman

ABSTRACT

The N3 position of thymidine was alkylated with different sized bromoalkyl phthalimide linkers in generally good yields, with no alkylation observed on the sugar ring. The free amino group, available after methylamine deprotection of the phthalimide linker, was protected with the levulinyl protecting group (e.g., **20**). Branched 'Y'-shaped nucleic acids containing branching monomer **20** were synthesized using standard solid phase synthetic methodology and complexes of these branched nucleic acids with one and two mole-equivalents of linear complement dA_{10} are investigated by thermal melting. At the branching point the levulinic amide exhibited poor lability to Letsinger's hydrazine solution and proved to be incompatible with the solid phase synthesis of branched nucleic acids. The primary amino group provided a handle which was used to extend the size of the linker incorporating a primary hydroxyl group at the site of levulinic protection (e.g, **37**, **38**). The levulinic ester showed much better lability to hydrazinolysis rendering it more compatible with the solid phase synthesis of branched nucleic acids. An extensive one and two dimensional NMR characterization of the functionalized nucleosides is reported.

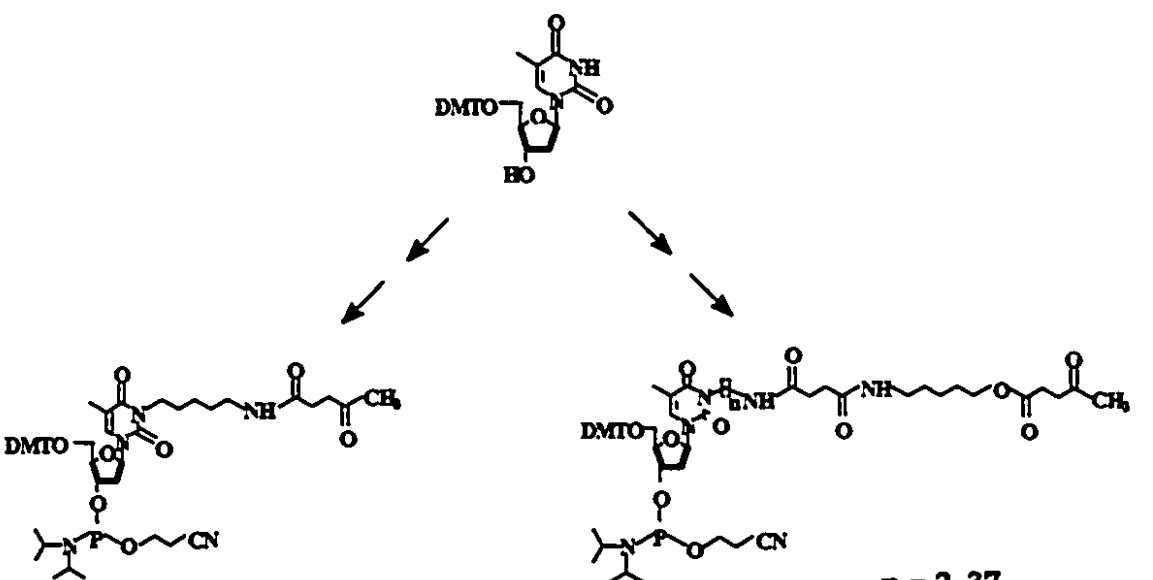

20

n = 2, 37
n = 5, 38

RÉSUMÉ

La position N3 de la thymidine a été alkylée régiospécifiquement et généralement avec de bons rendements par des dérivés bromoalkyles de la phthalimide. L' amine primaire disponible après la déprotection du groupement phthalimide avec la méthylamine a ensuite été protégée avec le groupement lévulinyle (ex, **20**). Des oligomères d'acides nucléiques avec une structure branchée en "Y" incorporant le monomère **20** ont été synthétisés en utilisant la synthèse automatisée en phase solide. Les complexes formées entre les acides nucléiques branchés et un ou deux équivalents de l'oligomère linéaire complémentaire dA_{10} ont été étudiés par dénaturation thermique. Au point de branchement, l'amide lévulinique a démontré une résistance à la solution d'hydrazine de Letsinger ce qui empêche son utilisation pour la synthèse en phase solide des acides nucléiques branchés. L' amine primaire a donc été modifiée par l'ajout d'une chaîne alkyle permettant d'augmenter la longueur du lien et contenant un groupement hydroxyle primaire qui permet l'utilisation de l'anhydride lévulinique comme groupement protecteur (ex, **37**, **38**). L'ester lévulinique comparativement à l'amide a demontré une plus grande aptitude à l'hydrazinolyse ce qui en fait un candidat de choix pour la synthèse en phase solide des acides nucléiques branchés. Une caractérisation complète par la RMN à une et deux dimensions des dérivés nucléosidiques est reportée.

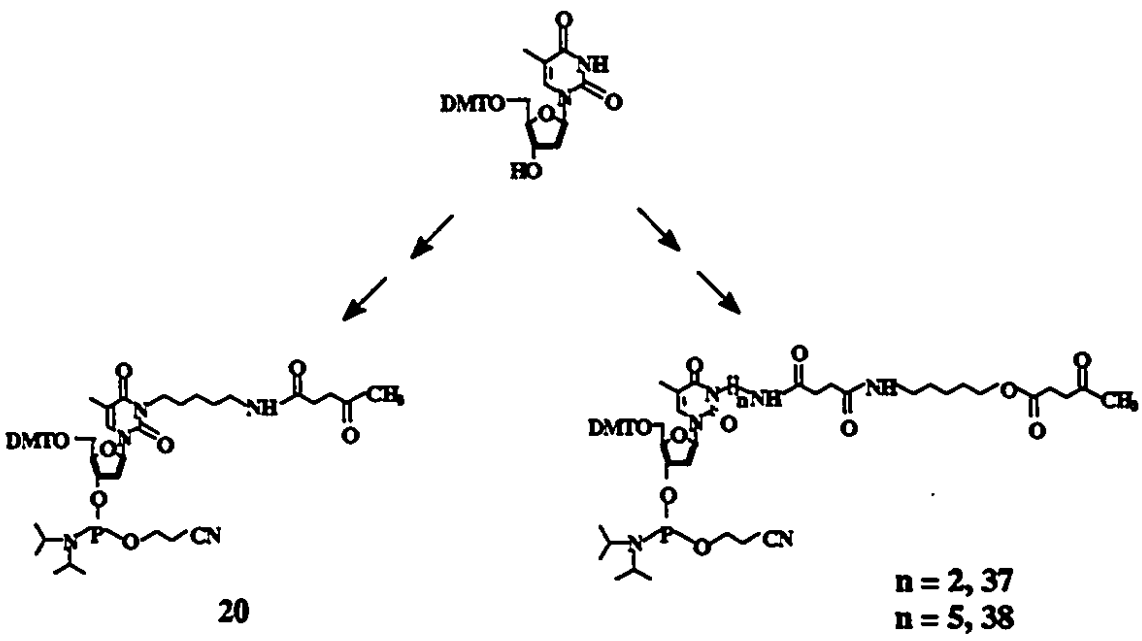

20

ACKNOWLEDGEMENTS

I would like to sincerely thank Dr. Masad Damha for his support, patience and faith in my abilities. His understanding and encouragement was greatly appreciated.

I would also like to express my gratitude to:

My colleagues in lab 207, especially Maggie Scartozzi, Anne Noronha and Sebastien Robidoux for their friendship and helpful discussions

Dr. Sauriol for her help in recording various spectra

Dr. Hamed and Dr. Mamer for recording the mass spectra

Tanya Tadey for providing CE characterizations

and

Sebastien Robidoux for translating the abstract

Finally, I would like to deeply thank my parents and brother for their encouragement and never ending support.

GLOSSARY OF SYMBOLS & ABBREVIATIONS

A	adenosine
Ac	Acetyl group
A_{260}	unity absorbance at 260 nm with a pathlength of one centimeter and volume of one milliliter
a	apparent (in NMR)
as	antisense
b	broad (in NMR)
BIS	N,N'-methylene-bis-acrylamide
BPP	Bromophenol Blue
CPG	control-pore-glass
CE	capillary electrophoresis
δ	chemical shift
d	doublet (in NMR)
dd	doublet of doublets (in NMR)
DCC	dicyclohexylcarbodiimide
DCU	dicyclohexylurea
DIEA	diisopropylethylamine
DMAP	4-dimethylaminopyridine
DMF	N,N-dimethylaminopyridine
DMT-Cl	4,4'-dimethoxytrityl chloride
DNA	deoxyribonucleic acid
ds	double stranded
eq	equivalent
FAB-MS	fast atom bombardment mass spectrometry
gr	gram

hr	hour
HIV	human immunodeficiency virus
J	coupling constant
$\lambda_{max(min)}$	wavelength at the maximum (minimum) of an absorption peak
L	liter
LCAA	long-chain alkylamine
Lv	levulinyl
LvOH	levulinic acid
Lv_2O	levulinic anhydride
m	multiplet
M	molar
m/z	mass-to-charge ratio
min	minute
mg	milligram
mL	milliliter
mmol	millimolar
mRNA	messenger ribonucleic acid
MS	mass spectrometry
NMR	nuclear magnetic resonance
O.D.	optical density unit
PAGE	polyacrylamide gel electrophoresis
py	pyridine
Py	pyrimidine
Pu	purine
ppm	parts per million
q	quartet (in NMR)

q^5	quintet (in NMR)
RNA	ribonucleic acid
rRNA	ribosomal RNA
R_f	relative mobility (TLC)
RNase	ribonuclease
RT	room temperature
RSV	Rous Sarcoma Virus
s	singlet (in NMR)
ss	single stranded
T	thymidine
TBAF	*tert*-butyl ammonium fluoride
TCA	trichloracetic acid
TEA	triethylamine
TBDMS-Cl	tert-butyldimethylsilyl chloride
TIPS-Cl	triisopropylsilyl chloride
THF	tetrahydrofuran
TEMED	N,N,N',N'-tetramethylenediamine
TMS-Cl	trimethylsilyl chloride
TLC	thin layer chromatography
tRNA	transfer RNA
TRIS	N-tris(hydroxymethyl)aminomethane
T_m	melting temperature
U	uridine
UV	ultraviolet
v	volume
VIS	visible
w	weight

TABLE OF CONTENTS

Chapter 1. Introduction and Literature Review

1.1 Oligonucleotide Drug Therapy

Researchers have always dreamt of discovering a drug that can, by some kind of magic, travel through the body and elicit a pharmaceutical effect, without producing any side effects. Such a "magic bullet" concept has been difficult to apply in the design of drugs that act by directly inhibiting disease related proteins, receptors or ion channels. The inherent problem stems from the difficulty in accurately determining the structural configuration of the receptor at the site of action of the proteins contributing to disease, since these receptors are responsible for the specificity with regard to the drugs with which they combine. In addition, obtaining the target protein using genetics and biochemistry and then rationally designing an inhibitory drug that can bind to it specifically and uniquely to produce a therapeutic effect is a long and demanding process.

In the space of a little over ten years two innovative therapies, the antisense[1-9] and antigene[10-16] strategies, have created great excitement and optimism in the search and design of effective antiviral and antitumor drugs. The approach is simple and elegant in nature. Synthetic oligonucleotides can be designed and aimed at the inhibition of gene expression based upon the targeting of specific nucleic acid base sequences. *Antisense synthetic oligonucleotides (ASO)* bind via Watson-Crick base pairing to complementary regions on the mRNA, resulting in the inhibition of protein biosynthesis. *Antigene or triple helix forming oligonucleotides (AGO)* bind to the major groove of double stranded DNA via Hoogsteen base pairing resulting in the inhibition of transcription. These two classes of potential nucleic acid therapies are applicable to many DNA characterized diseases and potential targets include viruses and oncogenes.

1.2 Antisense Strategy

The first example of specific inhibition of viral gene expression by synthetic oligodeoxynucleotides was proposed by Zamecnik and Stephenson in 1978.[17] They demonstrated the direct inhibition of Rous Sarcoma Virus (RSV) replication by using a 13-mer synthetic oligodeoxynucleotide complementary to the RNA of the virus. The reduced replication of the virus indicated that it had successfully blocked the biosynthesis of proteins needed for making new viral particles. The regulation of gene expression resulted from hydrogen-bonding between the *sense sequence*- the one bearing the genetic information, or in this case the viral sequence- and the complementary or *antisense sequence*. What makes this strategy extremely attractive is the high specificity resulting from hydrogen bonding between the base sequences of the sense and antisense strands. Therefore, the design of a synthetic antisense oligonucleotide as a potential chemotherapeutic agent can be considered for any gene whose sequence is known.

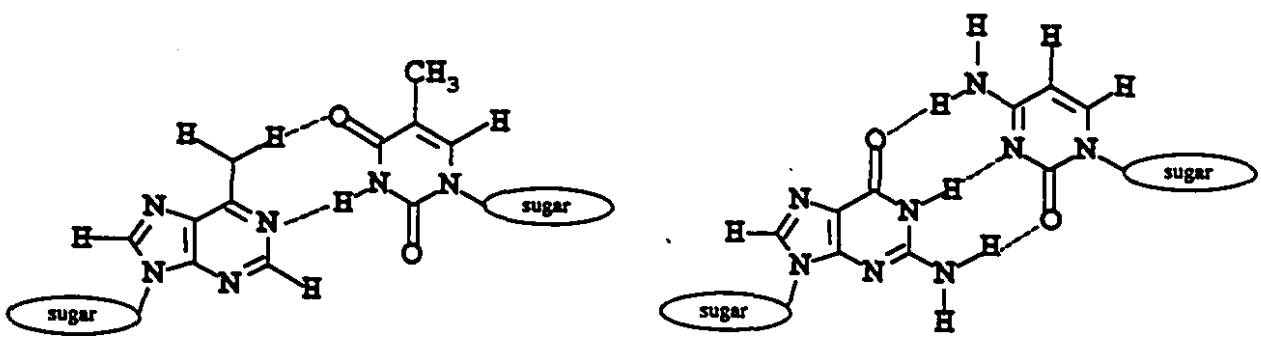

A-T G-C

Figure 1.1 Watson-Crick Hydrogen Bonding of Complementary Bases Between Adjacent Nucleic Acid Strands. G and C form three hydrogen bonds, while A and T(U) form two.

In principle, gene expression can be affected at different steps by targeting a specific nucleic acid sequence (figure 1.2). Targeting mRNA upstream of the AUG initiation codon with "passive" oligonucleotides (which do not modify the target mRNA) prevents, through a steric blocking or physical arrest mechanism, ribosomes from binding or scanning the message.[19-21] Alternatively, targeting of the coding region of mRNA followed by RNaseH degradation will prevent polypeptide chain elongation. RNaseH recognizes RNA-DNA hybrids and cleaves the RNA strand (figure 1.3a). Therefore, the contribution of these two mechanisms is primarily dependant on the location of the target along the mRNA. Inhibition will not occur when targeting the coding region of mRNA unless the resulting RNA-DNA complex is cleavable by RNaseH. For instance, derivatives such as α-antisense oligonucleotides do not elicit RNaseH cleavage when targeted downstream of the AUG initiation codon. Consequently, they must be targeted to a region from the 5' cap site to a few nucleotides upstream of the AUG initiation codon in order to elicit a physical arrest mechanism.

Nuclear nucleic acid sequences, such as pre-mRNA and even DNA can be targeted by antisense oligonucleotides. By doing so, nuclear events such as transcription (see next section), splicing, or the translocation of mature transcripts to the cytoplasm are prevented from occurring. Antisense oligonucleotides can also be linked to active groups such as metal complexes or photosensitizers (figure 1.3b). Such "reactive" oligonucleotides irreversibly damage the target mRNA by either cleavage or crosslinkage, respectively. As a consequence, the location of the target sequence is less important for "reactive" oligonucleotides than for passive ones since irreversibly damaged mRNA can no longer support protein synthesis.

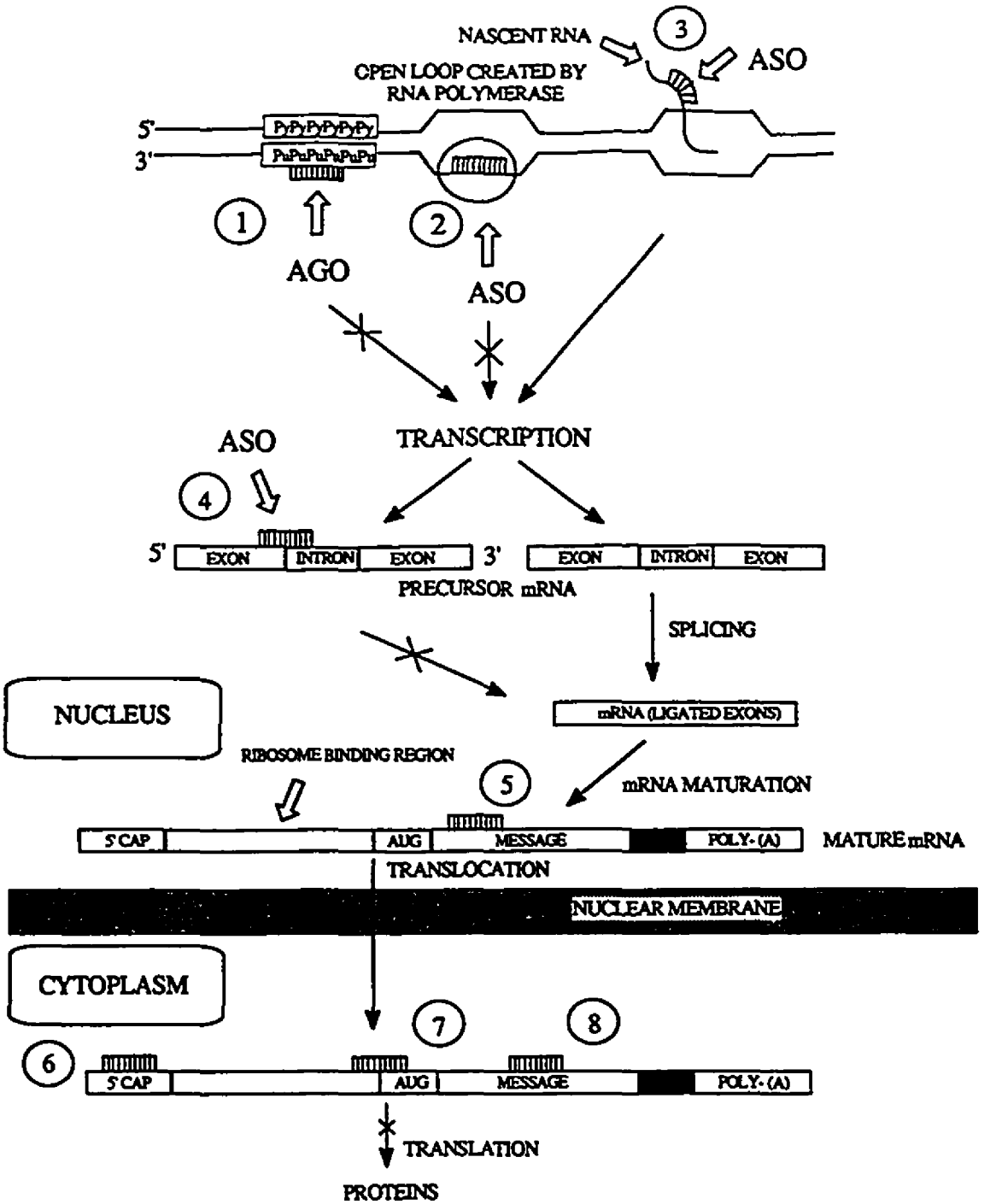

Figure 1.2 Summary of Possible Target Sites for Sequence Specific ASO's and AGO's. Inhibition of gene expression could occur : (i) at the level of transcription by triple helix formation (1), (ii) by hybridization of antisense nucleic acids to the open loop created by RNA polymerase (2) or nascent RNA (3) , (iii) by interfering with splicing at intron-exon junctions (4), (iv) by interfering with mRNA transport from nucleus to cytoplasm (5), (v) at the translational level by inhibiting the binding of initiation factors (6), the assembly of ribosomal subunits (7) or ribosomal sliding along the coding sequence (8). (figure adapted from reference 18).

a) RNase Function

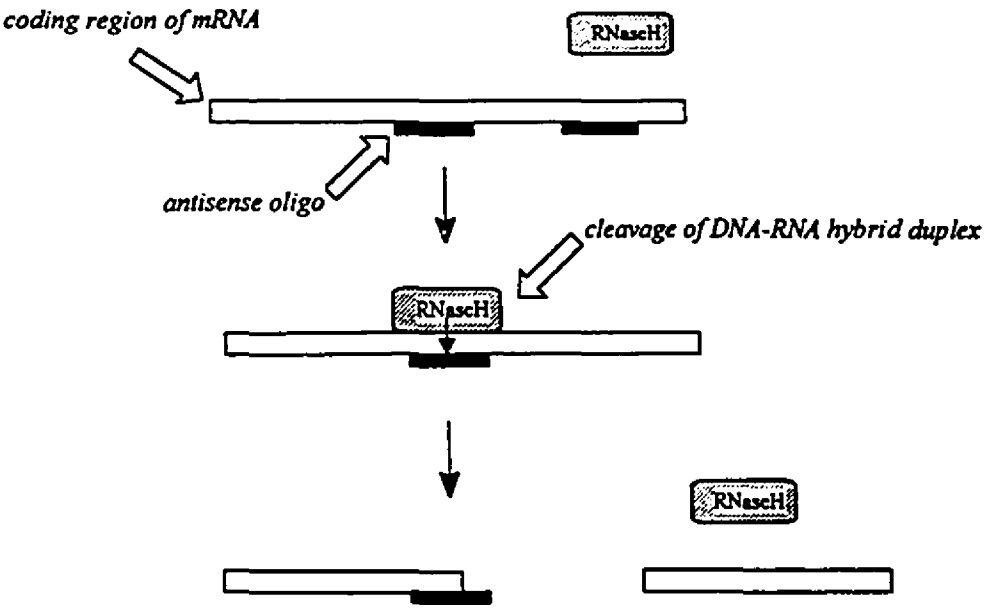

b) "Reactive" Antisense Oligonucleotides

(I) antisense oligomer linked to crosslinking agent

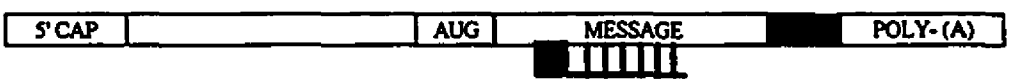

(II) antisense oligomer linked to cleaving agent

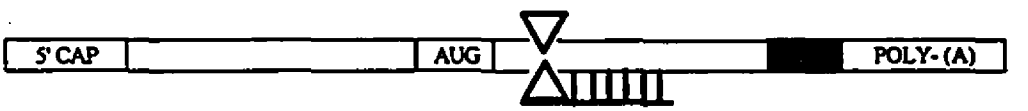

Figure 1.3 a) function of RNaseH, b) translation inhibition by reactive ASO's

1.3 Stability and Cellular Uptake of Synthetic Oligonucleotides

Although antisense oligonucleotides have generated a lot of excitement, several problems have created initial barriers to the therapeutic uses of these molecules. For instance, oligonucleotides with a natural phosphodiester back-bone are rapidly degraded by nucleases present within cells and in the serum. Antisense oligonucleotides must also reach the interior of the cell by passing through the membrane of a living cell. In order to increase the cellular uptake and nuclease resistance of antisense oligonucleotides a whole range of synthetic strategies has been developed (figure 1.4). Ideally, chemical modifications should result in structural analogs with hybridization properties similar to the parent molecule under physiological conditions.

Improving both cellular uptake and nuclease resistance was intensively investigated by Paul S. Miller and associates at John Hopkins University.[22,23] In particular, they replaced the non-bonding oxygen in each phosphate group with a methyl group. The resulting methylphosphonate oligomers showed greater extra- and intracellular resistance to nuclease degradation. Furthermore, the non-ionic nature of the internucleotide phosphate bridge improved lipid solubility and considerably enhanced cellular uptake. However, the methylphosphonate oligodeoxynucleotide analogs did not retain the hybridization characteristics of the parent phosphodiester oligodeoxynucleotides. A study by Heikkila *et al.*[24] demonstrated increasing destabilization in the hybrids formed between a chemically synthesized RNA 27-mer and an antisense oligodeoxynucleotide 15-mer with increasing substitution of terminal phosphodiester linkages of the antisense strand with methylphosphonates. In addition, methylphosphonate antisense oligomers do not elicit RNaseH cleavage of the target sense mRNA and therefore do not inhibit protein synthesis if targeted downstream of the initiation codon AUG.

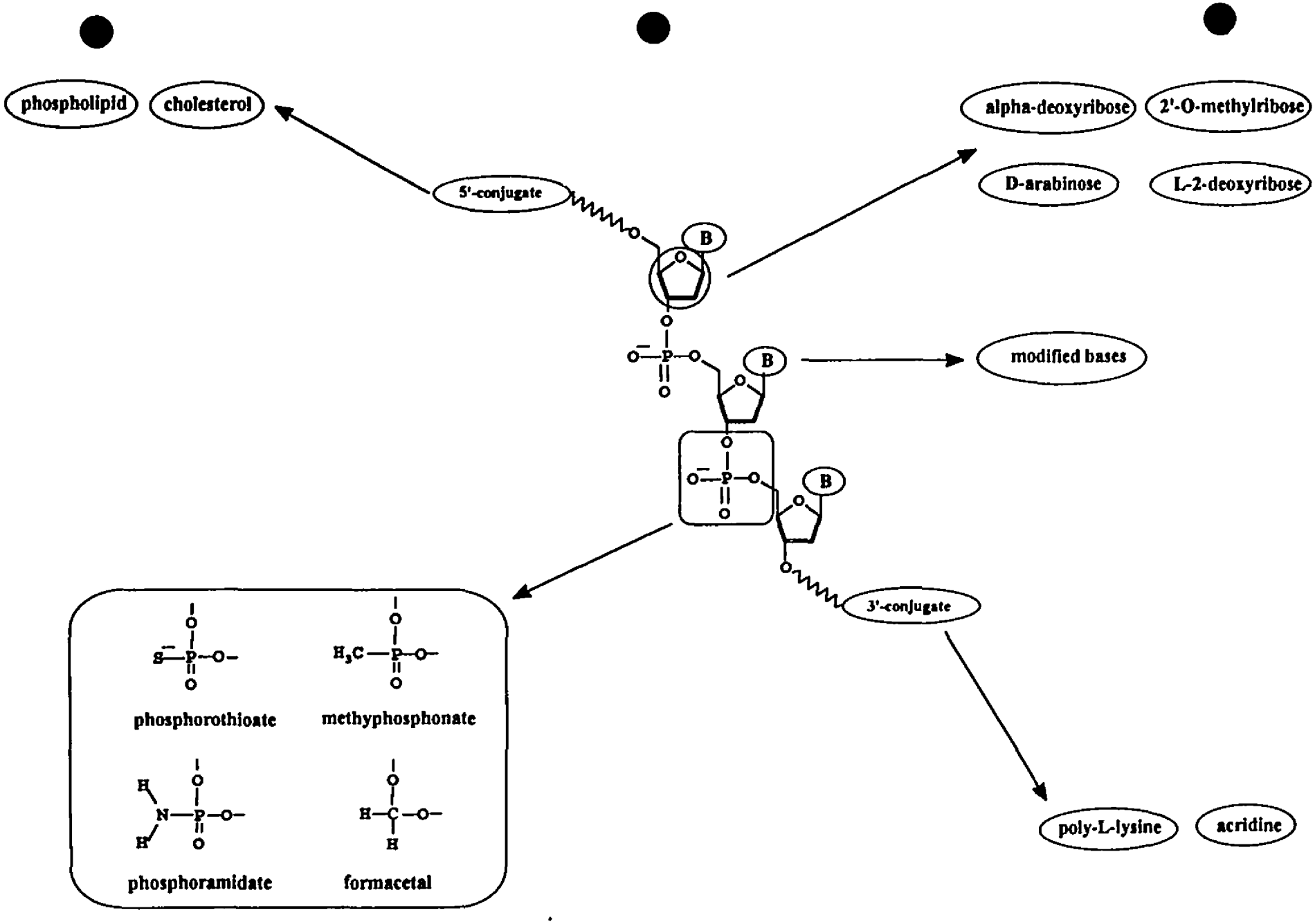

Figure 1.4 Possible Chemical Modifications of Natural Oligonucleotides

Matsukura *et al.*[25] introduced phosphorothioate oligomers (*S-Oligos*) in which the nonbridging phosphate oxygen atom is replaced by a sulfur atom. These modified oligomers showed increased resistance to nuclease degradation[26] and, unlike methylphosphonate oligomers, exhibit enhanced binding ability and elicit RNaseH activity.[27] Regretably, *S-Oligos* do not penetrate cells efficiently, requiring their use at relatively high concentrations. Despite this drawback, *S-Oligos* are quite popular and most antisense drugs today employ such a modification. Several other backbone modifications have been investigated and reviewed.[28]

Improvements to the cellular uptake of oligonucleotides may also be effected by covalent attachment of lipophilic groups (figure 1.4). Leonetti *et al.*[29] have demostrated enhanced cell delivery of oligodeoxynucleotides by 3'-conjugation to poly-L-lysine. Alternatively, Letsinger *et al.*[30] and Toulmé & Hélène[31] improved cellular uptake by linkage to cholesterol and acridine residues, respectively. Hèléne *et al.*[32] also demonstrated that covalently attaching an acridine residue to the 3' end of $(Tp)T_{11}$ increased the dissociation temperature from 33.5 °C to 47.5 °C. Therefore, covalently linking lipophilic molecules to an oligonucleotide effectively improves both its transport and hybridization properties.

Another way to increase duplex stability involves replacement of the natural bases with modified heterocyclic residues. Chollet *et al.*[33] investigated the effect of incorporating diaminopurine (DAPu) on duplex stability. The ability of thymine to form three hydrogen bonds with DAPu compared to only two with its natural partner, adenine, increased duplex stability significantly. The incorporation of other modified bases, such as isosteric purine 2'-deoxyribofuranosides[34,35,36] and the pyridopyrimidine bases[37] have also been studied and reviewed.[38]

Modification of an oligonucleotide may also be effected on the pentafuranosyl moiety. An interesting sugar modification involves incorporating α-anomeric nucleoside units[39,40] into antisense oligonucleotides. α-anomeric oligonucleotides can hybridize with

its complementary β-oligonucleotide forming an α-β duplex with parallel polarities.[41] α-anomeric antisense oligonucleotides exhibit nuclease resistance, yet do not elicit RNaseH activity after hybridization on a complementary sense RNA strand.[42,43] Antisense oligonucleotides incorporating 2'-O-methyl nucleoside units show a much greater binding affinity with complementary RNA than the corresponding natural DNA.[44-46] Other types of pentafuranose modifications, such as oligodeoxynucleotides containing both L- and D-deoxynucleotide residues[47], replacement of the sugar unit with glycerol[48,49] or replacement of both the sugar and phosphodiester moieties with a peptide backbone (peptide nucleic acid or PNA)[50,51] and morpholino-type backbone[52] have been investigated.

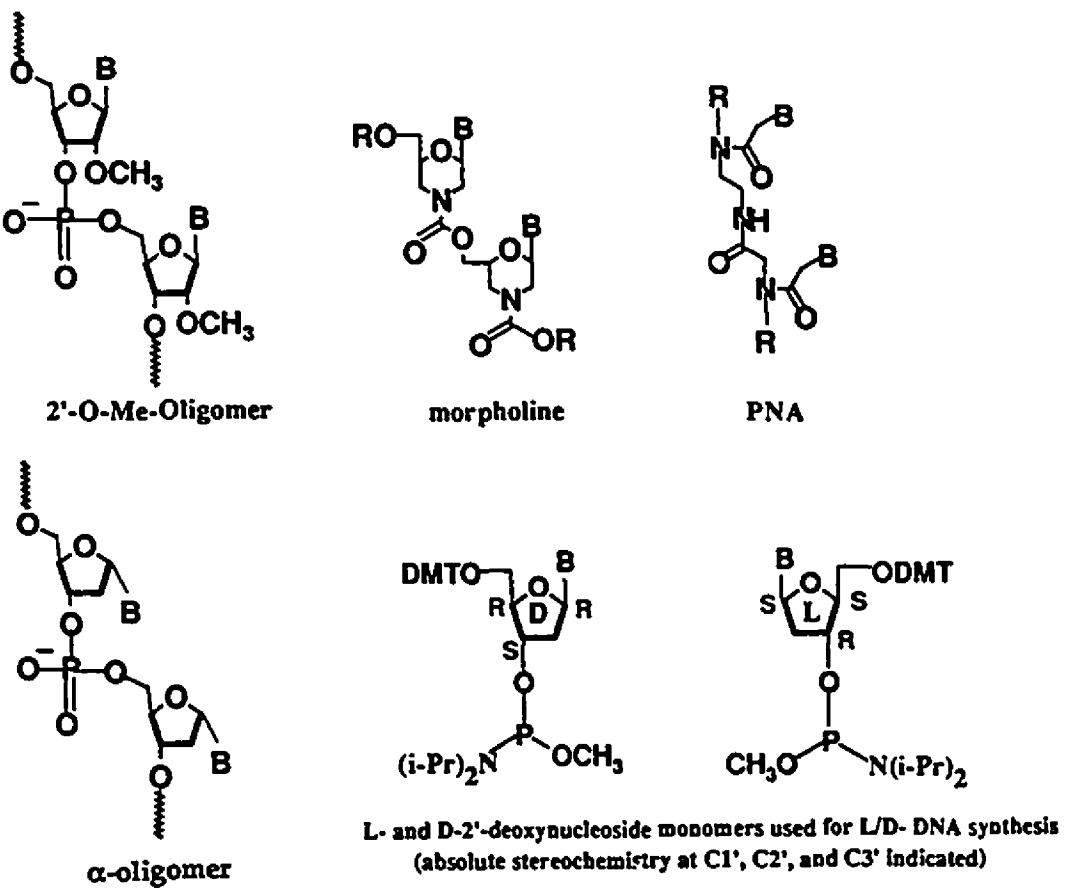

Figure 1.5 Backbone and Sugar Modified Oligonucleotides

1.4 Antigene Strategy

Recently, control of gene expression by triple helix forming oligonucleotides has been investigated, making the precursor DNA molecule itself the target. Such *antigene oligomucleotides* bind in a sequence specific manner to the major groove of double helical DNA to form a local triple helix or triplex structure directly interfering with gene expression at the transcriptional level. Triple helix formation can sterically inhibit protein-DNA interactions if the triplex structure overlaps the recognition sites of sequence-specific DNA binding-proteins that activate transcription.

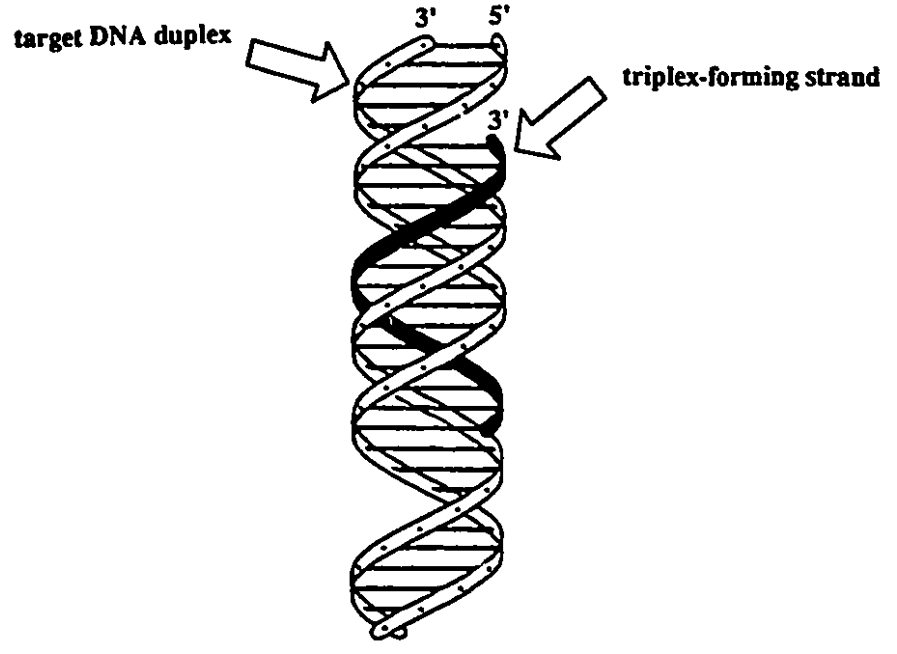

Figure 1.6 Schematic Representation of Triple Helix Formation. Triplex forming strand binds to major groove of double stranded DNA (adapted from reference 52)

1.5 Triple Helix Formation

Triple helical polynucleotides were first described over three decades ago.[53] Poly(U) and poly(A) were shown to form a stable 2:1 complex in the presence of magnesium ions. After this discovery a variety of other triple-stranded structures were observed.[54,55,56] Triplex forming strands make use of molecular recognition sites present in the major groove of a Watson-Crick DNA duplex. In particular, pyrimidine-rich or purine-rich oligonucleotides bind in a sequence specific manner to the major groove of double-stranded DNA through the formation of specific hydrogen bonds to homopurine sequences engaged in Watson-Crick hydrogen bonding to pyrimidines. On this basis, several recognition schemes have been suggested resulting in different triple helical motifs (Figure 1.7). In the "pyrimidine motif", specificity is derived from the formation of T•A-T and C^+•G-C isomorphous base triplets.[57,58,59] In this case a homopyrimidine oligonucleotide binds, through the formation of Hoogsteen hydrogen bonds[60], to the major groove of a complementary homopurine•homopyrimidine stretch. The triple helix forming homopyrimidine strand has a parallel orientation relative to the homopurine strand. For a parallel orientation of the third strand, the glycosidic bond of nucleosides in all three strands is required to be in the *anti* conformation. In contrast, in the "purine motif", derived from A•A-(T)U or G•G-C base triplets[61,62], a homopurine triplex forming strand binds, through the formation of Hoogsteen hydrogen bonds, in an antiparallel orientation with respect to the homopurine strand.[63] For this *anti* parallel orientation of the third strand, the glycosidic bond of all nucleosides is required to be in the *anti* conformation. Triple helix complexes containing cytosine on the third strand ("pyrimidine motif") are pH dependant since the N3 of cytosine must be protonated in order to form a base triplet with a G-C base pair (figure 1.7).

With the possibily of forming A•A-T(U) and G•G-C base triplets, the triple helical recognition code has been formally extended. However, the nonisomorphous nature of

these base triplets results in distortion of the phosphodiester backbone, introducing a energy penalty that often prevents triple helix formation. Nonetheless, it has been demonstrated that under certain conditions these base triplets can be accommodated within a double helix, resulting in a relatively stable triple helix.[64]

It has long been recognized that only homopurine•homopyrimidine sequences can be targeted for triple helix formation. Current research is directed towards the design of oligonucleotides that can recognize mixed pyrimidine/purine sequences on the target strand, since interruption of a homopurine sequence by a homopyrimidine sequences destabilizes triple helix formantion.

Recently, Horvan and Dervan[65] introduced the concept of "switchback" or alternate strand triple helix formation, which simply consists of two short hompyrimidine oligonucleotides joined at their 3' ends by 3'-3' linker (Figure 1.8). Such linked oligonucleotides are thus capable of similtaneously binding, in a parallel orientation, to both homopurine tracts on alternate strands of the target DNA duplex. Other studies have been conducted using the same "switchback" principle.[66,67,68]

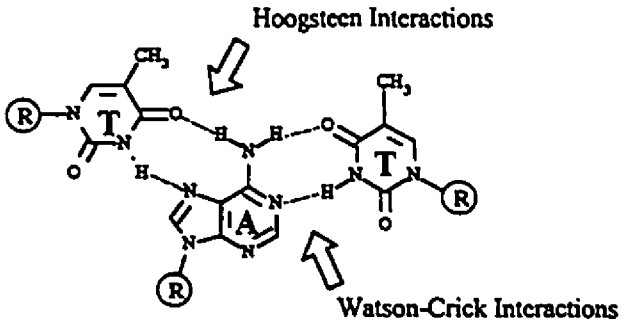

T•AT

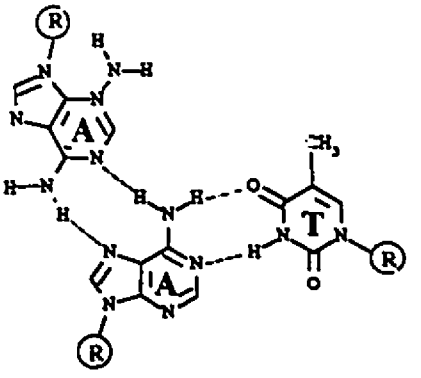

A•AT

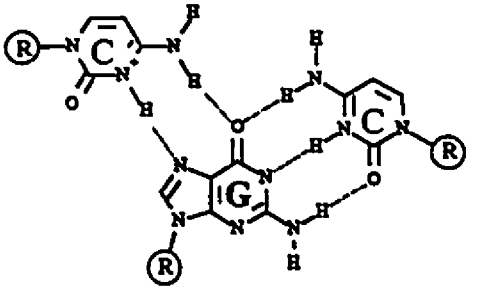

C^+•GC

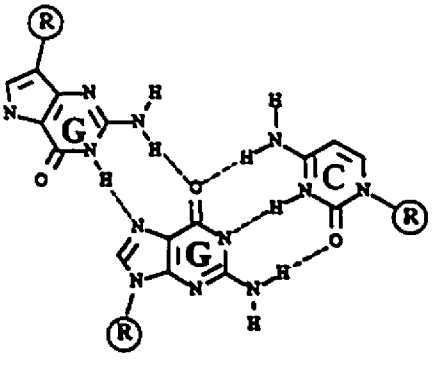

G•GC

PYRIMIDINE MOTIF

Pyr:Pur:Pyr

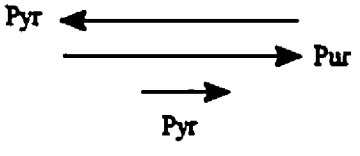

PURINE MOTIF

Pyr:Pur:Pur

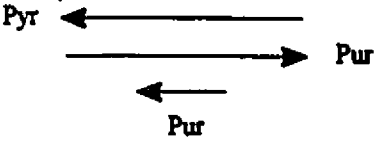

Figure 1.7 Triple Helix Base Recognition Motifs

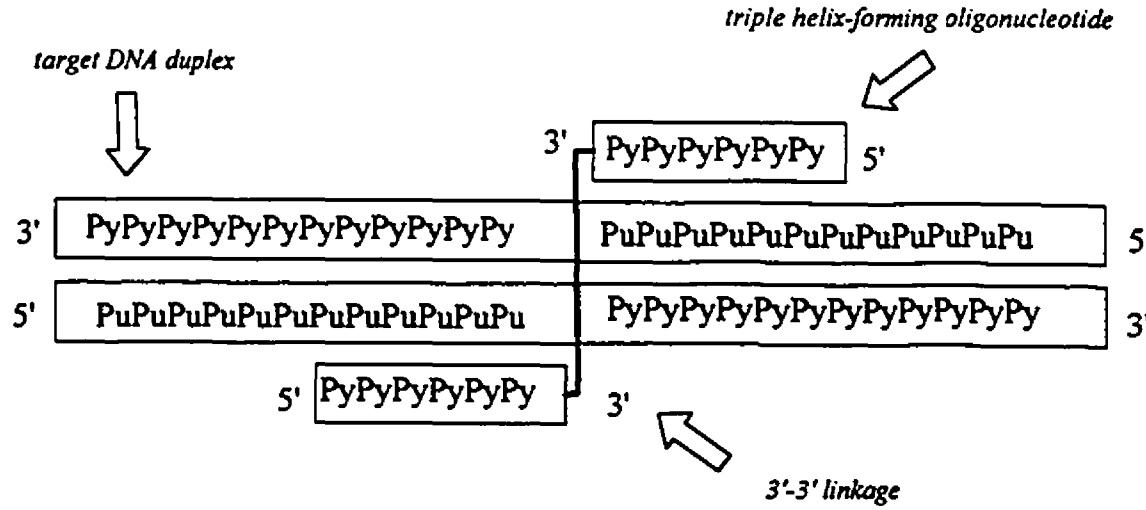

Figure 1.8 Alternate Strand or "Switchback" Triple Helix Formation

1.6 Antisense-Directed Antigene Strategy

In principle, synthetic oligonucleotides can be designed to form a triple helix on a single-stranded DNA or RNA sequence. Such an approach can be seen as an extension of the antisense approach with duplex formation followed by triple helix formation. This novel approach is referred to as *antisense-directed triple helix inhibition* and has been investigated with oligonucleotides linked through a flexible linker [69-72], branched nucleic acids[73] and circular DNA.[74-76] In particular, branched "Y" and "V"-shaped poly(dT) nucleic acids **I** and **II** with an adenosine unit at the branching point (figure 1.9) have been synthesized by Damha *et al.*[77] The hybridization properties of these branched nucleic acids with one and two-mole equivalents of a complementary linear deoxyadenosine decamer were studied by UV thermal-melting and circular dichroism spectroscopy and exhibited results consistent with triple helix formation.

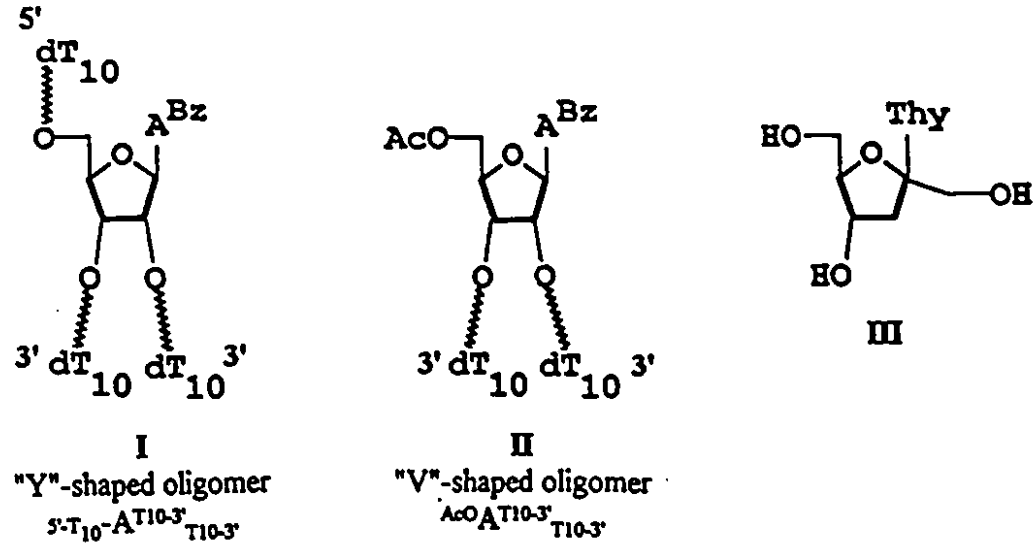

Figure 1.9 Branched(poly-dT) nucleic acids synthesized by Damha *et al.*[77]

In principle, a branched "Y"-shaped nucleic acid molecule can be designed with a mixed pyrimidine/purine base sequence and two polypyrimidine strands that can recognize and bind to a ssRNA molecule (figure 1.10). The mixed pyrimidine/purine "guide" sequence and the homopyrimidine, Py(B), sequence behave similarly to an antisense oligonucleotide by capturing the complementary target sequence on *ss*RNA through Watson-Crick base pairing. The second homopyrmidine (branch) sequence, Py(A), then mimics an antigene oligonucleotide and binds specifically, through Hoogsteen hydrogen bonds (or reverse-Hoogsteen hydrogen bonds), to the homopurine strand of the double helix to form a local triple helix. The result of such antisense-directed triple helix formation is the double recognition of *ss*RNA, once by the guide molecule and another by the homopyrimidine (branch) strand, thereby, maximizing the binding affinity to the target molecule and lowering the dosage needed to achieve inhibitory effects.

Flexible linker molecules can also be incorporated in the 2'- position of the sugar moiety or on the nucleobase in order to control the folding and binding properties of the third (branch) strand. Recently, Azhayev *et al.*[78] in Finland demonstrated the applicability of 3'-deoxy-β-D-psicothymidine III (figure 1.9) in the preparation of branched nucleic acids. Several intercalating agents can also be covalently attached to the third (branch)

strand in order to enhance the stability of the triple structure or cleave the *ds*DNA (figure 1.10).

PLAN OF STUDY

The primary goal of my project is to incorporate flexible linkers of different sizes into "Y"-shaped and "V"-shaped branched nucleic acids. By doing so, we hope that the linker will provide better flexibility than a phosphodiester linkage and therefore improve the folding of the third (branch) strand. In addition, we reasoned that the flexible linker will separate the two polypyrimidine " tails " such that the branch point will not present a steric barrier that limits the "tails" ability to fully base pair with complementary nucleic acids.

The fact that we were not restricted as to the type of flexible linker unit needed afforded us the luxury of some flexibility in our synthetic endeavor. Although several linkers can provide the necessary flexibility, we decided to start our project by incorporating different sized amino alkyl linkers at the sugar moiety. We reasoned that amino alkyl linkers will provide a reactive primary amino group at the branching point allowing the efficient assembly of our branched oligomers. The decision to use an amino alkyl linker was based on the consideration that the amino group can be protected with the phthalimido or levulinyl protecting groups. The use and compatibility of the phthalimido and levulinyl groups as potential protecting groups for the branching monomers will be investigated.

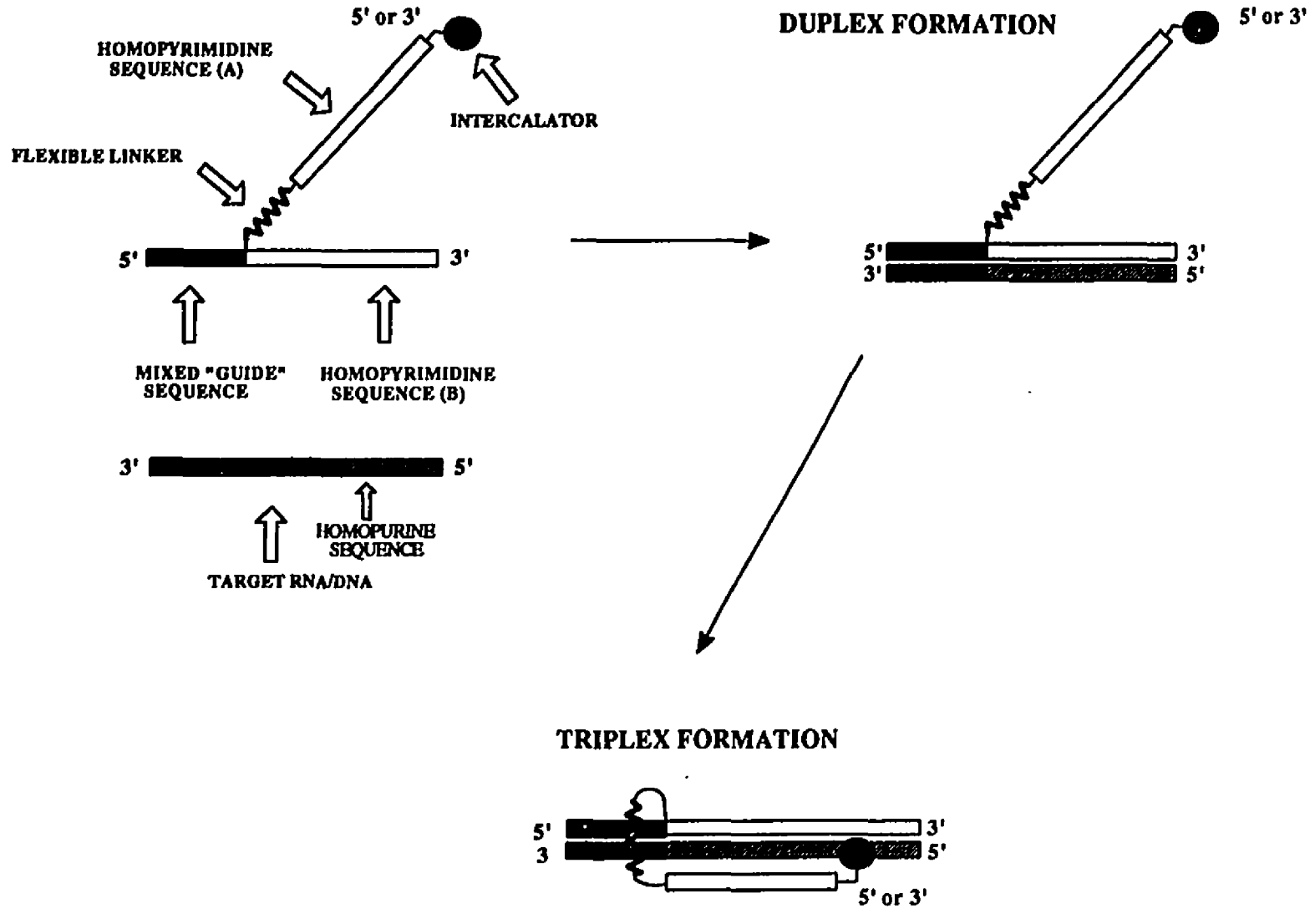

Figure 1.10 Antisense-Directed Triple Helix Formation by Branched Oligonucleotides. A Novel Approach Towards the Inhibition of Gene Expression.

CHAPTER 2 ATTACHMENT OF FLEXIBLE LINKER ON NUCLEOSIDE

2.1 Initial Synthetic Attempt

Considerable effort has been directed toward developing an efficient and general route for the preparation of 2'-O-alkylribonucleoside building blocks. Alkylating agents such as dimethylsulfate[79], organostannnous compounds[80], and diazomethane[81] have been utilized successfully. Our initial synthetic effort was directed toward the alkylation of a ribonucleoside at the 2' hydroxy position using the alkylating agent N-(5-bromopentyl)phthalimide. As a starting point, it was decided to use Manoharan's method[82] of functionalizing oligonucleotides at the 2' hydroxy position using the same alkylating agent (scheme 1). Manoharan observed 30% 2'-O-alkylation and <5% 3'-O-alkylation after treating the anion resulting from NaH/DMF of unprotected adenosine, at 0-5 ^{o}C, with N-(5-bromopentyl)phthalimide. Since we were not restricted as to the type of ribonucleoside needed, we decided to use 5'-O-DMT-N^{6}-benzoyl adenosine **1** as our starting material. This was prepared by reacting the free amino group of adenosine with benzoyl chloride according to Jones' transient protection procedure[83] and then protecting the 5'-hydroxy group as a 4,4'-dimethoxytrityl ether. Unlike Monaharan's results, our initial treatment of nucleoside **1** with NaH/DMF followed by alkylation, at 0-5 ^{o}C, of the resulting anion with 1.6 equivalents of N-(5-bromopentyl)phthalimide afforded **3** as the exclusive product (18-20%). We found that carrying out the reaction at ambient temperature produced a slightly higher yield of 26-28%. The structure of nucleoside **3** was confirmed by ^{1}H-NMR (figure 2.1) and mass spectrometry.

The fact that the sugar moiety was not alkylated was not entirely surprising. The intrinsic acidity of the amide (NH) group should be greater when compared to the weakly acidic properties (pKa $\cong$ 12.5) of the 2', 3' cis-diol groups.[84] This difference in acidity would render the NH group more susceptible to alkylation. In addition, efficient and

selective alkylations of the 2'- hydroxy of ribose sugars have proven to be difficult, unless very reactive electrophiles or strongly activated halides are utilized.[85] N-(5-bromopentyl)phthalimide is at best a weakly activated halide, thereby explaining the low yields obtained.

Scheme 1

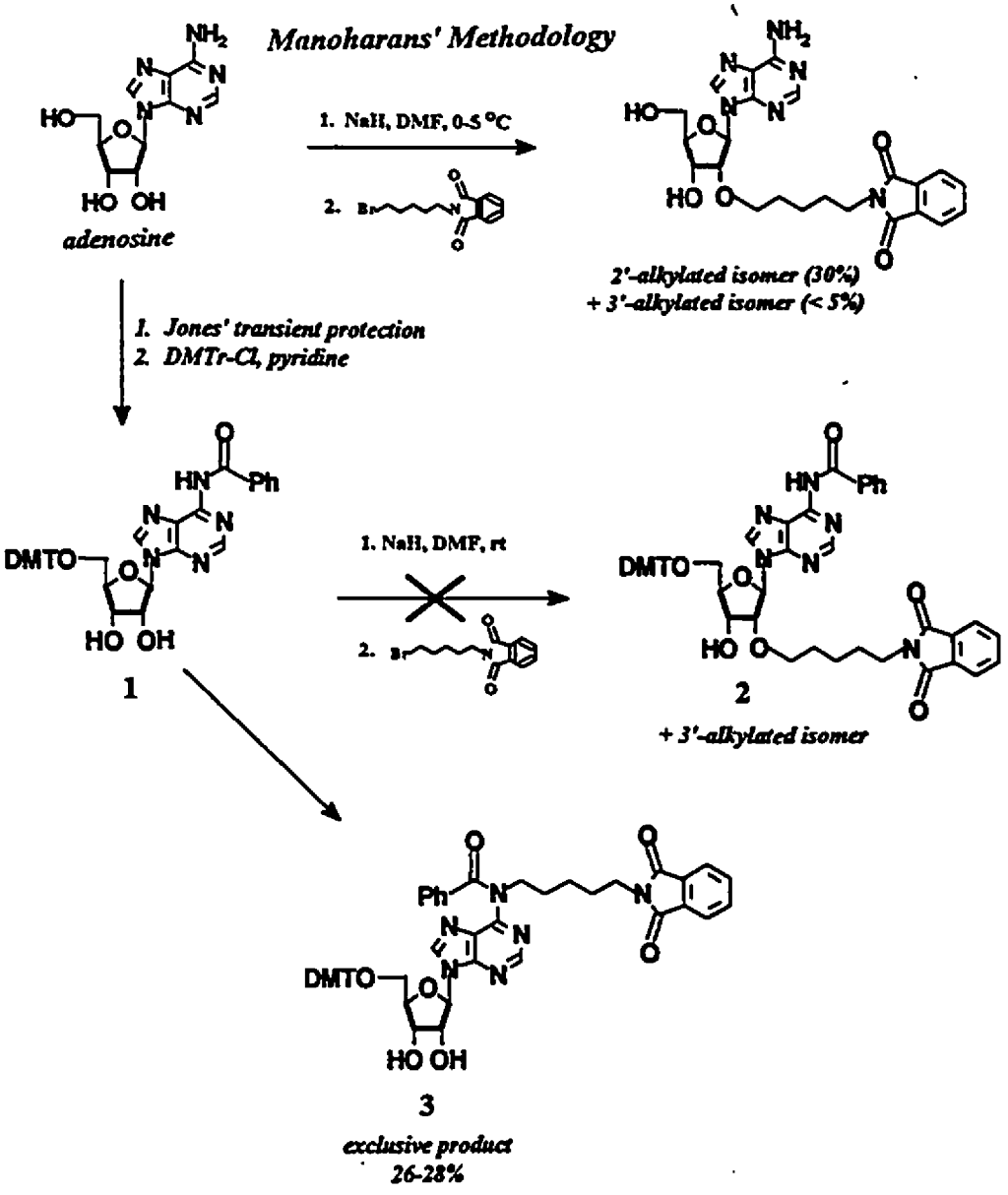

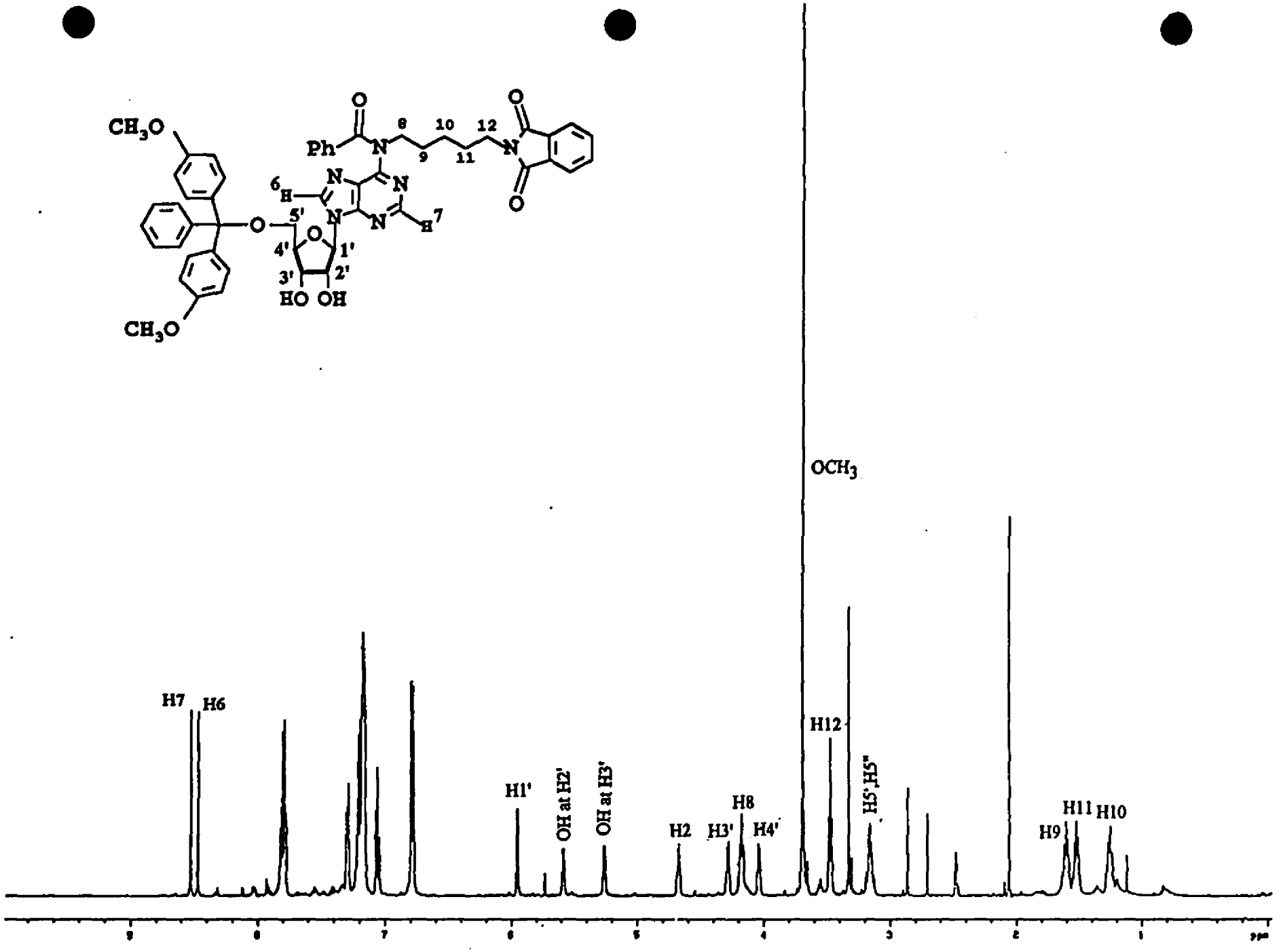

Figure 2.1 The 500 MHz spectrum of 3 in DMSO-d_6

We therefore decided to turn our attention to the pyrimidine nucleosides. This decision was based on our opinion that the intrinsic acidity of the imide (NH, pKa = 9.8)[86] group of uracil and thymidine would render them more susceptible to alkylation at this position. Furthermore, we were also not restricted as to the type of sugar (ribo or 2'-deoxy) or the site of attachment of the linker since flexibility would be provided by nucleoside units bearing the linker either on the base or the sugar moiety. We found that NaH/DMF treatment of 5'-O-(4,4'-dimethoxytrityl)uridine **4** or 5'-O-(4,4'-dimethoxytrityl) thymidine **5** followed by alkylation with N-(5-bromopentyl)phthalimide, at ambient temperature , resulted in selective alkylation on N^3 of the base, in consistently high yields of 86-88% and no alkylation on the sugar moiety.

Scheme 2

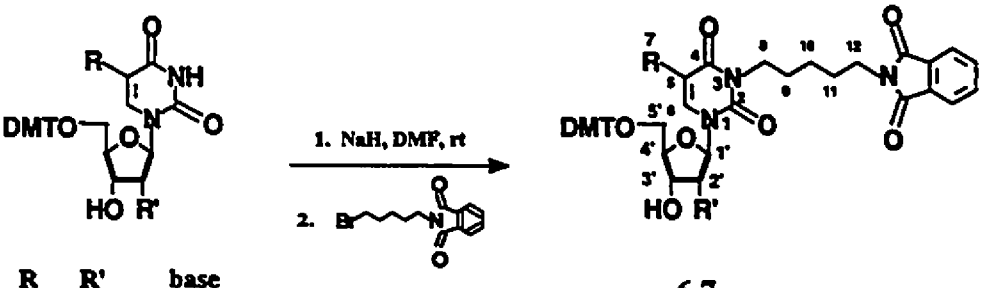

	R	R'	base
4	H	OH	*uridine*
5	CH_3	H	*thymidine*

6,7

It was decided at this point to use nucleoside **5** for subsequent work leading to the synthesis of our desired branching monomer. This choice also avoids additional protection/deprotection steps of the 2'- hydroxyl group of uridine.

The structures of nucleosides **6** and **7** were confirmed by ^1H and ^{13}C-NMR and mass spectrometry. Analysis of the ^1H-NMR spectrum of nucleoside **7** (figure 2.2) reveals the absence of the NH (imide) peak. This observation is consistent with either

N^3-alkylation or O^4-alkylation. In order to distinguish between both possibilities, ^{13}C-NMR analysis was necessary (figure 2.3). A report by Hata *et al.*[87] discussed the distinguishable difference between the C5 chemical shift between O^4- and N^3-acylated uridine derivatives. They found that the C5 chemical shift of N^3-acylated uridine derivatives appeared at a lower field compared with O^4-acylated uridine derivatives and at a similar chemical shift compared to the parent uridine. The C5 chemical shift of our alkylated nucleoside 7 appears at 110.39 ppm , which is very similar to the C5 chemical shift of the parent thymidine, 110.37 ppm. This observation is therefore consistent with N^3 alkylation.

In addition to ^1H- and ^{13}C-NMR, FAB mass spectrometry was employed as further structural proof. The fragmentation pattern observed (figure 2.4) was consistent with our proposed structure.

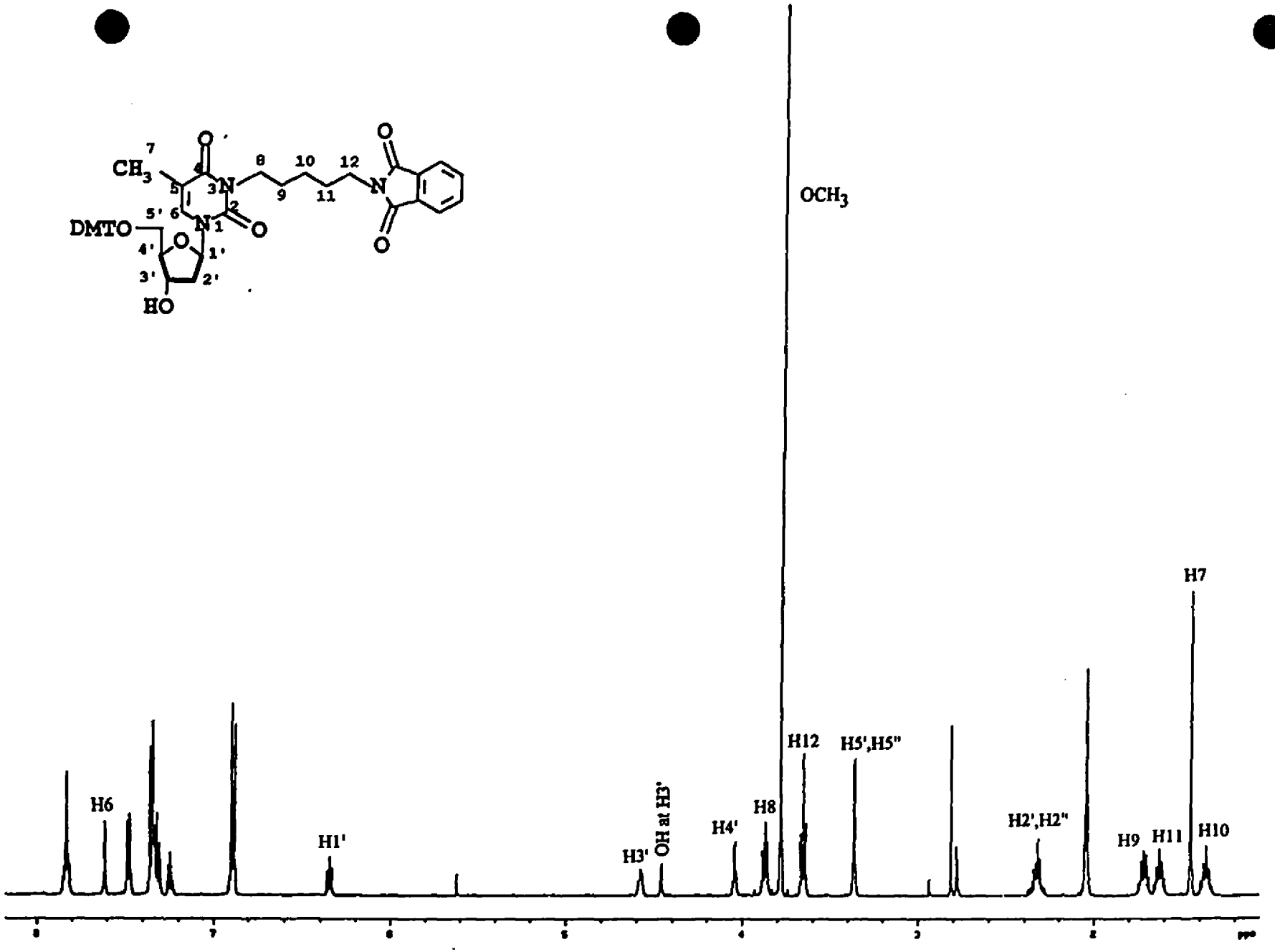

Figure 2.2 The 500 MHz ^{1}H-NMR spectrum of 7 in acetone-d_6 (chemical shifts are given in table 1).

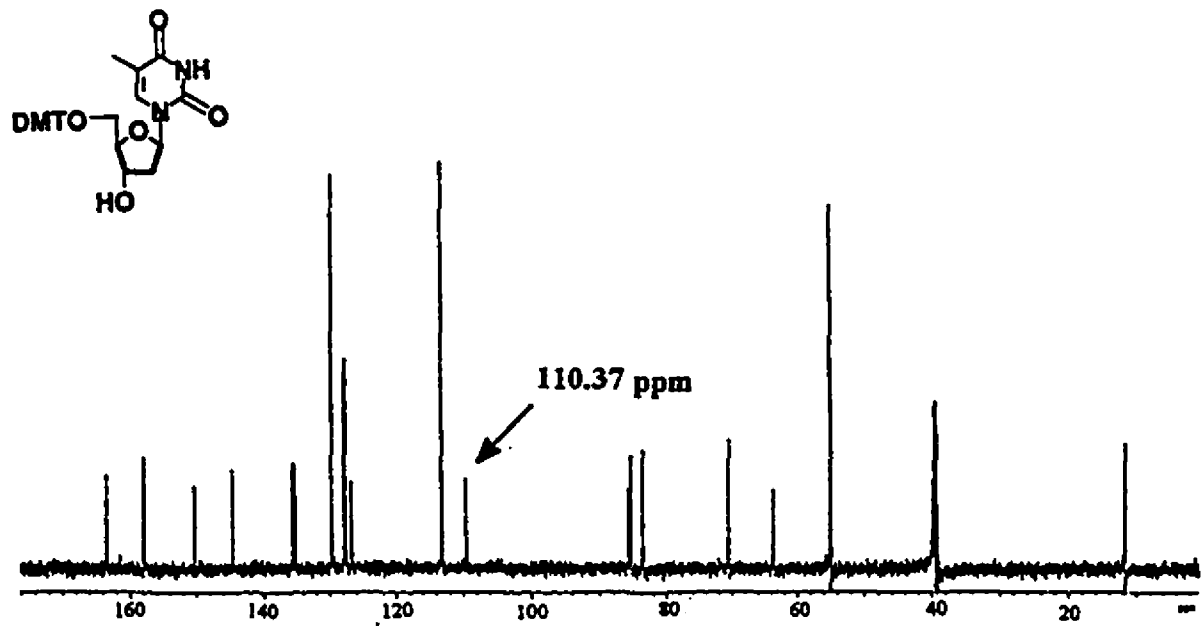

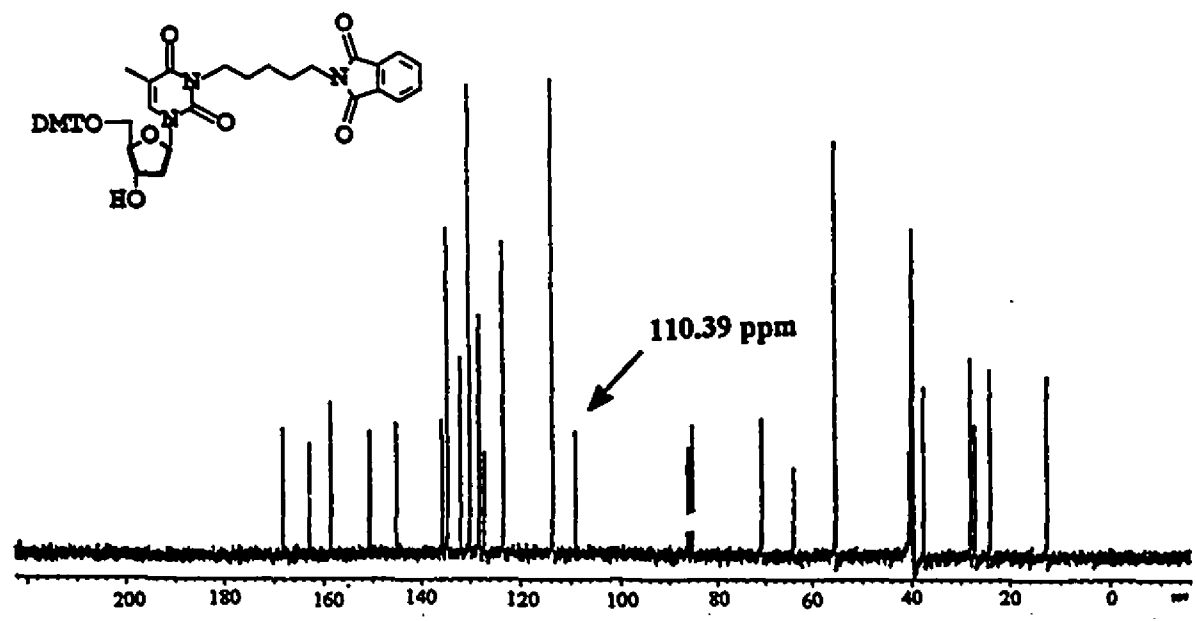

Figure 2.3 The 500 MHz ^{13}C-NMR spectrum of 5 and 7. The C5 resonance signal is indicated. (for other assignments see table 2)

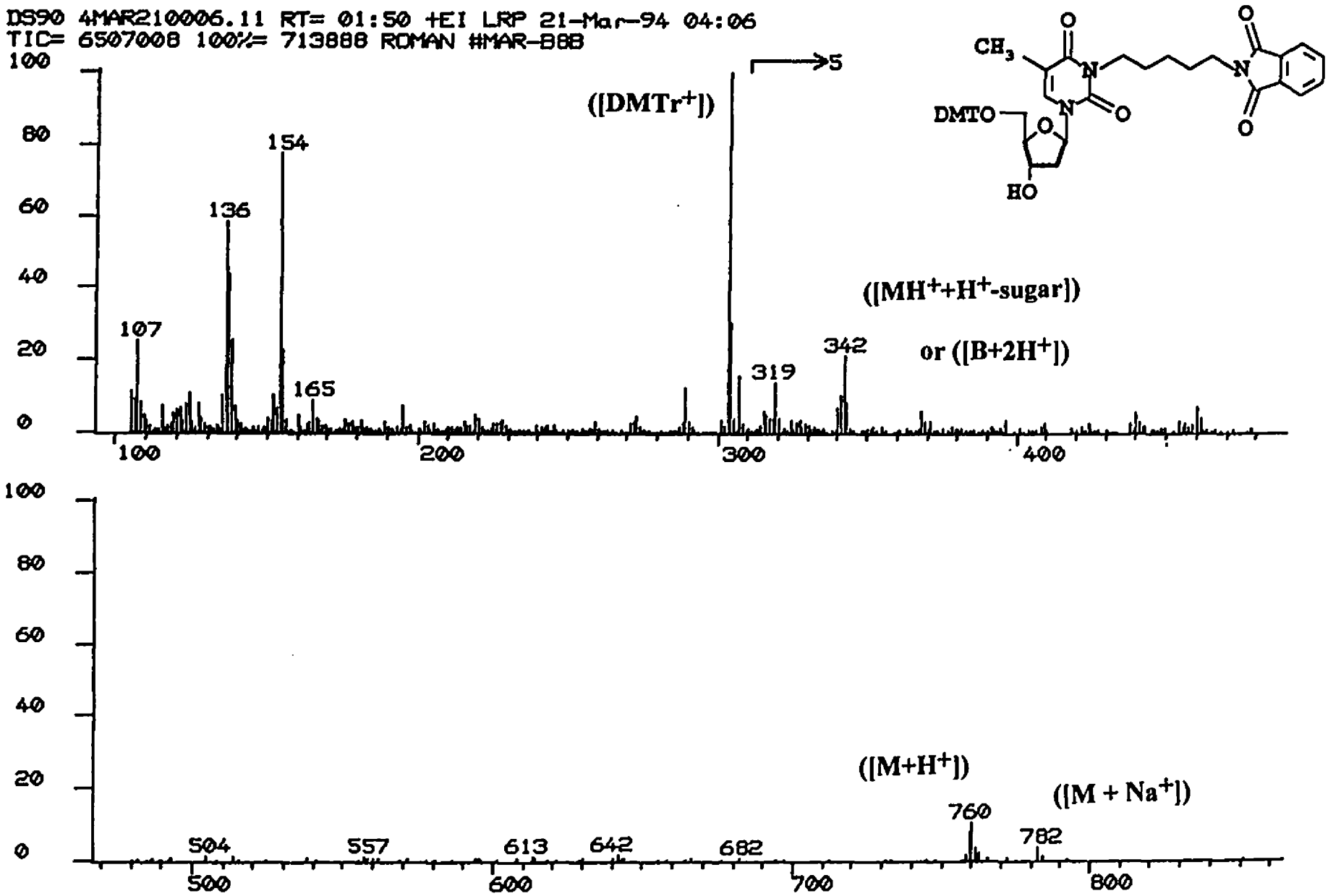

Figure 2.4 FAB mass spectrum of 7 in nitrobenzyl alcohol and NaCl

Encouraged by these results, we decided to attach different sized linkers ranging from N-(2-bromoethyl)phthalimide to N-(4-bromobutyl)phthalimide (scheme 3) in order to study the effect of different flexibilities on oligonucleotide binding. The same procedure was used as described for the synthesis of **7** and the functionalized nucleosides **8-10** were obtained in 52-82% yield after column chromatography and hexanes precipitation. Although a primary halide, N-(-2-bromoethyl)phthalimide is somewhat sterically hindered for efficient displacement by the incoming imide nucleophile, explaining the low yield observed. However, for linkers N-(3-bromopropyl)phthalimide to N-(5-bromopentyl)phthalimide the distance between the primary center and the large phthalimide group progressively increases rendering nucleophilic displacement more efficient as evidenced by the higher yields. ^{1}H-NMR and ^{13}C-NMR data were consistent with their structures and are reported in tables 1 and 2, respectively.

Scheme 3

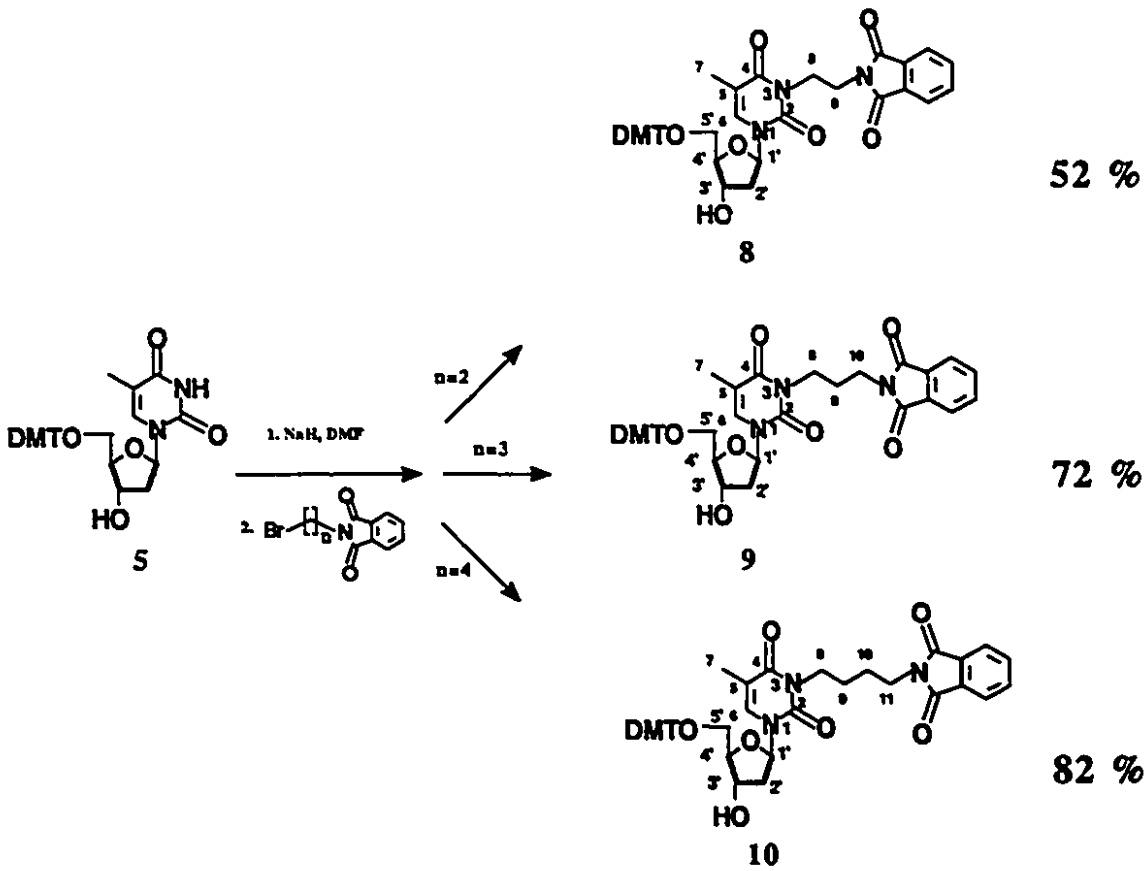

2.2 Synthesis of Amino Alcohol 11 - Removal of Phthalimido Group

A survey of the literature[88,89,90] revealed that the phthalimido protecting group is stable to a wide variety of reaction conditions. However, selective removal of the phthalimido group in the presence of highly sensitive functionalities has proven to be difficult and has overshadowed any obvious advantages it may have. Hydrazinolysis[91], base catalyzed aminolysis[92] and methylaminolysis[93,94] are three generally accepted procedures for removal of the phthalimido group. These three deprotection methods, however, would be incompatible with the automated solid phase synthesis of our desired branched oligonucleotides. Hydrazinolysis and the ensuing acidic workup would simply

TABLE 1 ^{1}H-NMR (500 MHz) Spectral Data[a] for Nucleosides **7**, **8**, **9** and **10** in acetone-d_6

COMPOUND	7 (n = 5)	8 (n = 2)	9 (n = 3)	10 (n = 4)
H1'	6.36 (t, 1H) J(H1', H2'AB) = 7.0	6.18 (t, 1H) J(H1', H2'AB) = 7.20, 6.35	6.35 (t, 1H) J(H1', H2'AB) = 7.45, 7.20	6.37 (dd, 1H) J(H1', H2'AB) = 7.45, 6.23
H2'	2.29-2.40 (m, 2H)	2.22-2.37 (m, 2H) J(H2', H3') = 6.23, 3.66 J(H2'A, H2'B) = 13.06	2.22-2.39 (m, 2H) J(H2', H3') = 5.86, 3.42 J(H2'A, H2'B) = 13.43	2.20-2.37 (m, 2H) J(H2', H3') = 6.10, 3.83 J(H2'A, H2'B) = 13.43
H3'	4.60 (m, 1H)	4.53 (m, 1H)	4.58 (m, 1H)	4.59 (m, 1H)
H4'	4.06 (q, 1H)	4.023 (q, 1H)	4.04 (q, 1H)	4.04 (q, 1H)
H5'	3.38 (d, 2H)	3.37 (d, 2H)	3.37 (d, 2H)	3.37 (d,2H)
OCH_3	3.78 (s, 3H)	3.79 (s, 3H)	3.78 (s, 3H)	3.94 (s, 3H)
H6	7.62 (s, 1H)	7.59 (s, 1H)	7.63 (s, 1H)	7.62 (s, 1H)
H7	1.457 (d, 1H) ^{3}J(H6, H7) = 1.0	1.39 (d, 1H) ^{3}J(H6, H7) = 1.0	1.464 (d, 1H) ^{3}J(H6, H7) = 1.0	1.472 (d, 1H) ^{3}J(H6, H7) = 1.0
H8	3.86 (t, 2H)	3.959 (m, 2H)	3.962 (m, 2H) J(H8'A, H9XY) =7.25, 7.50 J(H8'B, H9XY) =7.48, 7.18 J(H8'A, H8'B) =12.97	3.935 (m, 2H) J(H8'A, H9XY) =7.00, 7.12 J(H8'B, H9XY) =6.00, 6.88 J(H8'A, H8'B) =12.62
H9	1.707 (q^5, 2H)	4.21 (m, 2H)	2.05 (q, 2H)	1.67 (m, 2H)
H10	1.623 (q^5, 2H)		3.705 (t, 2H)	1.67 (m, 2H)
H11	1.357 (m, 2H)			3.695 (t, 2H)
H12	3.647 (t, 2H)			

[a] Assignments are based on the results of ^{1}H-^{1}H COSY

TABLE 2 ^{13}C-NMR Spectral Data for Nucleosides 7, 8, 9 and 10 in acetone-d_6

COMPOUND	7(n = 5)	8(n = 2)	9(n =3)	10(n =4)
C1'	86.11	86.28	86.18	86.11
C2'	41.28	41.30	41.26	41.27
C3'	72.30	72.02	72.24	72.31
C4'	87.12	87.17	87.15	87.15
C5'	64.65	64.53	64.64	64.67
OCH_3	55.48	55.49	55.47	55.48
C2	151.47	151.72	151.46	151.53
C4	163.60	163.88	163.59	163.65
C5	110.39	110.33	110.36	110.39
C6	134.80	134.91	134.96	134.86
C7	12.85	12.82	12.82	12.87
C8	41.17	40.21	39.35	41.03
C9	28.85	36.52	27.43	26.62
C10	24.85	168.77	36.36	25.78
C11	27.88	168.77	168.68	38.13
C12	38.23		168.68	168.68
C13	168.74			168.68
C14	168.74			

be too harsh and the oligomer would undergo modification (e.g., at the heterocyclic bases). If ammonia or methylamine were used as deprotection agents, the ester linkage attaching the oligomer to the solid support would be cleaved easily, leading to premature release of the DNA from the polymer support and affording an undesirable product. It is now clear that the phthalimido group must be replaced by a protecting group that can be removed under conditions compatible with oligonucleotide assembly (see next section).

Meanwhile, we decided to utilize methylamine to remove the phthaloyl group because of its simplicity and the ease with which the methylamine can be removed from the reaction mixture. As outlined in scheme 4, treatment of a benzene/ethanol solution (1:2, v/v) of 7 with excess 40% aqueous methylamine afforded, in 45 min, an intermediate whose spectral properties are consistent with the phthalamide structure **11** (figure 2.5 and 2.6). The ^{1}H-detected heteronuclear multiple bond connectivity (HMBC)[95,96] spectrum, which defines small (long-range) H-C couplings ($^{2}J_{CH}$ and $^{3}J_{CH}$), shows a strong cross peak from 14-C to 15-Me ($^{3}J_{CH}$) and a moderately weak peak from 13-C to both 12-H_2 ($^{3}J_{CH}$). When the reaction was allowed to proceed for 24 hr, the desired amino alcohol **12** was obtained, after reverse phase chromatography, in 80% yield (figure 2.7). This prolonged treatment would not be useful in branched DNA assembly since methylamine would easily cleave DNA covalently bound to CPG, affording an undesired product. A trityl analysis, revealed 50% cleavage after a 30 min methylamine treatment of CPG bound 5'-O-tritylated nucleosides (figure 2.8). Clearly, a 24 hr treatment would cleave all CPG bound DNA.

Scheme 4

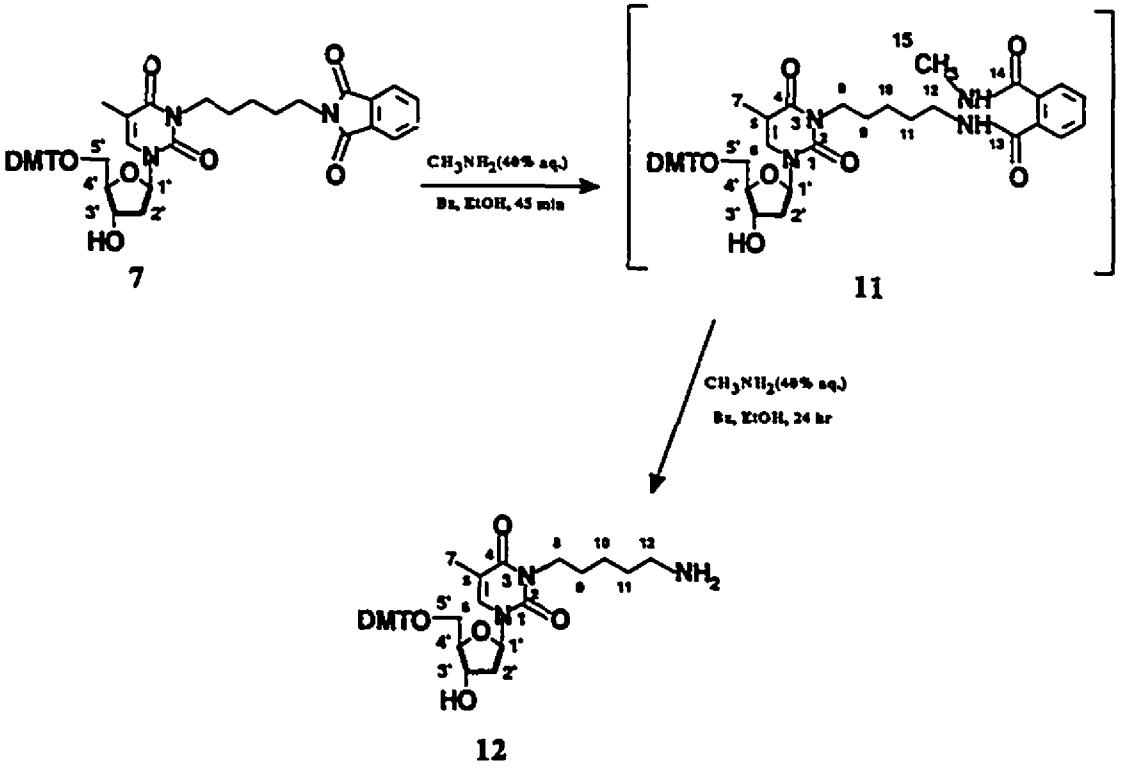

7 11 12

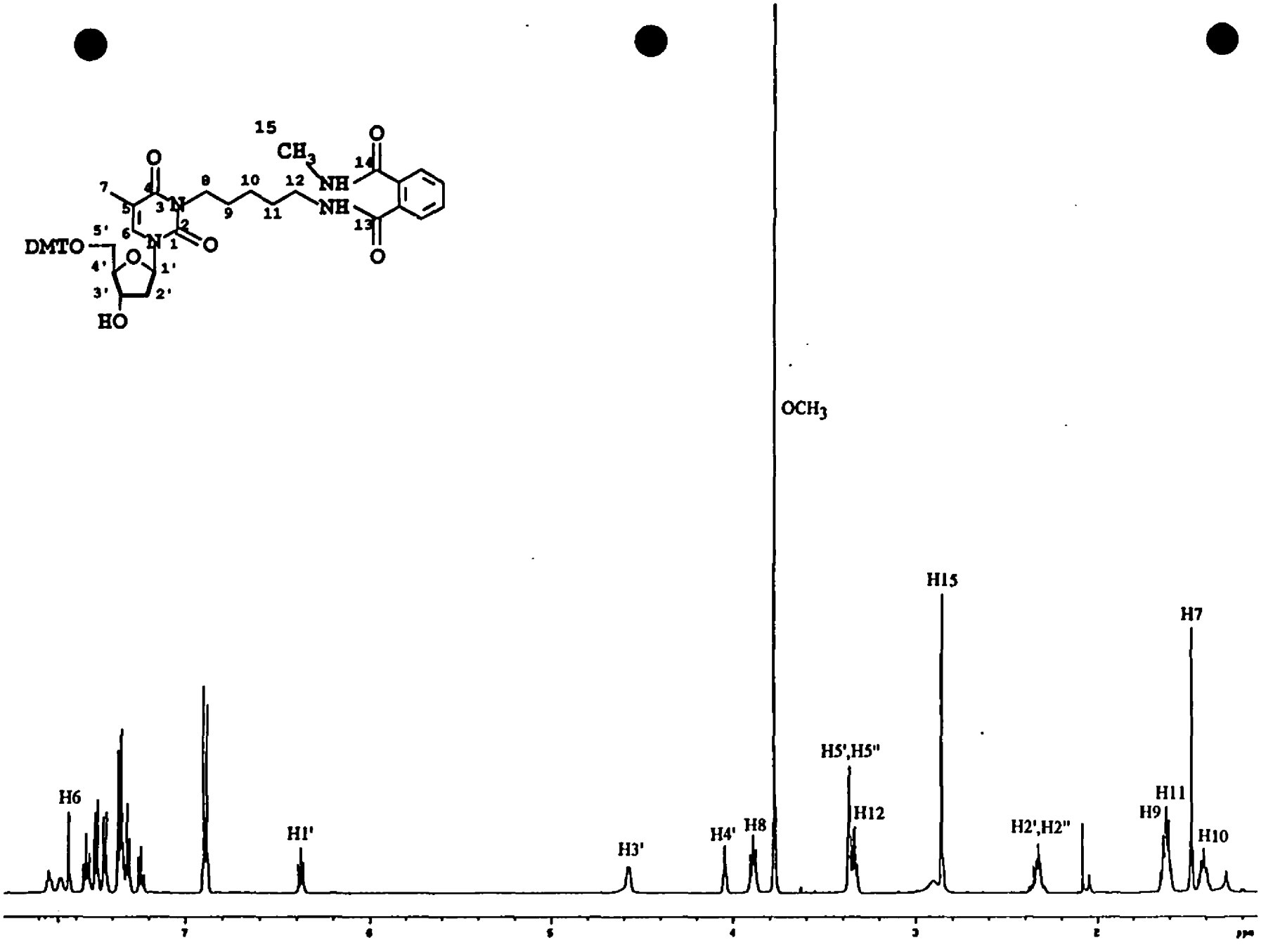

Figure 2.5 The 500 MHz ^{1}H-NMR spectrum of phthalamide 11 in acetone-d_6

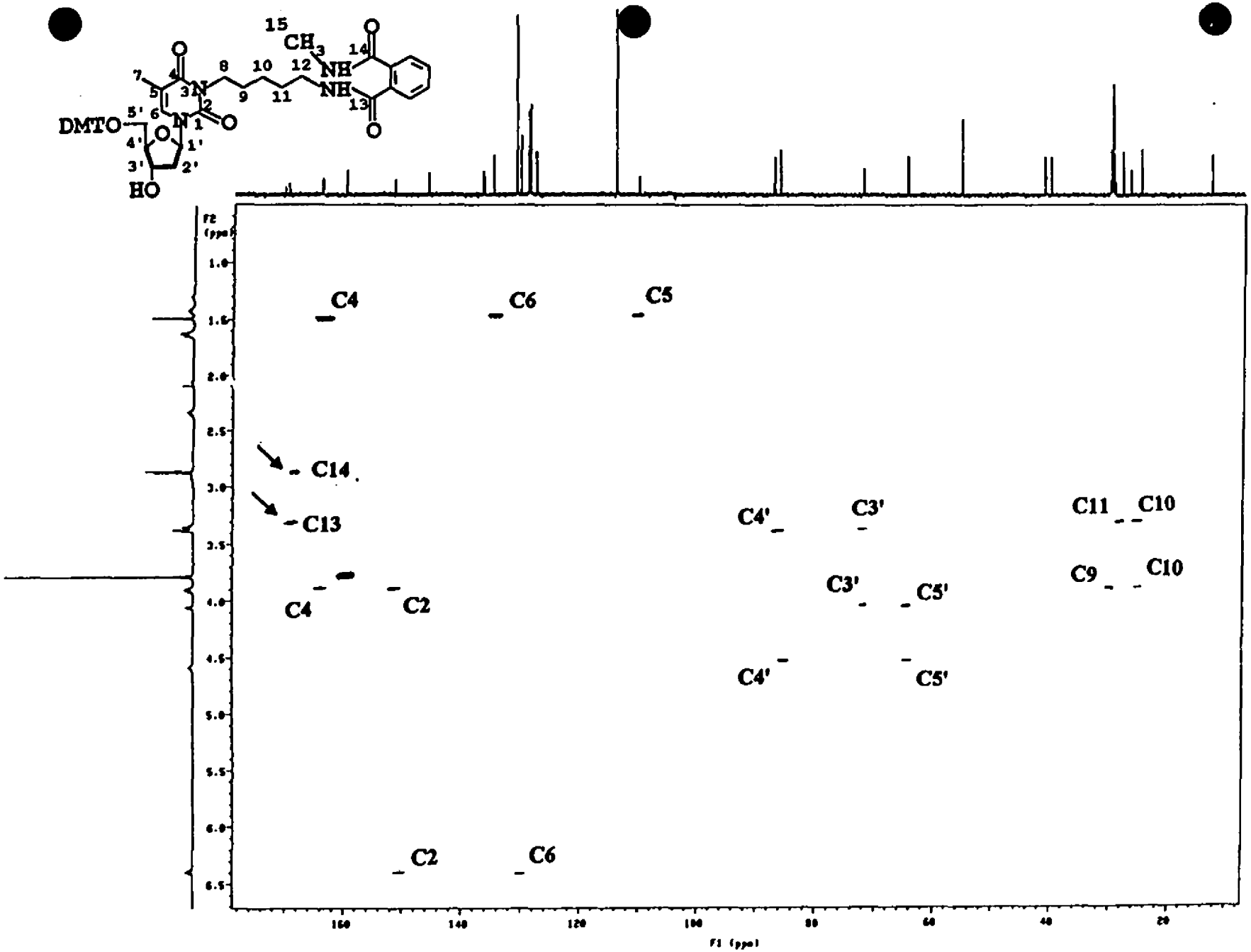

Figure 2.6 The 500 MHz HMBC spectrum of phthalamide 11 in acetone-d_6

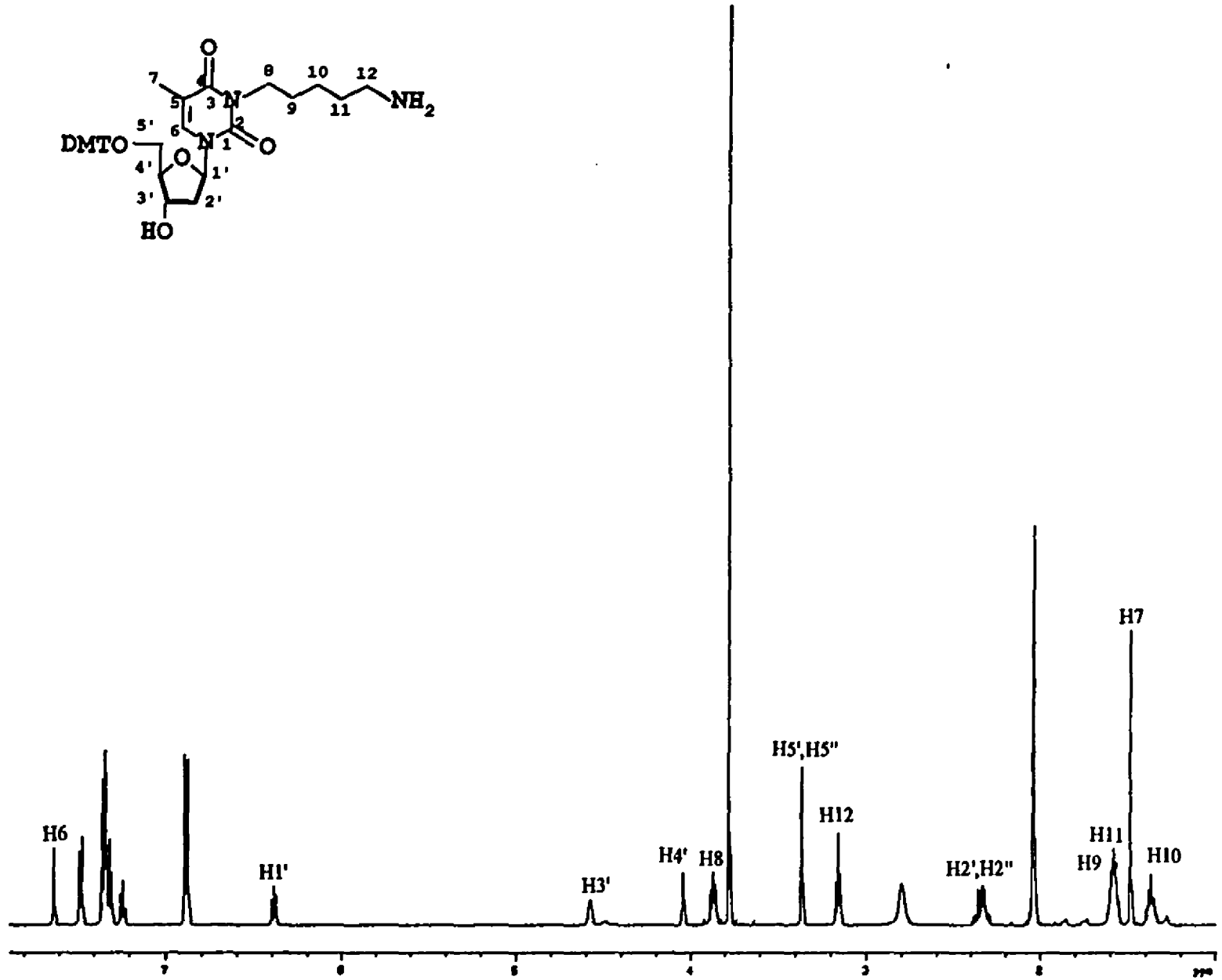

Figure 2.7 The 500 MHz ^{1}H-NMR spectrum of amino alcohol **12** in acetone-d_6

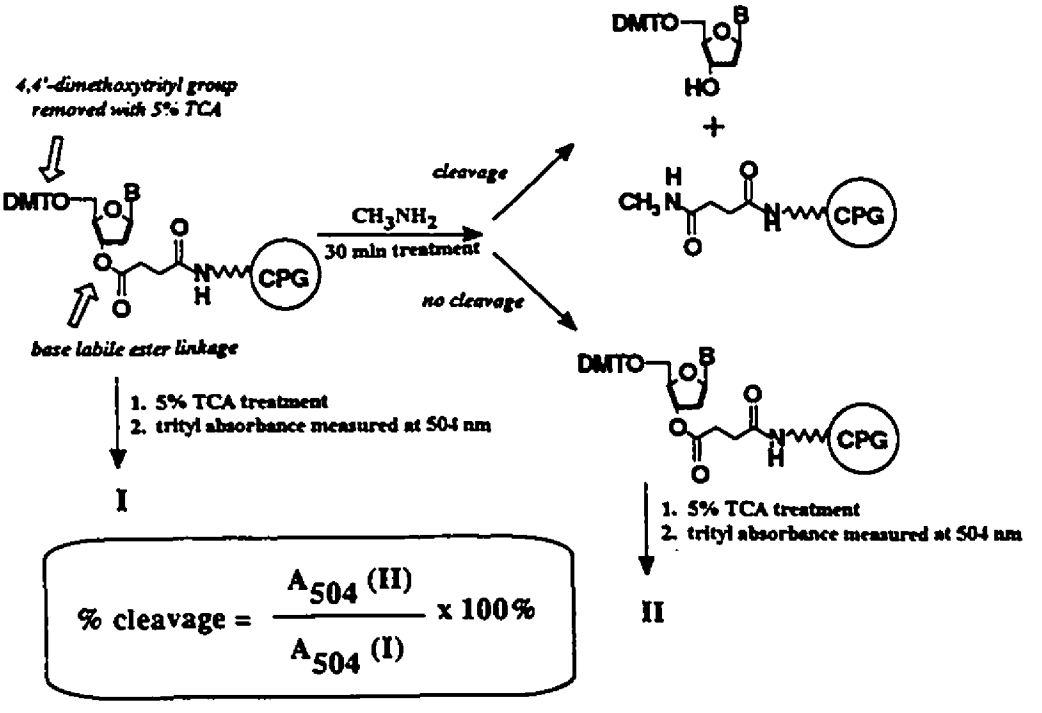

Figure 2.8 Methylamine treatment and Trityl Analysis of CPG bound 5'-O-tritylated nucleosides.

2.3 Synthesis of N- levulinated thymidine (16)

The synthetic studies in section 2.2 clearly demonstrated that the phthalimido protecting group must be replaced by another protecting group that is more compatible with the solid phase synthesis of oligonucleotides and can be removed selectively in the presence of other functional groups. We decided to investigate the levulinyl group as a possible canditate. The levulinyl group was introduced as a protecting group in nucleic acid chemistry by Hassner *et al.*[97] and later used by Van Boom and Burgers[98] as a 5'- hydroxyl protecting group during oligonucleotide synthesis. The levulinate protecting group seemed ideal for our purposes because it is stable to the general conditions used in oligonucleotide assembly and can be removed rapidly and selectively under "neutral" conditions, i.e., 0.5 M hydrazine hydrate in pyridine:AcOH buffer (4:1, v/v) for 5-15

minutes[99-100] (scheme 5). Under these mild conditions, the heterocyclic nucleic acid bases and ester linkages will not undergo any modification.

Scheme 5

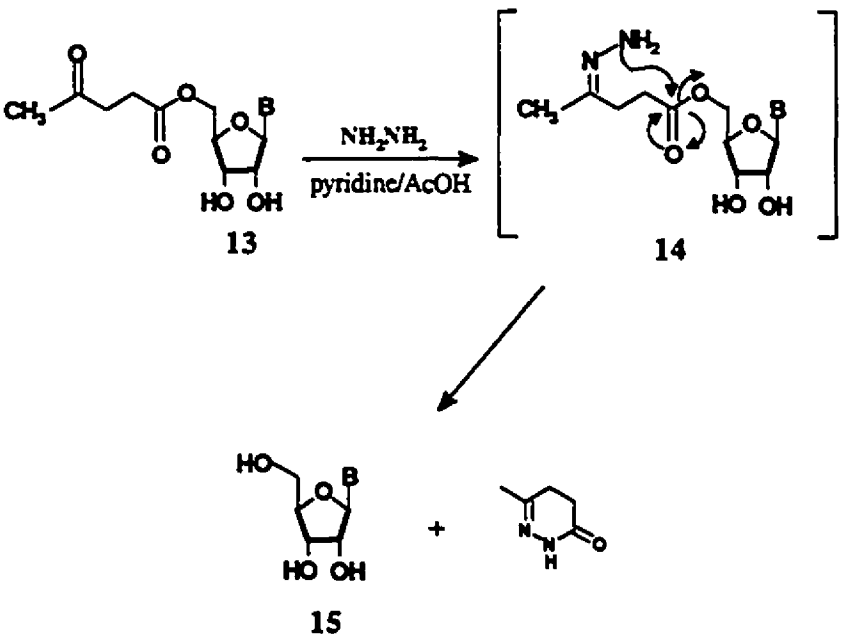

The direct N-levulination of our amino alcohol **12** seemed improbable without first protecting the free 3'-hydroxyl group. However, it was hoped that N-levulination might be accomplished in a single step by employing a simple procedure developed by Ugarkar *et al.*[101] for the selective N-acylation of cytosine nucleosides. We found that reacting amino alcohol **12** with freshly prepared levulinic anhydride, employing N,N'-dimethylformamide as a solvent, afforded high yields (>80%) of the desired nucleoside **16**, whose spectral properties (figure 2.9) are consistent with the proposed structure.

Scheme 6

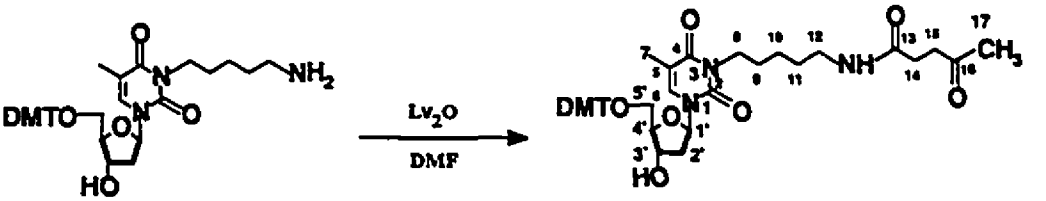

12 16

At this stage we felt that a detailed investigation of the delevulination of **16** in pyridine:AcOH conditions (Letsinger's hydrazine solution)[99,100] would give us a better indication of its usefulness in branched DNA assembly. We hoped that, under these conditions, N-delevulination would be achieved as efficiently as O-delevulination. In fact, Ogilvie *et al.*[102] used these conditions to cleanly remove the levulinyl group on cytosine within 5 to 15 minutes (**17** → **18**, scheme 7).

Unlike the rapid deprotection of **17**, a 90 min treatment of **16** with 10 equivalents of the "neutral" hydrazine solution afforded only 70%, as judged by TLC, of the expected amino alcohol **12** and a second less polar product of unknown structure (R_f = .40 in CH_2Cl_2/MeOH, 9:1, v/v). It was found that an 18 hr treatment provided the best results affording *ca.* 90% of the amino alcohol **12** and *ca.* 5-10% of the undesired product.

Scheme 7

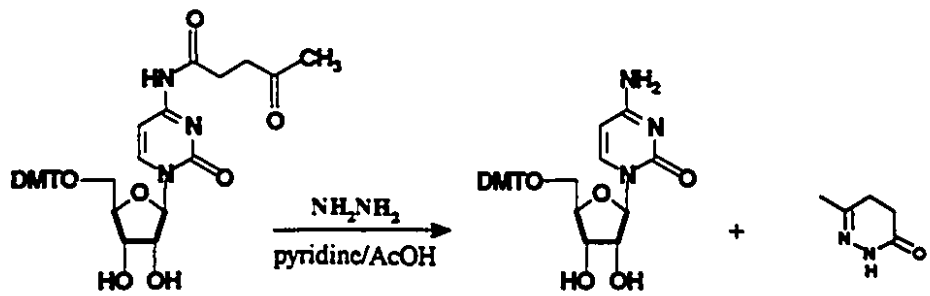

17 18

It was apparent that complete deprotection was not possible which was quite discouraging because coupling yields at the branching point would be adversely affected (see chapter 4). Despite our best efforts, the intermediate at R_f = .40 could not be obtained in the pure state since it partially reverted back to the starting material during silica gel chromatography. This observation led us to suspect that the intermediate compound is hydrazone **19** (scheme 8). We also realized that intramolecular cleavage of the amide intermediate **19** would be much more difficult when compared to intramolecular cleavage of ester intermediate **14** explaining the difference in deprotection time between O- and N-delevulination. In addition, we realized that the nature of the leaving group would also have a significant effect on the rate of N-delevulination explaining the difference in deprotection time between **17** and **16**. These observations suggest that although amide **16** is somewhat labile to Letsinger's hydrazine solution, complete deprotection would be difficult since the leaving group in this case in not nearly as good as in **17** and esters are expected to be more reactive than amides.

Scheme 8

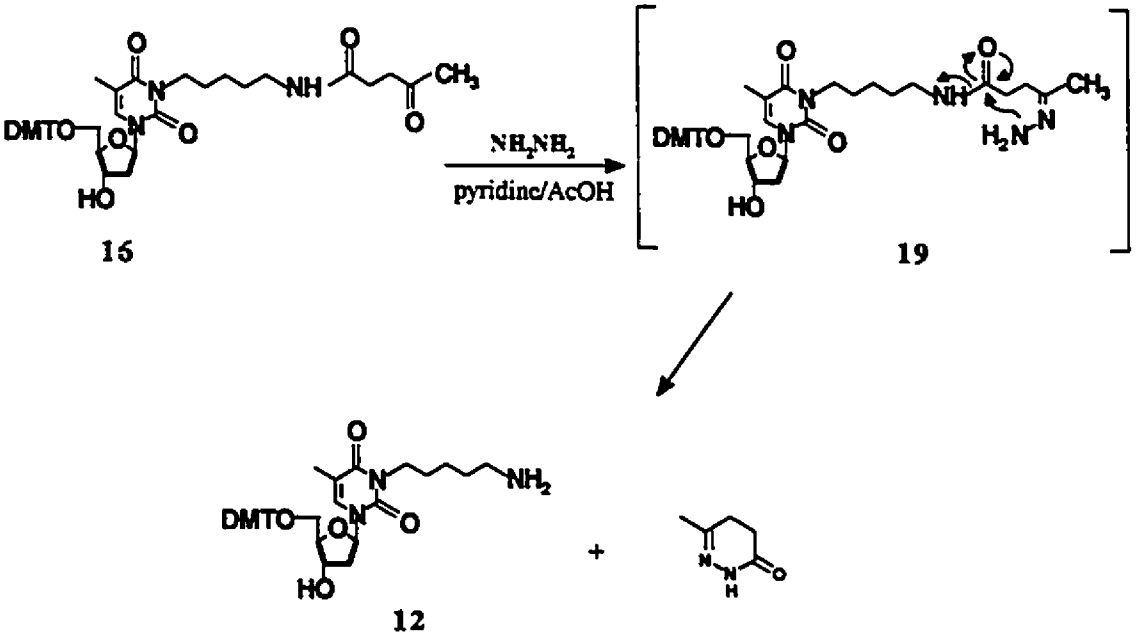

Treatment of **16** with N,N'-diisopropyl(β-cyanoethyl)phosphonamidic chloride in THF containing DMAP and diisopropylethylamine afforded phosphoramidite **20** in 85% yield. ^{31}P-NMR analysis indicated the presence of two phosphorus resonances at 147.695 and 148.075 ppm corresponding to the two diastereomers of **20** (figure 2.10).

Scheme 9

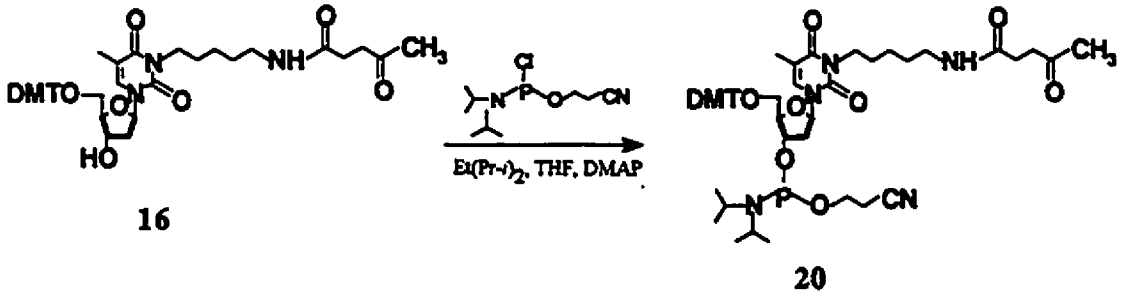

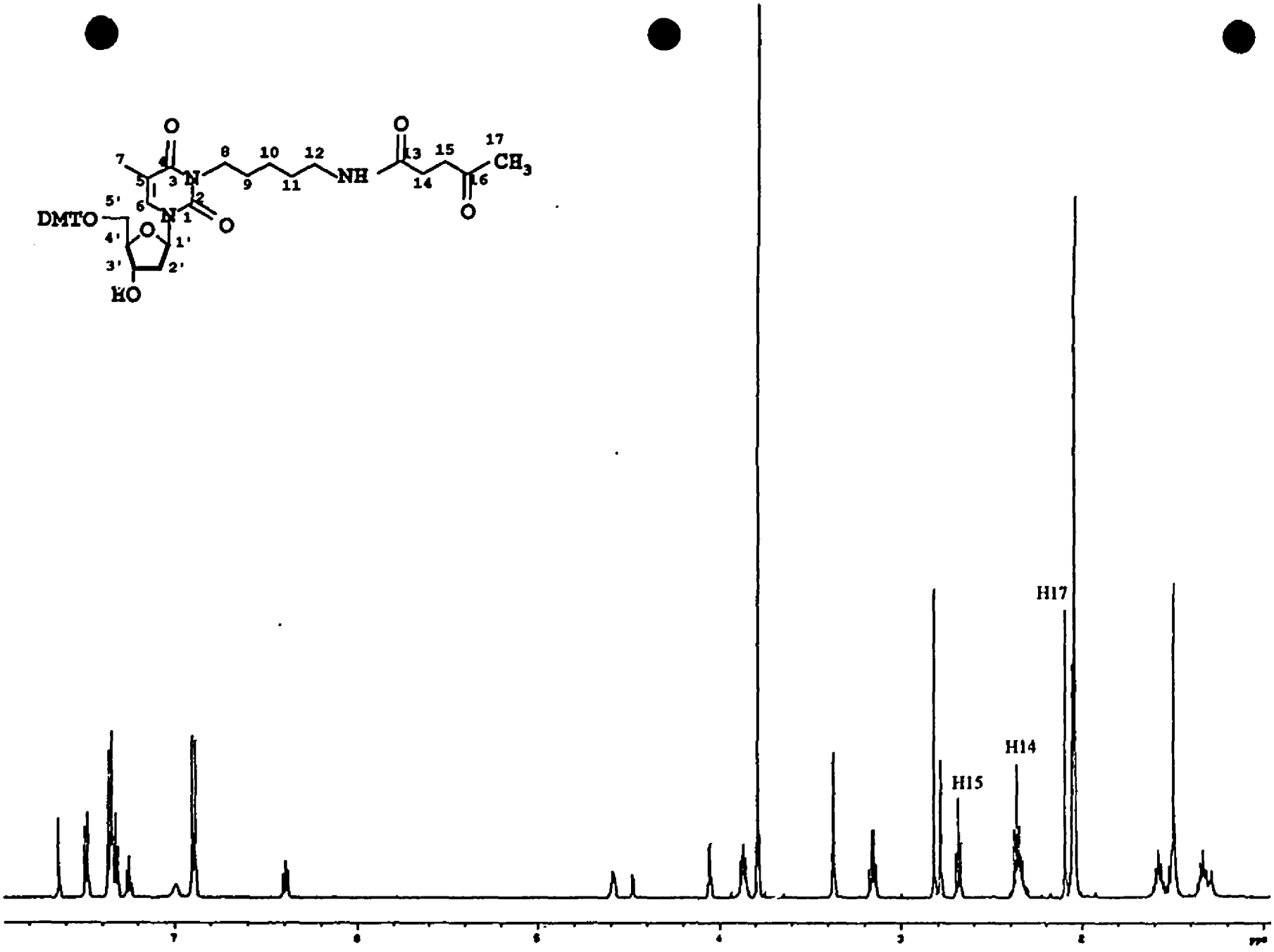

Figure 2.9 The 500 MHz ^{1}H-NMR spectrum of levulinic amide **16** in acetone-d_6

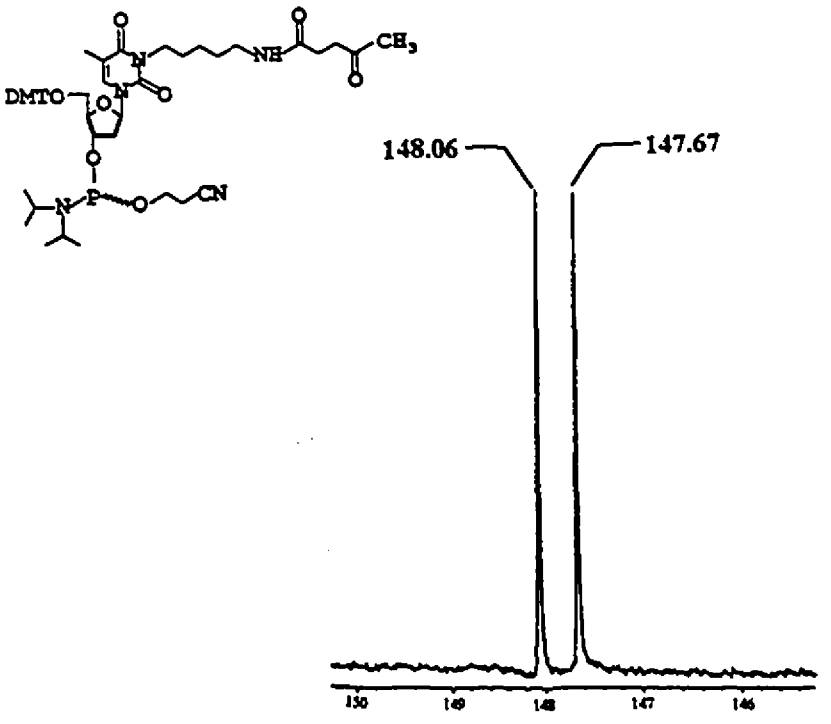

Figure 2.10 ^{31}P-NMR of amidite 20

CHAPTER 3 SYNTHESIS OF O-LEVULINATED EXTENDED LINKER

3.1 Overview of Synthetic Plan

To solve the problem of incomplete hydrazine deprotection of levulinic amide nucleoside **16**, we turned our attention to the synthesis of a flexible linker containing a primary alcohol moiety (rather than a primary amine) at the site of protection. The key feature of this method would be the formation of a hydrazine-labile protecting group which would solve the problem of deprotection time and render it more suitable for oligonucleotide synthesis. The fact that we were not restricted as to the type and size of linker afforded us the luxury of some flexibility in the final structure of the linker moiety (figure 3.1). With nucleoside **7** in hand, we systematically dissected a few possibilities and ultimately decided to employ a procedure originally developed by Itakura *et al.*[103] and later modified by Usman *et al.*[104] In order to investigate the effect of flexibility on oligonucleotide binding, it was decided at this stage of the synthetic plan to use nucleosides **7** and **8** for subsequent synthetic steps.

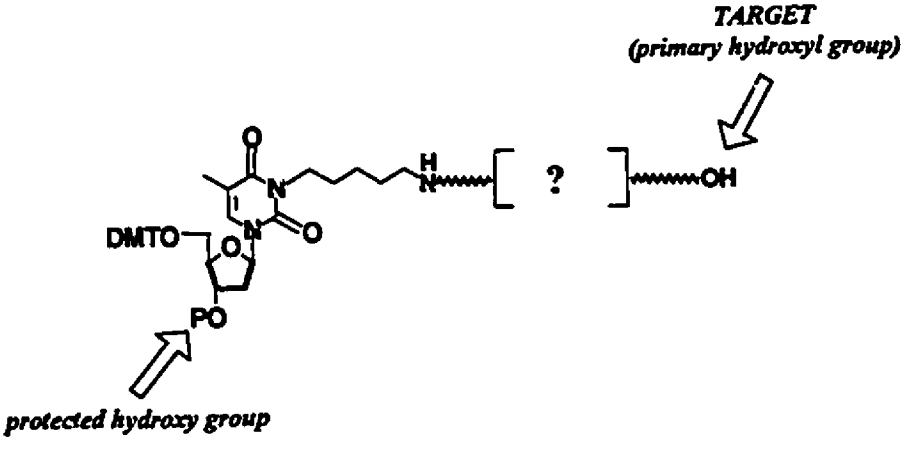

Figure 3.1 Final target of linker system

3.2 Synthesis of Amines 25 and 26

Before applying Itakura's modified procedure, the 3'-hydroxy of nucleoside 7 must be protected and the phthaloyl group must be removed. While there are a number of possible protecting groups that may be used for masking the 3'- hydroxy moiety, we chose the triisopropylsilyl (TIPS) group because of its good stability to basic conditions.[105] The general procedure for the preparation of 3'-O-silylated phthalimides **21** and **22** is shown in scheme 9. Silyl protection was carried out according to the procedure developed by Ogilvie and co-workers.[106] Dissolving functionalized nucleosides **7** and **8**, two equivalents of triisopropylsilyl chloride, and imidazole in anhydrous DMF afforded silylated nucleosides **21** and **22** in >90% yields. Triisopropylsilylation was followed by dephthaloylation using 40% aqueous methylamine, as described previously, to afford amines **25** and **26** in moderate yields (78-80%).

Scheme 9

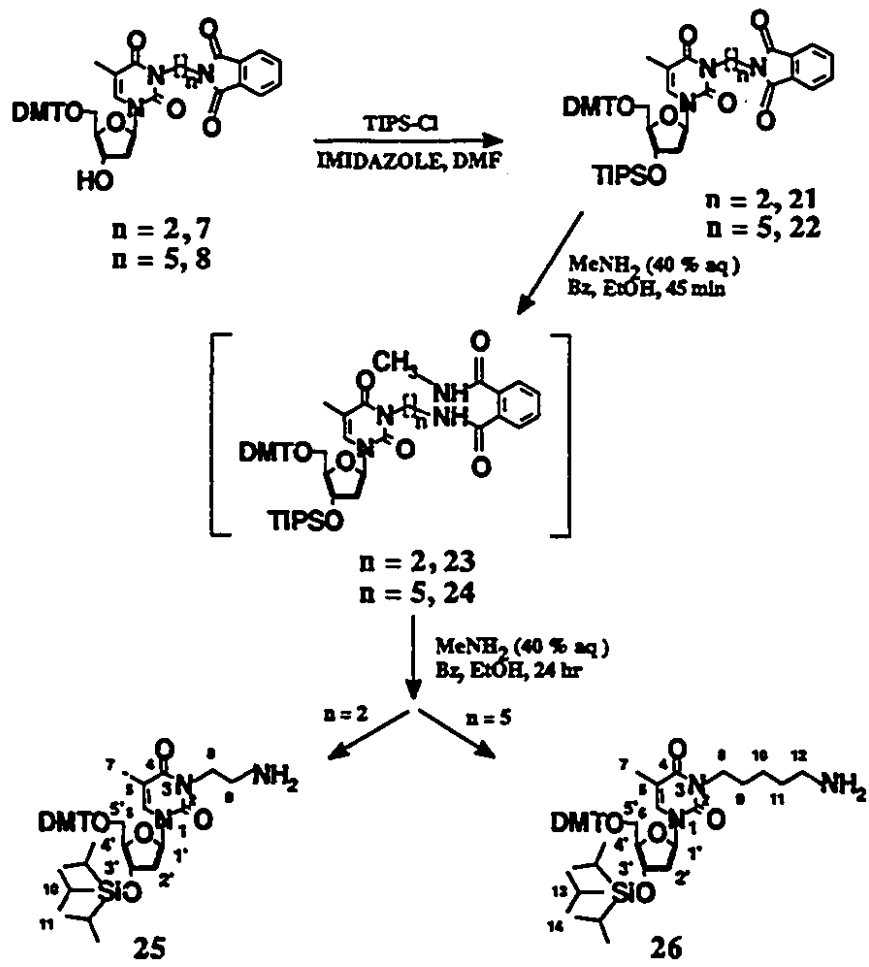
DMTO
HO
n = 2, 7
n = 5, 8
TIPS-Cl
IMIDAZOLE, DMF
TIPSO
n = 2, 21
n = 5, 22
MeNH2 (40 % aq)
Bz, EtOH, 45 min
CH3
NH
NH
n = 2, 23
n = 5, 24
MeNH2 (40 % aq)
Bz, EtOH, 24 hr
n = 2
n = 5
NH2
SiO
25
26

3.3 Synthesis of Alcohols 31 and 32

With amines **25** and **26** in hand, we decided to apply Itakura's methodology in the synthesis of pentachlorophenyl esters **29** and **30** as depicted in scheme 10. Thus, reaction of 3'-silylated amine **25** with succinic anhydride and a catalytic amount of DMAP in pyridine afforded succinate **27** in quantitative yield. The longer succinate **28** was obtained in a similar manner. An important feature provided by the succinylation step is that it allows the introduction of two amides which may reduce the number of degrees of freedom of the linker making it more "entropically" favorable for the third (branch) strand to fold over and form a triple helix. Crude succinates **27** and **28** were then treated with pentachlorophenol and dicyclohexylcarbodiimide in DMF at ambient temperatures for 48 hr to afford, after hexanes precipitation, activated pentachlorophenyl esters **29** and **30** in near quantitative yield. The crude pentachlorophenyl esters **29** and **30** were used in the next step without any purification.

We then investigated the ability of 5-amino-1-pentanol to displace the pentachlorophenyl ester, reasoning that the primary amine moiety would react preferentially and provide our desired target molecule. In order to minimize undesirable displacement by the hydroxy group, a 20% solution of pentachlorophenyl ester **29** was added, at ambient temperature, over a 15 min interval to a solution of 5-amino-1-pentanol in pyridine containing triethylamine. TLC analysis in 7.5% CH_2Cl_2/MeOH showed complete reaction after 24 hr with the formation of a single more polar UV active and ninhydrin negative compound of $R_f = .32$. This compound was identified as alcohol **31** by NMR (see section 3.5) and was obtained in 76% yield overall yield after flash chromatography. In addition, we felt it was possible for the hydroxyl moiety of 5-amino-1-pentanol to displace the pentachlorophenol ester **29** yielding the unwanted amine side-product. However, TLC analysis did not reveal a ninhydrin positive and UV active

compound. Alcohol 32 was obtained in 72% overall yield with no apparent amine formation.

Scheme 10

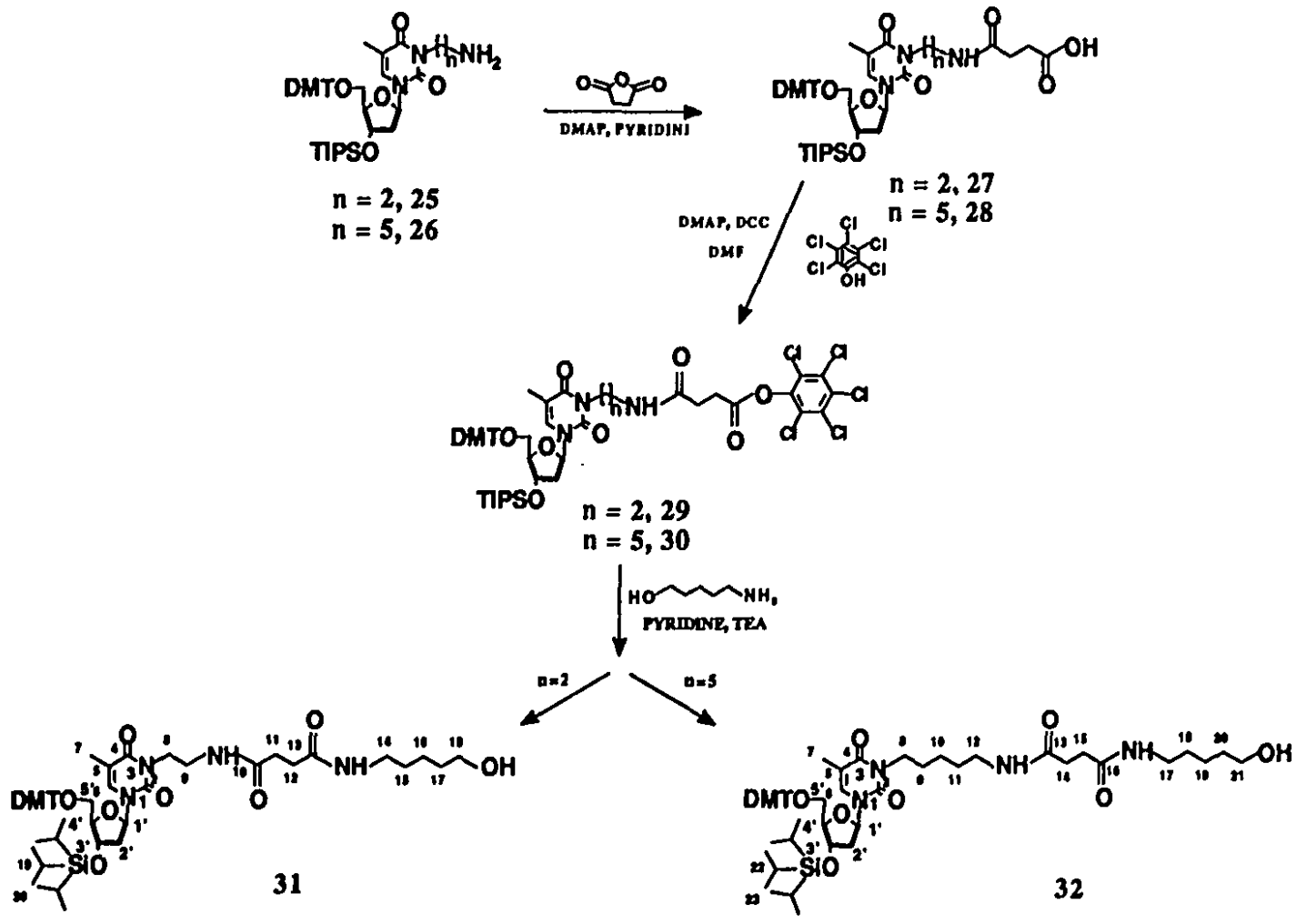
DMTO
TIPSO
n = 2, 25
n = 5, 26
DMAP, PYRIDINE
n = 2, 27
n = 5, 28
DMAP, DCC
DMF
n = 2, 29
n = 5, 30
PYRIDINE, TEA
n=2
n=5
31
32

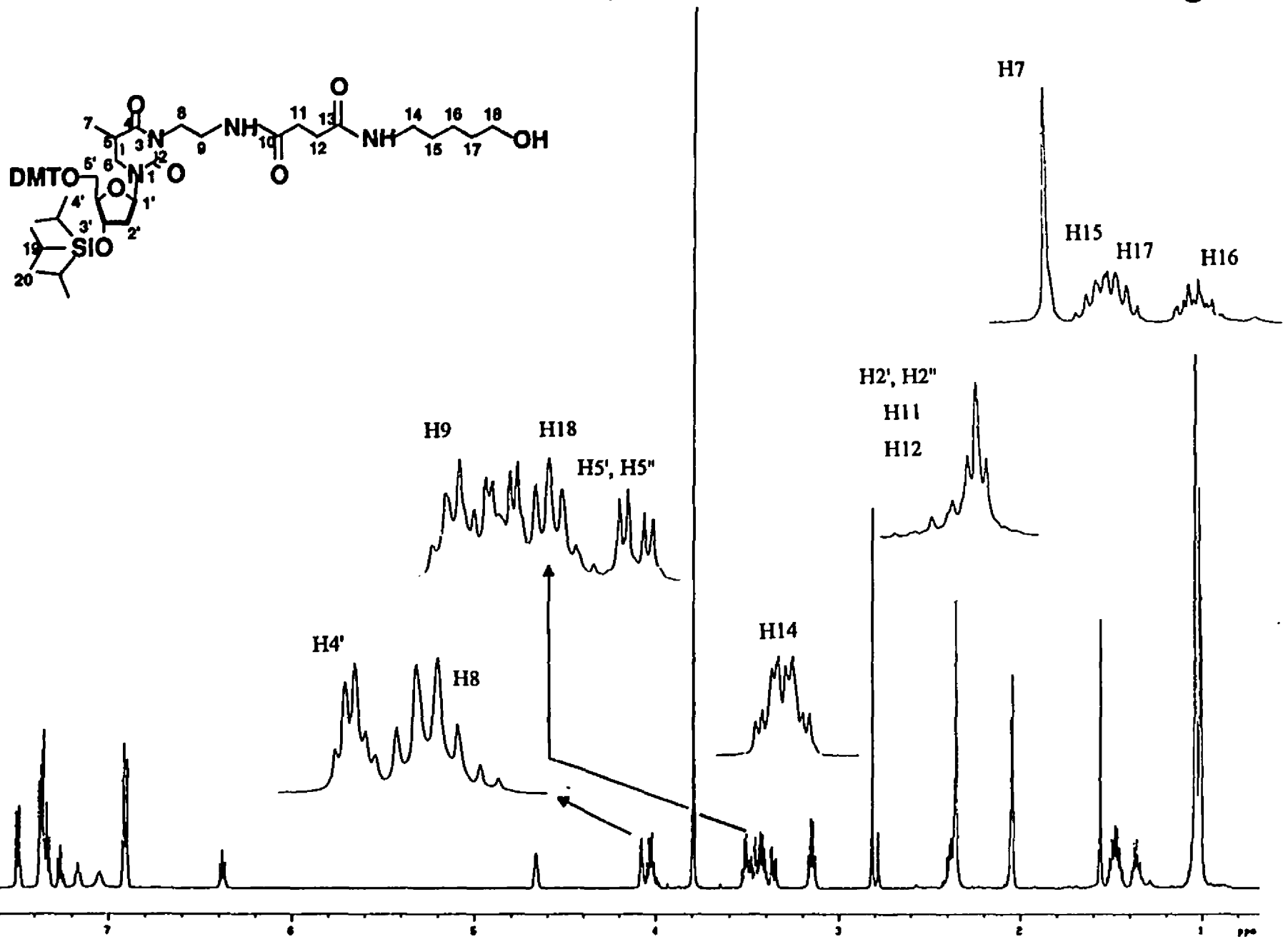

Figure 3.2 The 500 MHz ^{1}H-NMR spectrum of alcohol **31** in acetone-d_6

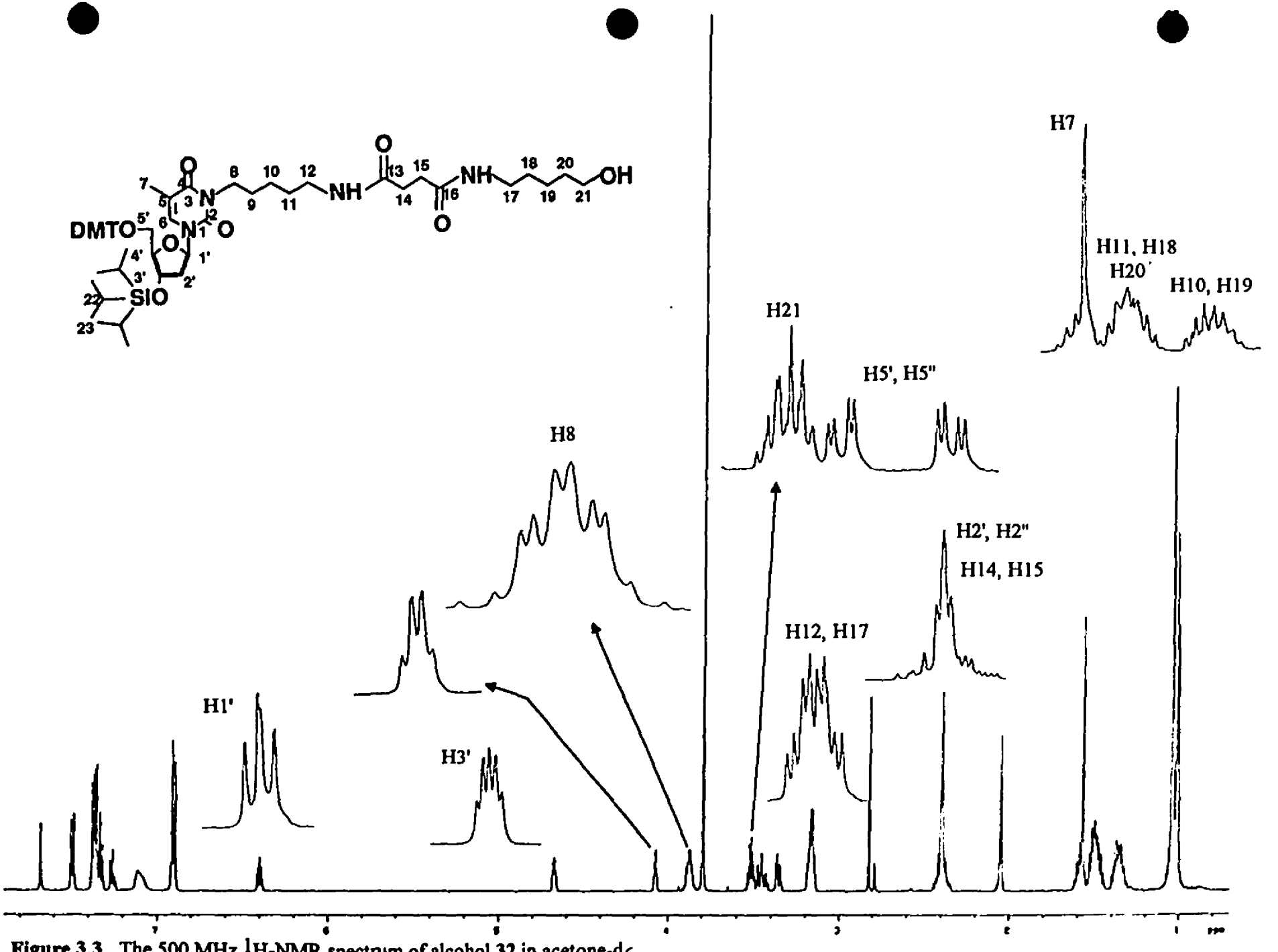

Figure 3.3 The 500 MHz ^{1}H-NMR spectrum of alcohol **32** in acetone-d_6

3.4 Synthesis of Levulinic Esters 33 and 34

Treatment of primary alcohols 31 and 32 with freshly prepared levulinic anhydride in anhydrous pyridine provided levulinates 33 and 34 in >80% yield after flash chromatography. To our satisfaction, treatment of levulinates 33 and 34 with 10 equivalents of hydrazine in pyridine:acetic acid buffer (4:1, v/v) successfully and efficiently removed the levulinyl protecting group in less than 5 min, thereby fullfilling our synthetic goal.

Scheme 11

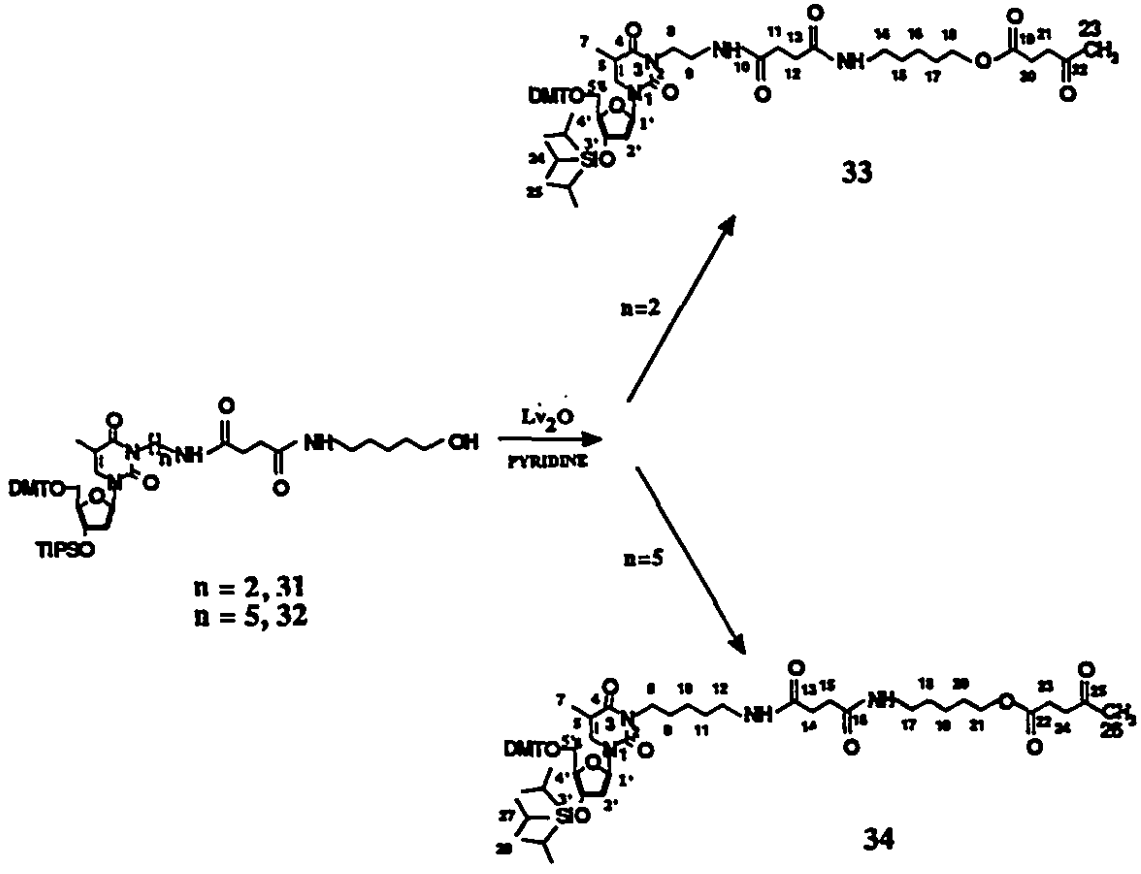

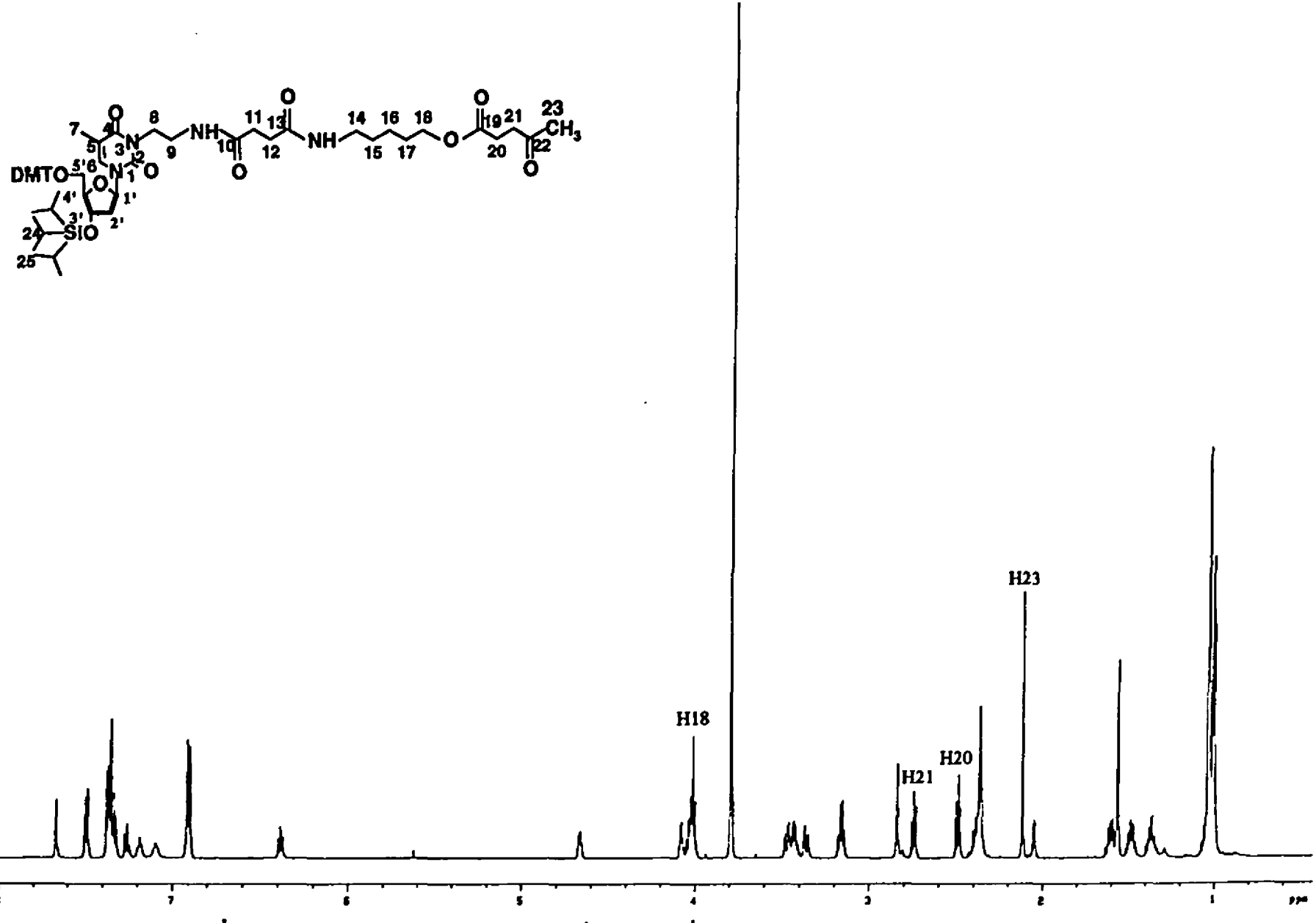

Figure 3.4 The 500 MHz ^{1}H-NMR spectrum of levulinic ester 33 in acetone-d_6

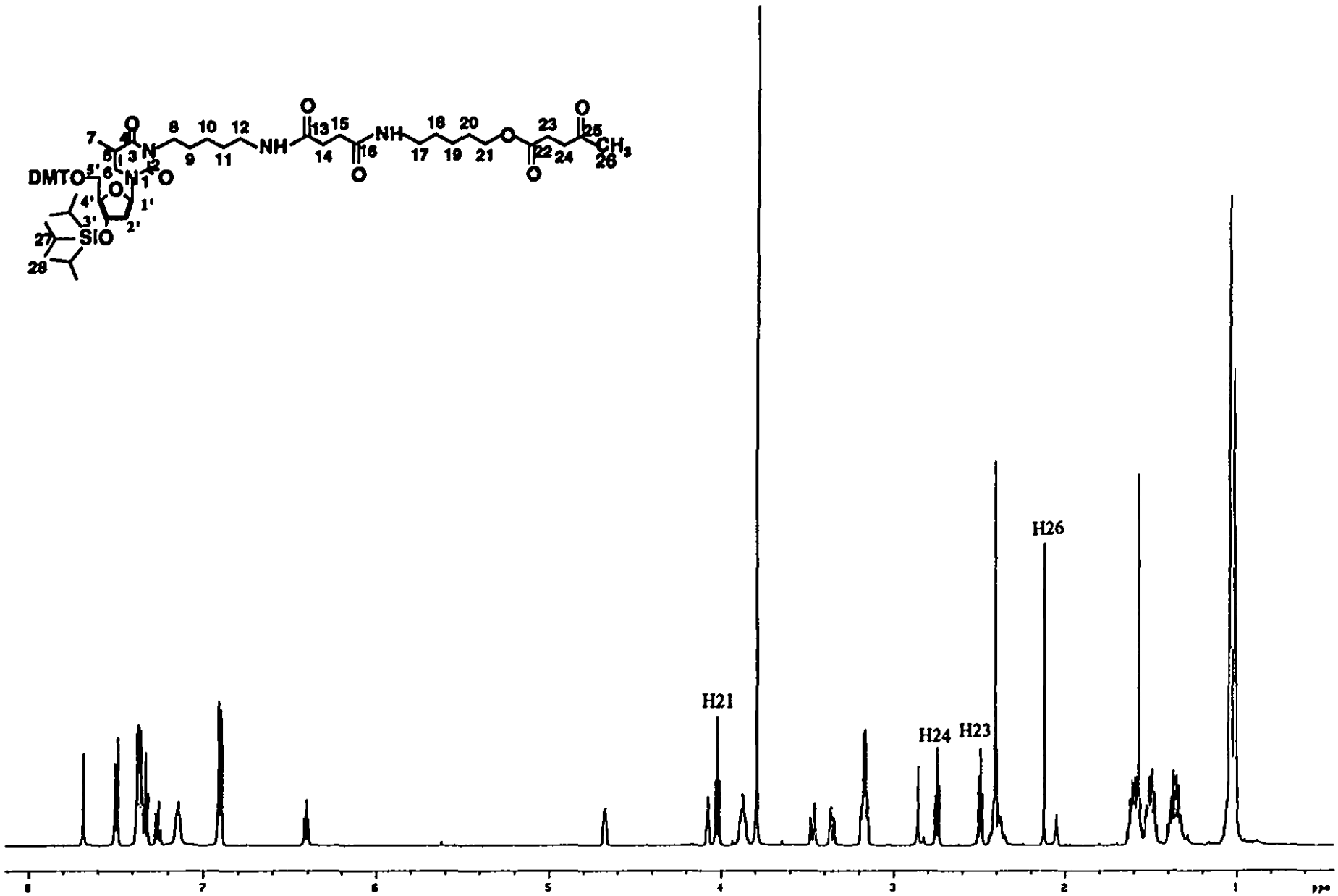

Figure 3.5 The 500 MHz ^{1}H-NMR spectrum of levulinic ester **34** in acetone-d_6

3.5 NMR and FAB Mass Spectrometry Characterization

The structures of **31, 32, 33,** and **34** were assigned on the basis of mass spectrometry and both one and two dimensional NMR analysis. Detailed ^{1}H-NMR and ^{13}C-NMR assignments of all newly synthesized compounds are summarized in Tables 3, 4, and 5. As representative examples, we show the complete NMR assignments of alcohols **31** and **32**. Supplementary spectra appear in appendix I.

The FAB mass spectra of **31** and **32** in a nitrobenzyl alcohol matrix doped with NaCl showed molecular ion peaks at m/z 951 and 993 corresponding, respectively, to the sodium molecular ion peaks of each alcohol (spectra not shown). In addition, the peaks at m/z 355 and 397 correspond to the functionalized base moiety plus two hydrogen atoms which are transferred from the sugar moiety.[107] Assignments of other peaks are given in the experimental section.

Although the ^{1}H-NMR spectra of **31** and **32** (figures 3.2 and 3.3) showed the presence of the flexible linker moieties, unambiguous structural assignments for each peak was difficult due to extensive overlap. This is especially true for the congested linker methylene protons of both alcohols and the heavily congested region near δ 3.5 for alcohol **31** (see expansions, figure 3.2). A more detailed investigation was needed and a number of 2D-NMR experiments, including homonuclear correlated spectra (COSY), ^{1}H-detected heteronuclear multiple quantum coherence spectra (HMQC), and heteronuclear multiple bond connectivity spectra (HMBC) were performed to unambigously assign the structures (figures 3.6-3.9). To give an example, in the HMQC spectrum of **31** (figure 3.7), the ^{13}C peaks at 30.23 and 33.37 ppm were identified as methylene C15 and C17, respectively. Similarly, in the HMQC spectrum of **32** (figure 3.9) the C13 peak at 33.195 ppm was identified as methylene C20.

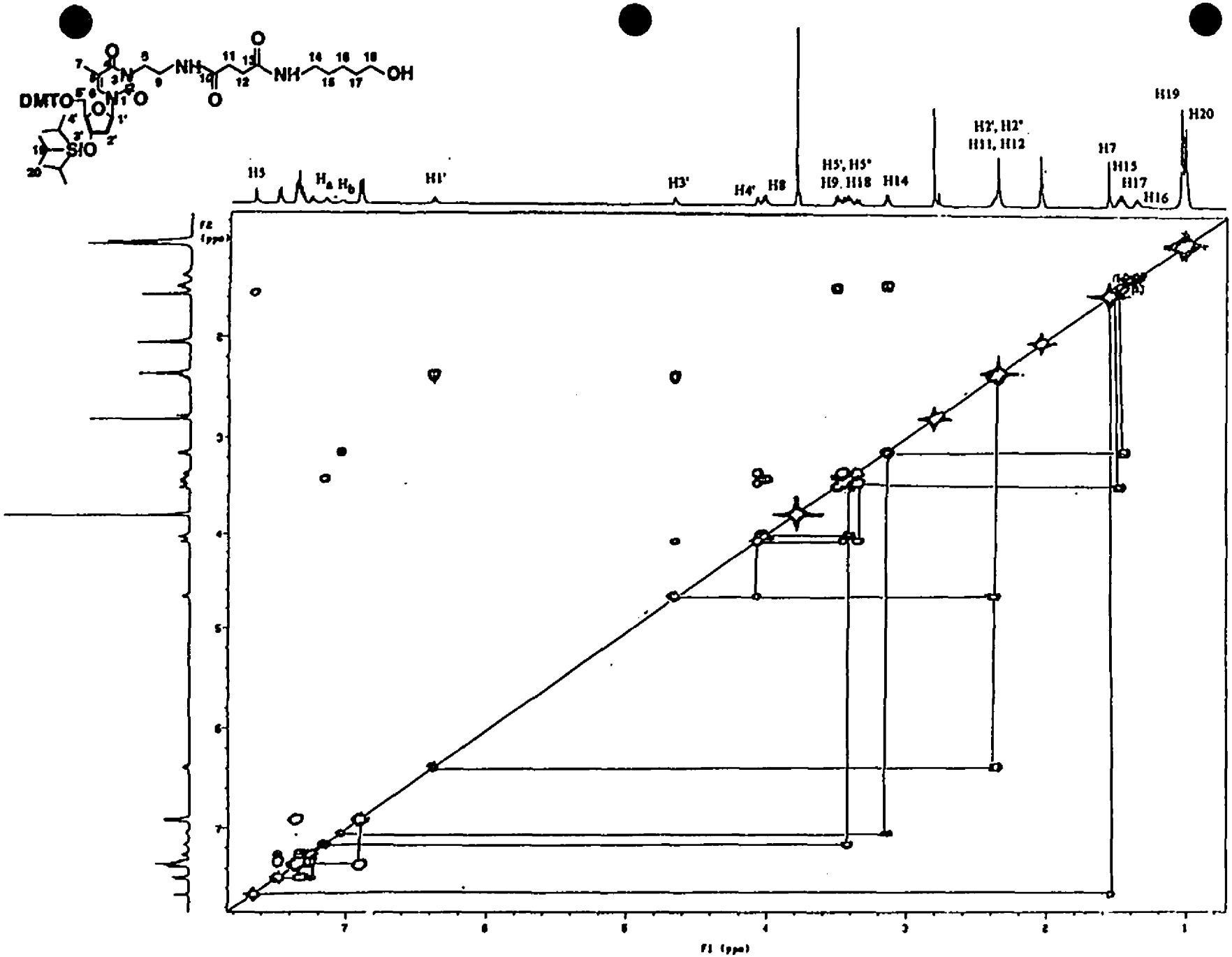

Figure 3.6 The 500 MHz COSY spectrum of alcohol **31** in acetone-d_6

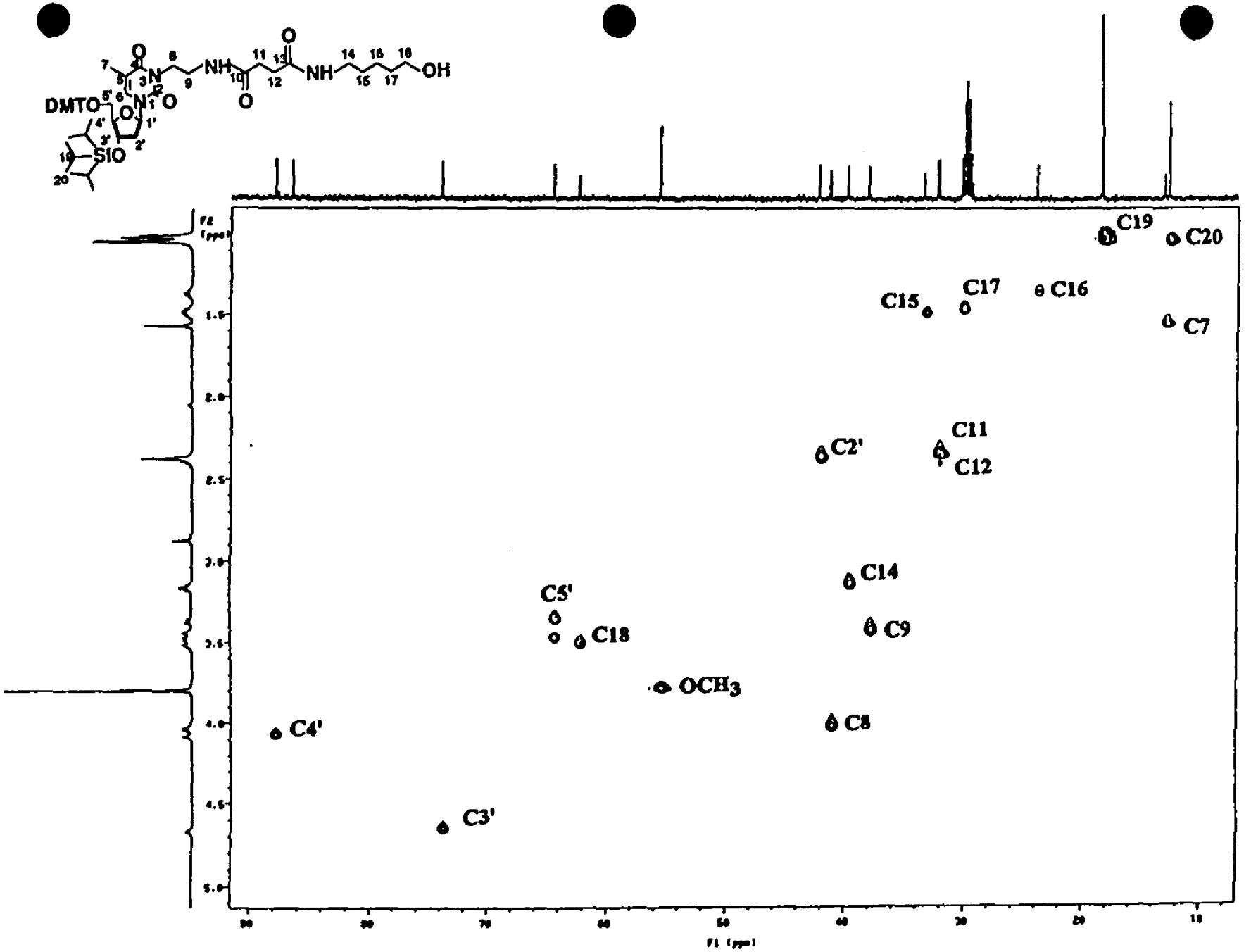

Figure 3.7 The 500 MHz HMQC spectrum of alcohol **31** in acetone-d_6

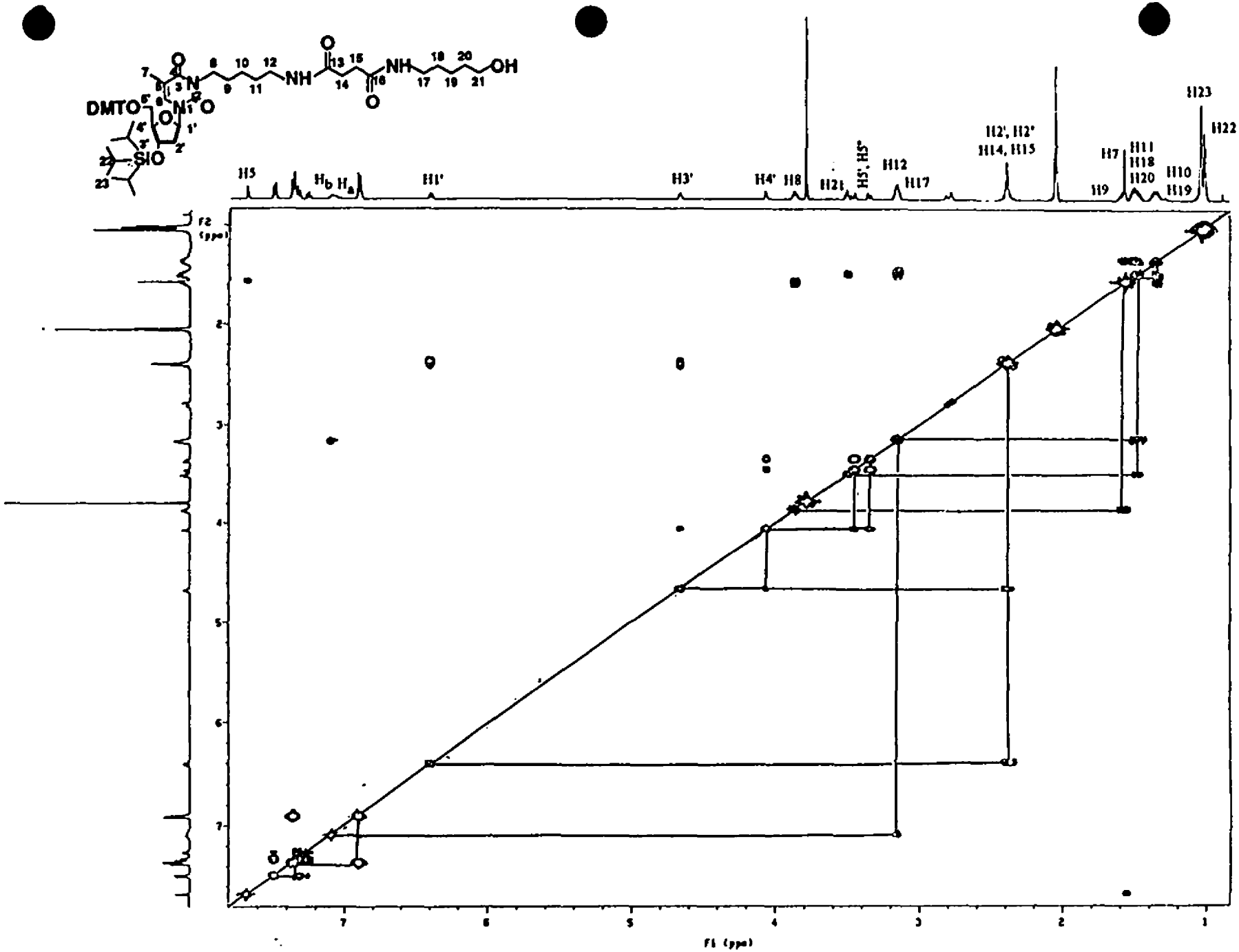

Figure 3.8 The 500 MHz COSY spectrum of alcohol **32** in acetone-d_6

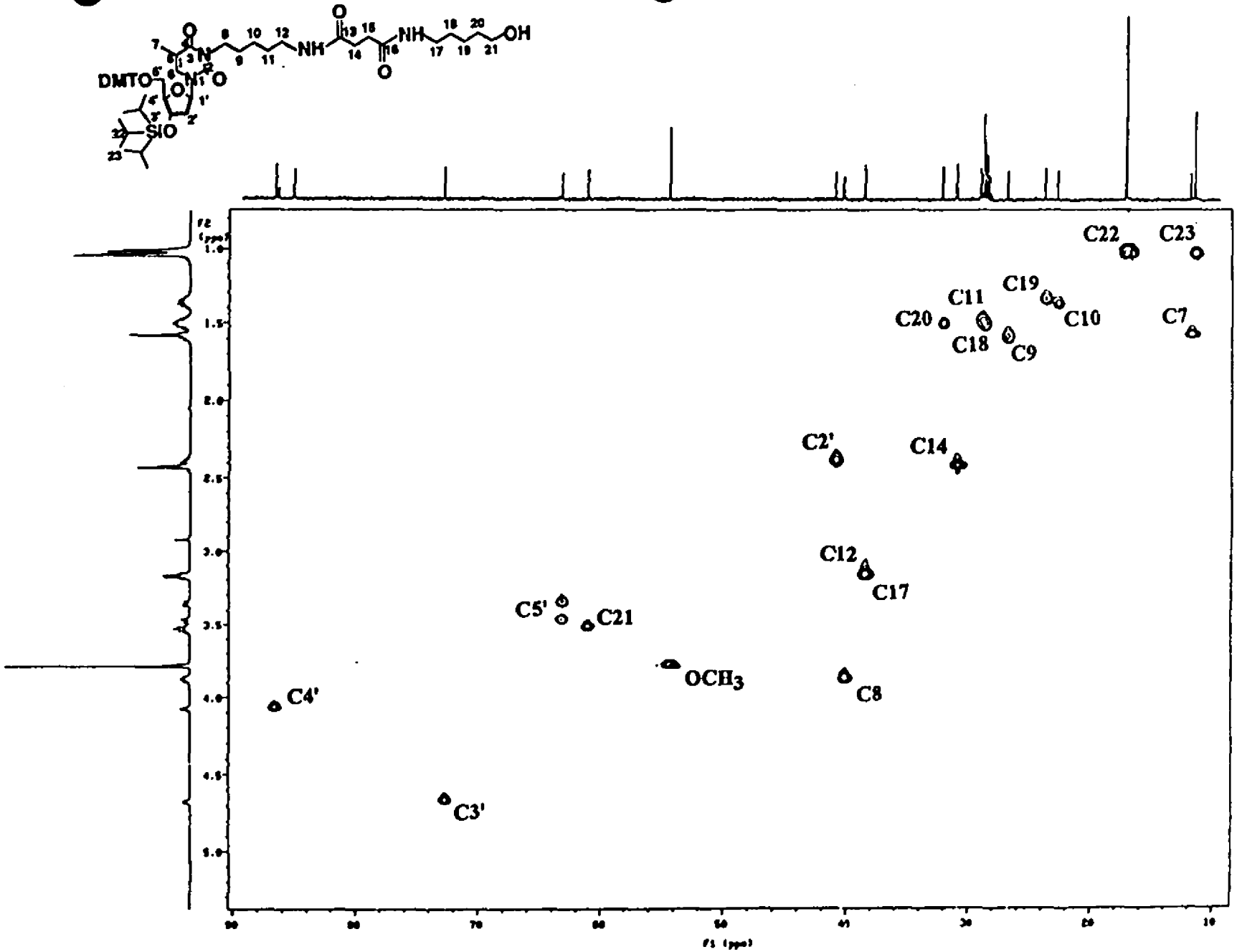

Figure 3.9 The 500 MHz HMQC spectrum of alcohol **32** in acetone-d_6

TABLE 3 ^{1}H-NMR (500 MHz) Spectral Data for Nucleosides **21, 25, 31, 33, 35,** and **39** in acetone-d_6

COMPOUND	H1'	H2'	H3'	H4'	H5'
21	6.126 (t, 1H) J(H1',H2'AB) = 6.35	2.05-2.28 (m,2H)[a]	4.558 (m, 1H)	4.030 (M, 1H)[a] J(H4',H5'A) = 2.93 J(H4',H5'B) = 3.42	3.38 (ddd, 2H) J(H5'A,H5'B) = 10.75
25	6.397 (t, 1H)	2.34-2.48 (m, 2H)[a]	4.668 (m, 1H)	4.028 (m, 1H) J(H4', H5'A) = 2.93	3.467 (A of ABX, dd, 1H) 3.37 (B of ABX, 1H)[a]
31	6.389 (dd, 1H) J(H1',H2'AB) = 6.10,7.57	2.34-2.42 (m, 1H)	4.664 (m, 1H) J(H3', H4') = 6.59	4.082 (qt, 1H) J(H4', H5'B) = 3.91	3.50 (A of ABX, 1H)[a] 3.36 (B of ABX, 1H) J(H5'A, H5'B) = 10.75
33	6.384 (dd, 1H) J(H1',H2'AB) = 6.10, 7.57	2.325-2.420 (m, 2H)[a]	4.663 (m, 1H) J(H3', H4') = 6.35	4.084 (qt, 1H) J(H4', H5'A) = 3.17 J(H4', H5'B) = 3.91	3.47 (A of ABX, 1H) J (H5'A, H5'B) = 10.75
35	6.371 (t, 1H)	2.32-2.40 (m, 2H)[a]	4.586 (m, 1H)	4.062 (m, 1H)[a]	3.384[a]
39	6.366 (t, 1H)	2.32-2.42 (m, 2H)[a]	4.578 (m, 1H)	4.083 (m, 1H)[a]	3.404[a]

[a] obscured by overlapping with other signals

TABLE 3 (cont'd)

OCH_3	TIPS	H6	H7	H8	H9
3.795 (s, 3H)	1.014-1.043 (m, 21H)	7.628 (s, 1H)	1.445 (d, 3H) ^3J(H6, H7) = 1.5	3.965 (AB, m, 2H)	4.219 (AB, m 2H)
3.795 (s, 3H)	1.014-1.043 (m, 21H)	7.675 (s, H)	1.572 (d, 3H) ^3J(H6, H7) = 1.0	4.069 (AB, m, 2H)[a]	3.365 (AB, m, 2H)
3.793 (s, 3H)	1.014-1.043 (m, 21H)	7.50 (s, 1H)	1.57 (d, 3H) ^3J(H6, H7) = 1.0	4.03 (AB, m, 2H) J(H8, H9) = 5.86, 7.20 J(H8A, H8B) = 12.94	3.15 (AB, m, 2H)[a]
3.798 (s, 3H)	1.015-1.043 (m, 21H)	7.502 (s, 1H)	1.566 (d, 3H) ^3J(H6, H7) = 1.0	4.022 (AB, m, 2H)[a]	3.433 (AB, m, 2H)[a]
3.795 (s, 3H)	-------	7.50 (s, 1H)	1.496 (d, 3H) ^3J(H6, H7) = 1.0	4.017 (AB, m, 2H)[a]	3.429 (AB, m, 2H)
3.783 (s, 3H)	-------	7.496 (s, 1H)	1.535 (d, 3H) ^3J(H6, H7) = 1.0	4.028 (AB, m, 2H)[a]	3.425 (AB, m, 2H)[a]

[a] obscured by overlapping with other signals

TABLE 3 (cont'd)

H11	H12	H14	H15	H16	H17
	2.374 (ABCD, m, 4H)[a]	3.158 (aq, 2H)	1.493 (m, 2H)[a]	1.367 (m, 2H)	1.487 (m, 2H)[a]
	2.366 (ABCD, m, 4H)[a]	3.161 (aq, 2H)	1.486 (m, 2H)[a]	1.366 (m, 2H)	1.606 (m, 2H)[a]
	2.373 (ABCD, m, 4H)[a]	3.162 (aq, 2H)	1.489 (m, 2H)[a]	1.365 (m, 2H)	1.604 (m, 2H)[a]
	2.382 (ABCD, m, 4H)[a]	3.140 (aq, 2H)	1.490 (m, 2H)[a]	1.365 (m, 2H)	1.485 (m, 2H)[a]

[a] obscured by overlapping with other signals

TABLE 3 (cont'd)

H18	H20	H21	H23	H24
3.436 (m, 2H)				
4.015 (m, 2H)[a]	2.49 (t, 2H)	2.121 (s, 3H)		
4.023 (m, 2H)[a]	2.493 (t, 2H)	2.747 (t, 2H)		
3.488 (m, 2H)[a]				

[a] obscured by overlapping with other signals

TABLE 4 ^{1}H-NMR (500 MHz) Spectral Data for Nucleosides **22, 26, 32, 34, 36,**and **40** in acetone-d_6

COMPOUND	H1'	H2'	H3'	H4'	H5'
22	6.408 (dd, 1H) J(H1', H2'AB) = 6.50, 7.92	2.34-2.45 (m,2H) J(H2', H3') = 6.28, 3.67 J(H2'A, H2'B) = 13.00	4.672 (m, 1H)	4.072 (m, 1H) J(H4', H5'A) = 2.93 J(H4', H5'B) = 3.42	3.466 (A of ABX) 3.356 (B of ABX) J(H5'A, H5'B) = 10.75
26	6.415 (dd, 1H) J(H1', H2'AB) = 6.23, 7.69	2.348-2.449 (m,2H) J(H2', H3') = 5.86, 3.17 J(H2'A, H2'B) = 13.31	4.672 (m, 1H)	4.074 (m, 1H) J(H4', H5'A) = 2.93 J(H4', H5'B) = 3.42	3.454 (A of ABX) 3.346 (B of ABX) J(H5'A, H5'B) = 10.94
32	6.410 (dd, 1H) J(H1', H2'AB) = 7.57, 5.86	2.35-2.45[a]	4.672 (q^5, 1H)	4.076 (q, 1H) J(H4', H5'A) = 2.93 J(H4', H5'B) = 3.42	3.474 (A of ABX, 1H) 3.356 (B of ABX, 1H) J(H5'A, H5'B) = 10.75
34	6.408 (dd, 1H) J(H1', H2'AB) = 7.72 6.24	2.34-2.44[a]	4.673 (q^5, 1H)	4.075 (q, 1H) J(H4', H5'A) = 3.17 J(H4', H5'B) = 2.93	3.467 (A of ABX, 1H) 3.355 (B of ABX, 1H) J(H5'A, H5'B) = 10.75
36	6.404 (t, 1H)	2.34-2.44[a]	4.593 (m, 1H)	4.073 (q, 1H)	3.372 (d, 2H)
40	6.409 (t, 1H)	2.35-2.50[a]	4.598 (m, 1H)	4.119 (m, 1H) J(H4', H5'A) = 3.92 J(H4', H5'B) = 2.93	3.396 (A of ABX, 1H) 3.341 (B of ABX, 1H) J(H5'A, H5'B) = 10.25

[a] obscured by overlapping with other signals

TABLE 4 (cont'd)

OCH_3	TIPS	H6	H7	H8	H9
3.795 (s, 3H)	1.046-1.106 (m, 21H)	7.467 (d, 1H)	1.572 (d, 1H) ^{3}J(H6, H7) = 1.0	3.887 (AB, m, 2H) J(H8'A, H9XY) = 7.30, 6.75 J(H8'B, H9XY) = 6.92, 6.78 J(H8A, H8B) = 12.83	1.621[a]
3.790 (s, 3H)	1.040-1.108 (m, 21H)	7.669 (d, 1H)	1.559 (d, 1H) ^{3}J(H6, H7) = 1.0	3.890 (AB, m, 2H)	1.627[a]
3.795 (s, 3H)	1.008-1.044 (m, 21H)	7.680 (s, 1H)	1.572 (d, 1H) ^{3}J(H6, H7) = 1.0	3.749 (AB, m, 2H) J(H8'A, H9XY) = 7.93, 7.10 J(H8'B, H9XY) = 7.08, 7.45 J(H8A, H8B) = 13.06	1.589[a]
3.796 (s, 3H)	1.008-1.031 (m, 21H)	7.676 (s, 1H)	1.572 (d, 1H) ^{3}J(H6, H7) = 1.0	3.873 (AB, m, 2H) J(H8'A, H9XY) = 7.93, 7.10 J(H8'B, H9XY) = 7.08, 7.45 J(H8A, H8B) = 13.06	1.602[a]
3.790 (s, 3H)	----------	7.643 (s, 1H)	1.493 (s, 1H)	3.870 (AB, m, 2H)	1.602[a]
3.784 (s, 3H)	----------	7.653 (s, 1H)	1.570 (d, 1H)	3.883 (AB, t, 2H)	1.597[a]

[a] obscured by overlapping with other signals

TABLE 4 (cont'd)

H10	H11	H12	H14	H15	H17
1.390 (m, 2H)	1.605[a]	3.236 (t, 2H)			
1.382 (m, 2H)	1.596[a]	3.193 (t, 2H)			
1.377[a]	1.503[a]	3.172 (q, 2H)		2.424 (ABCD, m, 4H)[a]	3.172 (q, 2H)
1.354[a]	1.498[a]	3.170 (q, 2H)		2.408 (ABCD, m, 4H)[a]	3.172 (q, 2H)
1.354[a]	1.498[a]	3.163 (q, 2H)		2.410 (ABCD, m, 4H)[a]	3.165 (q, 2H)
1.350[a]	1.504[a]	3.145 (q, 2H)		2.470 (ABCD, m, 4H)[a]	3.145 (q, 2H)

[a] obscured by overlapping with other signals

TABLE 4 (cont'd)

H18	H19	H20	H21	H23	H24	H26
1.503[a]	1.359[a]	1.503[a]	3.527 (m, 2H)			
1.515[a]	1.374[a]	1.595[a]	4.202 (t, 2H)	2.494 (t, 2H)	2.747 (t, 2H)	2.124 (s, 3H)
1.515[a]	1.374[a]	1.595[a]	4.021 (t, 2H)	2.494 (t, 2H)	2.748 (t, 2H)	2.122 (s, 3H)
1.504[a]	1.375[a]	1.504[a]	3.492(t, 2H)			

[a] obscured by overlapping with other signals

TABLE 5 ^{13}C-NMR Spectral Data for Nucleosides **21, 22, 25, 26, 31, 32, 33, 34, 39,**and **40** in acetone-d_6

COMPOUND	C1'	C2'	C3'	C4'	C5'	TIPS	OCH_3	C2	C4	C5	C6	C7	C8	C9	C10	C11
21	86.58	42.14	73.82	87.87	64.22	18.31 12.66	55.51	151.68	163.83	134.81	109.99	12.96	40.19	36.51	168.76	168.76
25	86.38	42.17	73.90	87.76	64.36	18.31 12.69	55.51	151.52	163.65	134.81	110.15	12.99	42.08	48.90		
31	86.35	42.16	73.87	87.54	64.38	18.32 12.71	55.53	151.80	164.02	134.74	110.16	13.06	41.22	38.00	172.75	32.28
33	86.34	42.16	73.88	87.54	64.39	18.31 12.70	55.52	151.80	163.99	134.71	110.15	13.05	42.16	37.99	172.16	32.09
39	86.23	41.36	72.19	87.16	64.66	------	55.52	151.89	164.00	134.91	110.07	12.95	41.22	38.02	172.28	32.11
22	86.32	42.13	73.94	87.76	64.39	18.32 12.68	55.51	151.46	163.59	134.28	110.12	12.98	41.21	28.88	24.88	27.90
26	86.28	42.10	73.92	87.72	64.37	18.32 12.69	55.50	151.46	163.63	134.63	110.15	12.74	41.54	28.13	25.46	31.13
32	86.12	41.95	73.77	87.60	64.21	18.16 12.53	55.35	151.30	163.49	134.52	110.00	12.87	41.26	27.86	23.75	30.10
34	86.10	42.10	73.78	87.59	64.22	18.13 12.52	55.34	151.30	163.45	134.50	109.99	12.84	41.41	28.02	23.87	30.00
40	86.19	41.36	72.28	87.34	64.74	------	55.50	151.59	163.67	134.89	110.07	12.90	41.33	28.02	24.00	30.00

TABLE 5 (cont'd)

COMPOUND	C12	C13	C14	C15	C16	C17	C18	C19	C20	C21	C22	C23	C24	C25	C26	C27
21																
25																
31	32.12	172.21	39.75	33.37	23.92	30.27	62.28									
33	32.26	172.22	39.52	29.98	23.88	29.04	64.70	172.64	28.50	38.22	206.08	29.63				
39	32.26	172.70	39.55	29.88	23.85	29.04	64.73	173.07	28.52	38.23	206.10	29.34				
22	38.24	168.75	168.75													
26	51.34															
32	39.58	172.23	32.05	32.01	172.18	39.53	30.07	24.77	33.20	62.11						
34	39.50	172.07	32.18	32.21	172.25	39.65	29.98	24.93	29.04	64.52	173.18	28.51	38.22	206.41	29.33	
40	39.53	172.30	32.36	32.39	172.42	39.66	29.95	24.90	29.04	64.76	173.06	28.53	38.24	206.52	29.34	

3.6 Synthesis of Phosphoramidites 37 and 38

The next step was the deprotection of the triisopropylsilyl protecting group, which was accomplished in near quantitative yield by treatment with tetra-*n*-butylammonium fluoride in THF. Treatment of alcohols **35** and **36** with N,N'-diisopropyl(β-cyanoethyl)phosphonamidic chloride in THF containing diisopropylethylamine and a catalytic amount of DMAP afforded the phosphoramidites **37** and **38** in >70% yield. ^{31}P-NMR analysis indicated the presence of two diastereomers for each amidite, and their chemical shifts were consistent with their structures.

Scheme 12

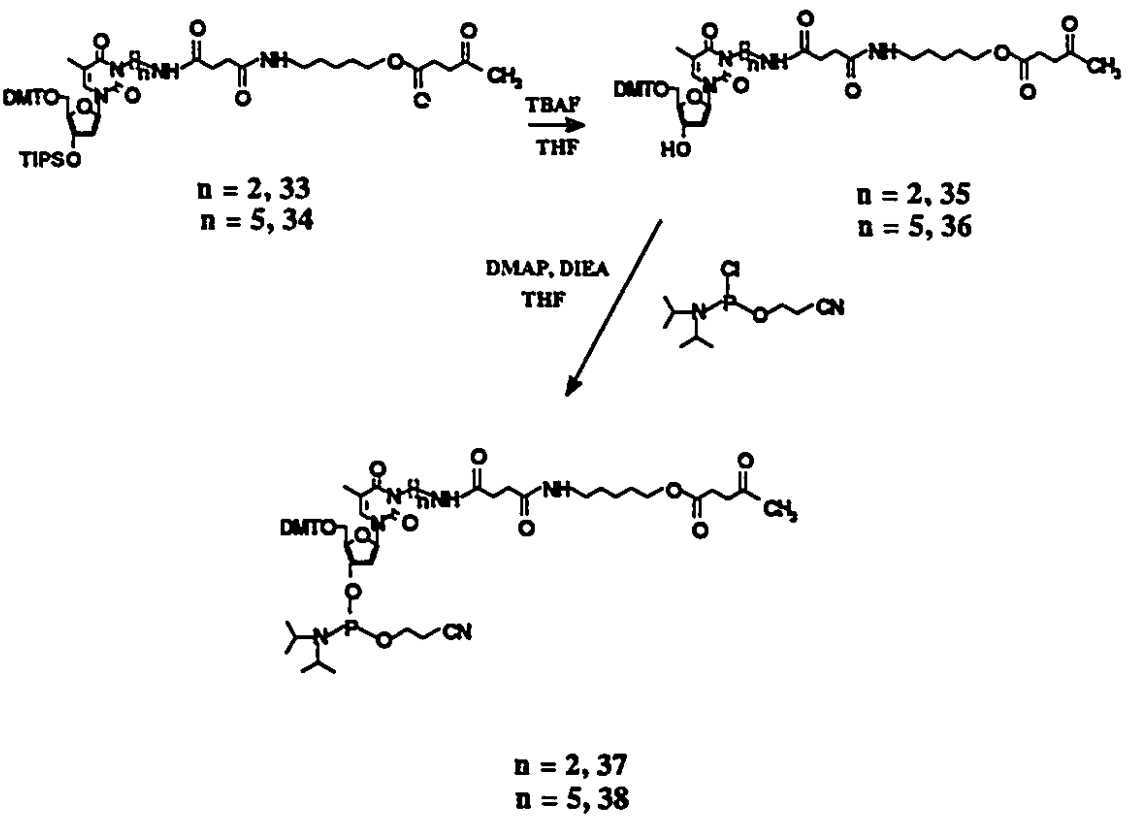

n = 2, 33
n = 5, 34

n = 2, 35
n = 5, 36

n = 2, 37
n = 5, 38

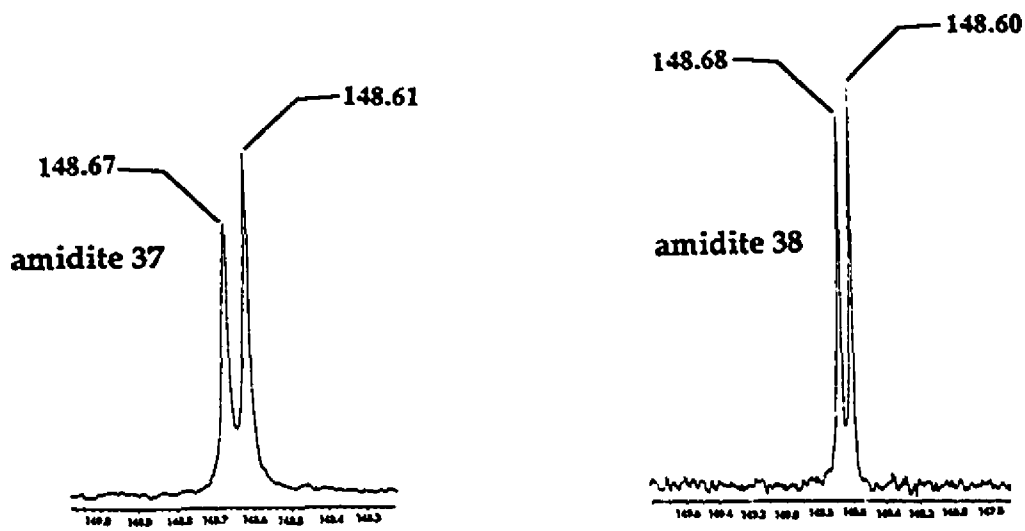

Figure 3.9 ^{31}PNMR of phosphoramidites 37 and 38 in acetone-d_6

3.7 Synthesis of Bisamidites 41 and 42

We also envisioned incorporating bis(phosphoramidite) synthons **41** and **42** in the automated solid phase synthesis of our branched oligonucleotides (see chapter 4). The preparation of **41** and **42** began with the desilylation of alcohols **31** and **32**, accomplished in quantitative yield by using tetra-*n*-butylammonium fluoride in THF. Treatment of diols **39** and **40** with 2.3 equivalents of N,N'-diisopropyl(β-cyanoethyl)phosphonamidic chloride in THF containing DMAP and 10 equivalents of diisopropylethylamine afforded bis(phosphoramidites) **41** and **42** in 52% and 70% yields, respectively. Eight resonance signals were expected in the ^{31}P-NMR spectra of **41** and **42**, corresponding to the four diastereomers formed for each amidite. However, only three signals were observed suggesting the coincidental overlap of signals or the formation of less than four isomers. Nonetheless, FAB mass spectrometry provided a fragmentation pattern which is consistent with our proposed structures.

Scheme 13

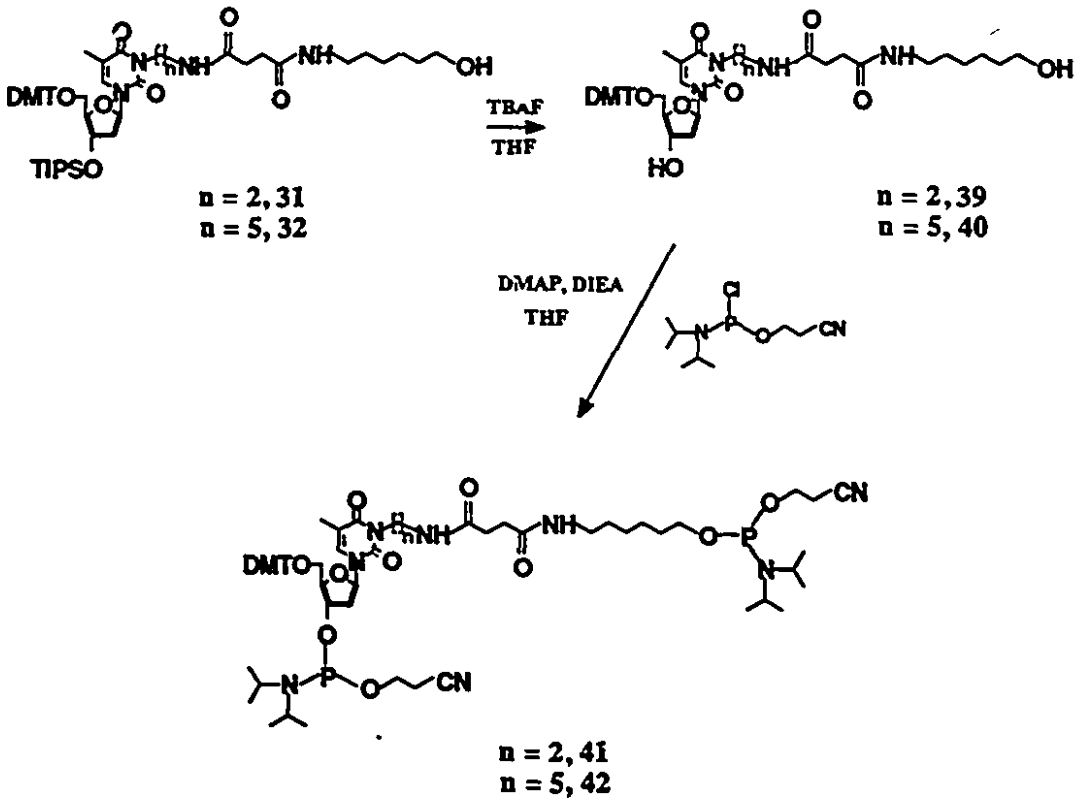

n = 2, 31
n = 5, 32

n = 2, 39
n = 5, 40

n = 2, 41
n = 5, 42

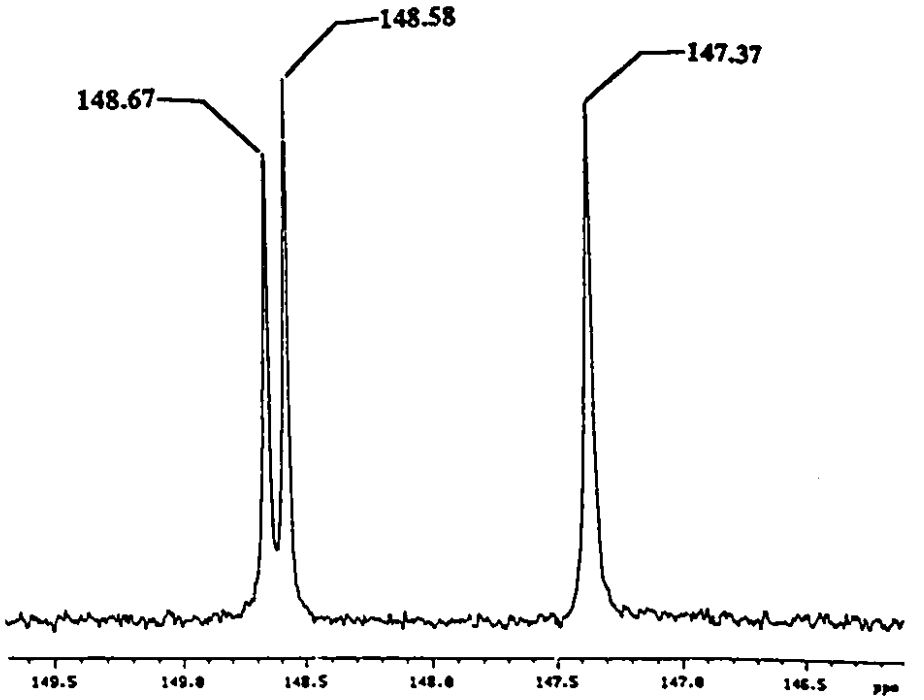

Figure 3.11 ^{31}P-NMR of bis(phosphoramidite) 42 in acetone-d_6

3.8 Synthesis of Phosphoramidite 46

Chemical synthesis of nucleic acids in the 5'- to 3'- direction rather than conventional 3'- to 5'- direction requires 5'-phosphoramidite-3'-dimethoxytrityl nucleoside monomers.[108] Scheme 14 shows the synthetic strategy used for preparing the amidite synthon **46** which will be incorporated into the assembly of our branched nucleic acids at the branching point (see section 4.1). The synthesis of **46** began with the selective protection of the 5'- hydroxy of thymidine as a *tert*-butyldimethylsilyl ether, prepared according to Ogilvie's methodology.[106] The 3'-hydroxy of crude **43** was then protected as a 4,4'- dimethoxytrityl ether using 4,4- dimethoxytrityl chloride and a catalytic amount of DMAP in anhydrous pyridine. Subsequent desilylation of crude **44** using tetra-*n*-butylammonium in THF afforded **45** in 76% overall yield after flash chromatography. Phosphitylation of pure **45** afforded the desired phosphoramidite **46** in 92% yield.

Scheme 14

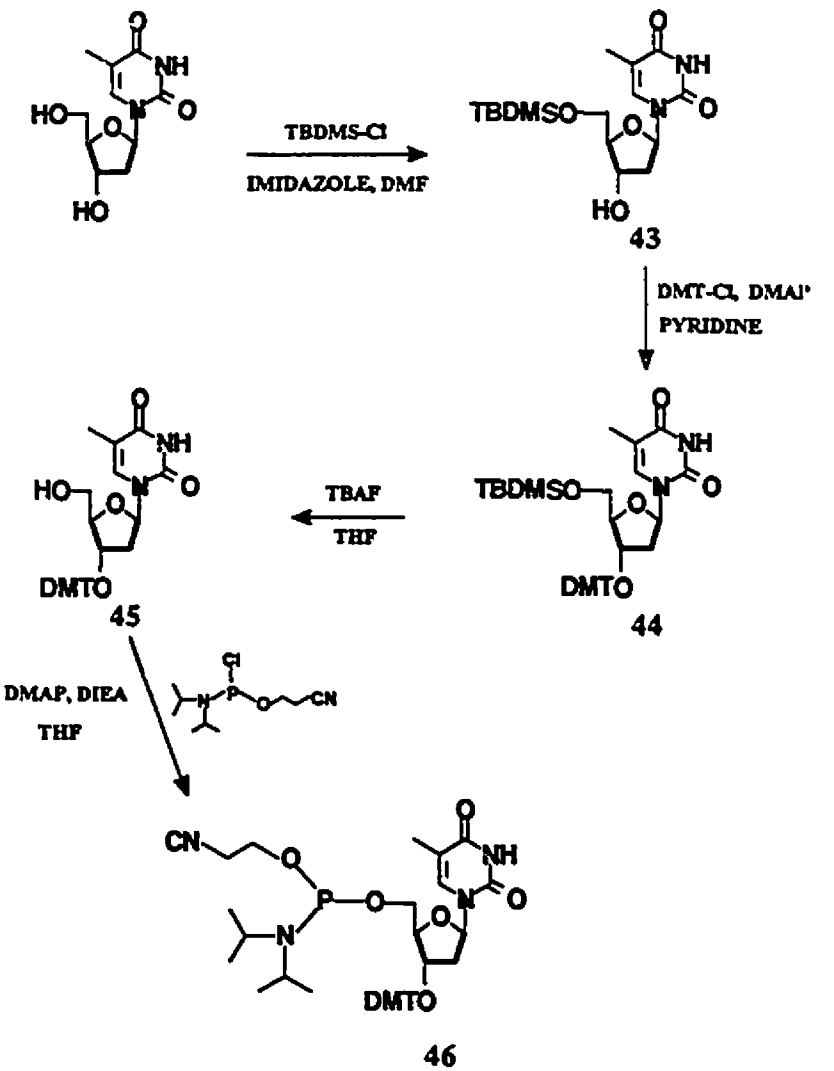
TBDMS-Cl
IMIDAZOLE, DMF
43
DMT-Cl, DMAP
PYRIDINE
TBAF
THF
44
45
DMAP, DIEA
THF
46

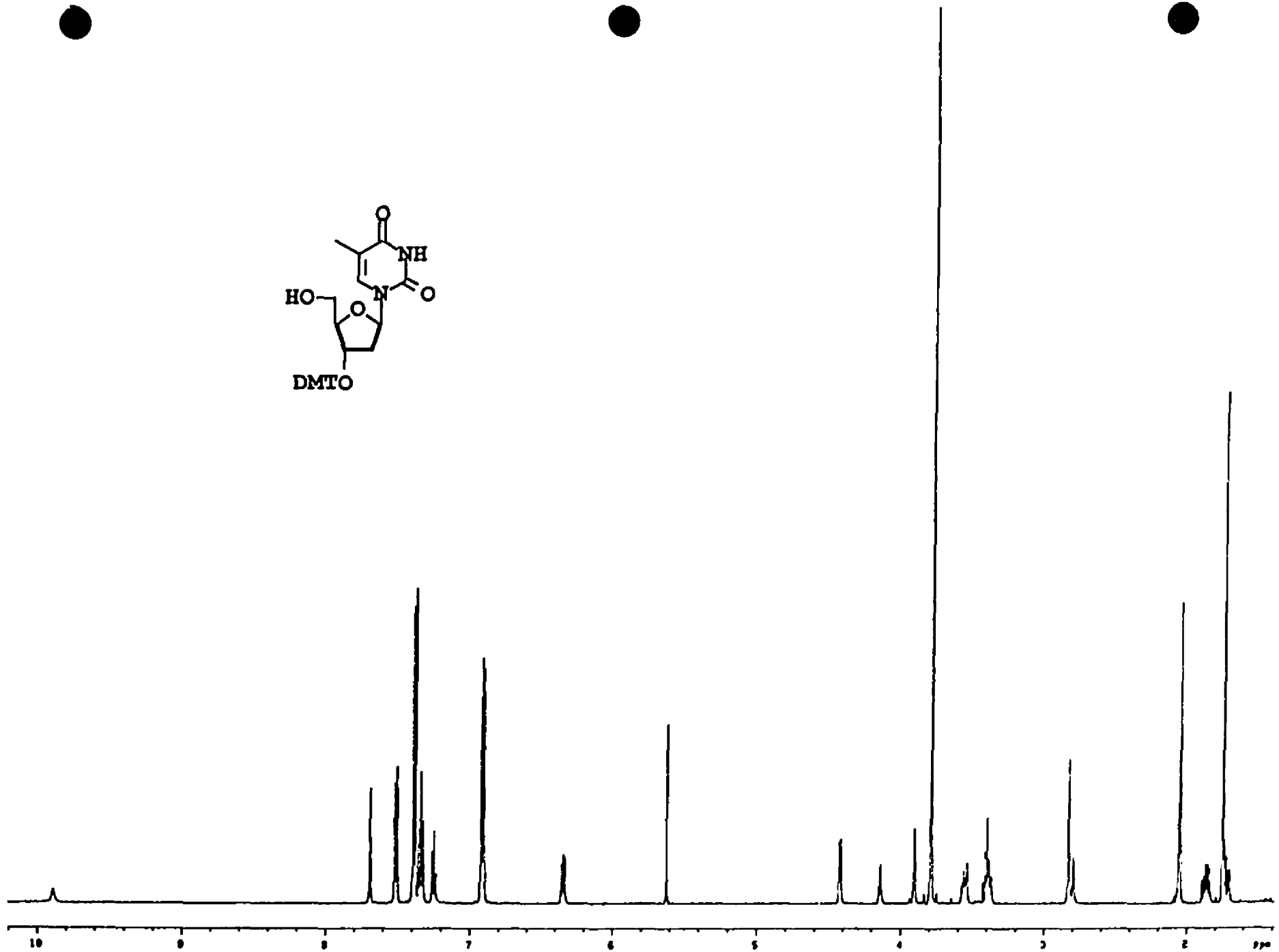

Figure 3.12 The 500 MHz ^{1}H-NMR spectrum of 45 in acetone-d_6

CHAPTER 4 SOLID-PHASE SYNTHESIS OF BRANCHED OLIGONUCLEOTIDES CONTAINING A FLEXIBLE LINKER.

4.1 Solid Phase Methodology for the Introduction of Branching Monomer 20

Damha's protocol[109] for the solid phase synthesis of branched oligomers containing vicinal (2'-5')- and (3'-5')- phosphodiester linkages was applied to the synthesis of our branched DNA molecules (scheme 15). Normal derivatization of long chain alkylamine control-pore-glass (LCAA-CPG) with 5'-DMT protected thymidine (5'-O-dimethoxytrityl-thymidine-3'-succinyl-LCAA-CPG)[110] is followed by the solid phase assembly of a thymidine decamer, T_{10}, on the solid support. During chain assembly the 5'-hydroxy of support-bound nucleotides that fail to undergo coupling are terminated or capped by acetylation. Acetylation of failure sequences is followed by the iodine/water oxidation of the newly formed 3'-5'- internucleotide phosphite linkages to the corresponding phosphotriesters. Cleavage of the dimethoxytrityl group at the 5' end with trichloroacetic acid provides T_{10} with a free 5'-hydroxyl group which is then reacted with an excess of branching monomer **20** employing standard tetrazole catalysis. Once the branching monomer has been introduced, synthesis of our "V"- and "Y"-shaped branched molecules is carried out by the following steps (scheme 15):

"V"-Shaped Oligomers I and II

i) Removal of the dimethoxytrityl group at the 5'-end of the oligonucleotide T^*T_{10} with trichloroacetic acid.

ii) acetic anhydride capping of the free 5'- hydroxy group

iii) removal of the N-levulinyl group employing Letsinger's hydrazine solution

iv) branch strand assembly in 3' → 5' (oligomer I) or 5' → 3' (oligomer II) directions employing thymidine 3' or 5' phosphoramidites, respectively.

"Y"-Shaped Oligomers III and IV

i) Removal of the dimethoxytrityl group at the 5'-end of the oligonucleotide T^*T_{10} with trichloroacetic acid.

ii) extension of thymidine decamer in the 3' → 5' direction to assemble a linear 21 unit long oligomer $[T_{10}(T_{linker})T_{10}]$.

iii) removal of the N-levulinyl group employing Letsinger's hydrazine solution.

iv) third (branch) strand assembly in the 3' → 5' (oligomer **III**) or 5' → 3' (oligomer **IV**) directions employing thymidine 3'- or 5'- phosphoramidites, respectively.

The newly synthesized branched DNA oligomers were deprotected, purified and handled according to procedures described by Damha and Ogilvie.[111]

Scheme 15

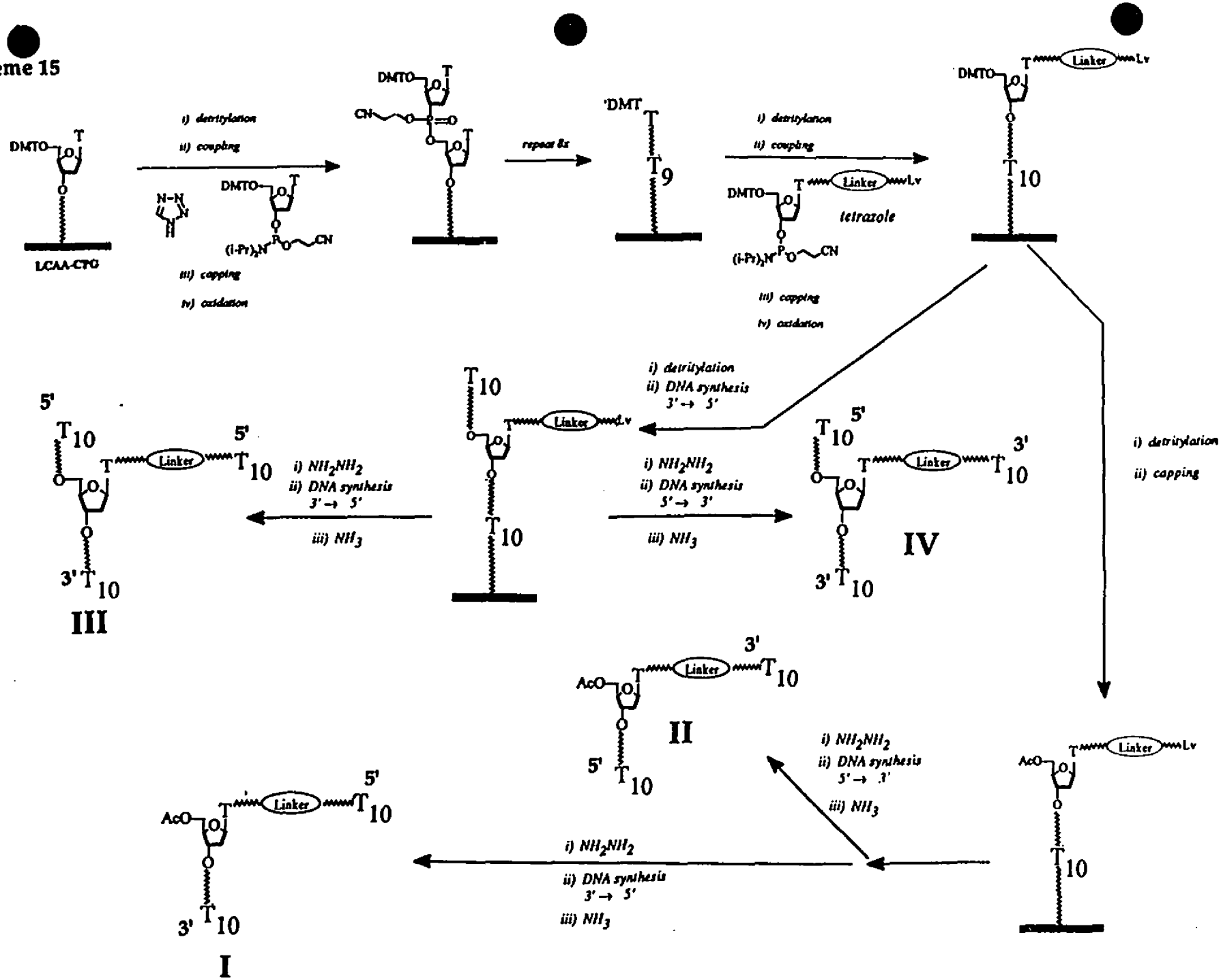
LCAA-CPG
i) detritylation
ii) coupling
iii) capping
iv) oxidation
repeat 8x
tetrazole
Linker
i) NH2NH2
ii) DNA synthesis
3'→ 5'
iii) NH3
5'→ 3'
I
II
III
IV

4.2 Synthesis of Branched Molecules Incorporating Branching Monomer 20.

The branching monomer **20** was used in the synthesis of "Y"-shaped, 31-mers **III** and **IV**, as described above. Both sequences were prepared on a .2 μmol scale. After assembly, the oligomers were cleaved from the solid support by standard treatment with 29% aqueous ammonia solution at room temperature for 24-48 hours. This step also removed the cyanoethyl phosphate protecting groups. Yields of the crude oligomers, as determined by UV quantification, were generally quite high ranging from 70 to 80 A_{260} units.

The oligomers were then analyzed and purified by polyacrylamide gel electrophoresis (PAGE), a method that separates oligonucleotide fragments according to their mass-to-charge ratio. On a 16 % polyacrylamide gel, the crude oligomers **III** and **IV** were actually a mixture of three distinct bands (lanes 3 and 4; figure 4.1). This band structure or "fingerprint" pattern is very similar to the one observed by Damha *et al.* in their synthesis of branched nucleic acids with an adenosine 2'-3'-bisphosphoramidite branch point.[109] The fast moving band (**c**) (with a similar electrophoretic mobility to an authentic linear 11-mer T_5AT_5 oligodeoxynucleotide) has been assigned to T_{10} and is present as a result of the incomplete coupling of the branching monomer. The middle band (**b**) with an electrophoretic mobility similar to an authentic linear 21-mer $T_{10}AT_{10}$ oligodeoxynucleotide, has been assigned to $T_{10}(T_{linker\text{-}NH2})T_{10}$ and may arise from incomplete deprotection of the N-levulinyl group (see section 2.3) at the branching point. Finally, it was speculated that the slower moving band (**a**) contained our desired branched oligomers **III** and **IV**. Relative to the linear 31-mer $T_{10}AT_{20}$ oligomer, branched oligomers **III** and **IV** exhibited similar but reduced electrophoretic mobilities. Such retarded mobility is characteristic of branched nucleic acids.[109]

Coupling yields, as determined by the release of the dimethoxytrityl cation, depicted a normal synthesis in the assembly of the 21-mer $T_{10}(T_{linker\text{-}NHLv})T_{10}$

oligonucleotide. At the branching point, Letsinger's hydrazine solution was applied for 10 min and 30 min, respectively, to remove the levulinyl group and allow the assembly of the third (branch) strand in the 3' → 5' direction (oligomer **III**) or the 5' → 3' direction (oligomer **IV**) Analysis of the electropherogram revealed nearly equal amounts of the by-product $T_{10}(T_{linker\text{-}NH2})T_{10}$ (*ca.* 10% of crude mixture **III** or **IV**, band (**b**)) suggesting similar efficiencies (~90%) in the removal of the levulinyl protecting group. However, the lower concentration of the T_{10} by-product in lane **3** (*ca.* 20% of crude mixture **III**, band (**c**)) suggests a greater coupling efficiency at this point for branching monomer **20** and as a consequence, a greater amount of branched oligomer **III** was obtained (*ca.* 70% of crude mixture **III**, band (**a**)).

For each synthetic case, a preparative denaturing PAGE gel was used to purify 25 A_{260} units of the crude mixture. The appropriate bands, viewed under UV shadowing, were excised with a razor blade and incubated in water at 37 °C to recover the oligonucleotides. Finally, these oligomers were desalted by reverse-phase chromatography (C18 SEP-PAK™ cartridges). Two to three A_{260} units of purified branched oligomers were obtained (*ca.* 10% yield). This was sufficient to carry out preliminary hybridization studies (next section).

To verify the purity of the oligomers, the branched molecules were subjected to high performance capillary gel electrophoresis (figure 4.2). It was apparent that our branched oligomers were contaminated with smaller failure sequences (N-1 or 30-mer, N-2 or 29-mer,...etc, where **N** represents the full 31-mer branched oligomer **III** or **IV**). This was somewhat surprising as the standard PAGE analysis indicated the presence of a single (slow moving) band. However, it is known that the resolving power of capillary gel electrophoresis surpasses the technique of PAGE for oligcnucleotide analysis.[112] In addition, it is also possible that degradation of our oligomers may have occurred when excising the bands obtained after preperative gel electrophoresis explaining the presence of

the smaller (failure) sequences. Nonetheless, we decided to provide some preliminary binding studies of our branched nucleic acids with complementary adenylic oligomers.

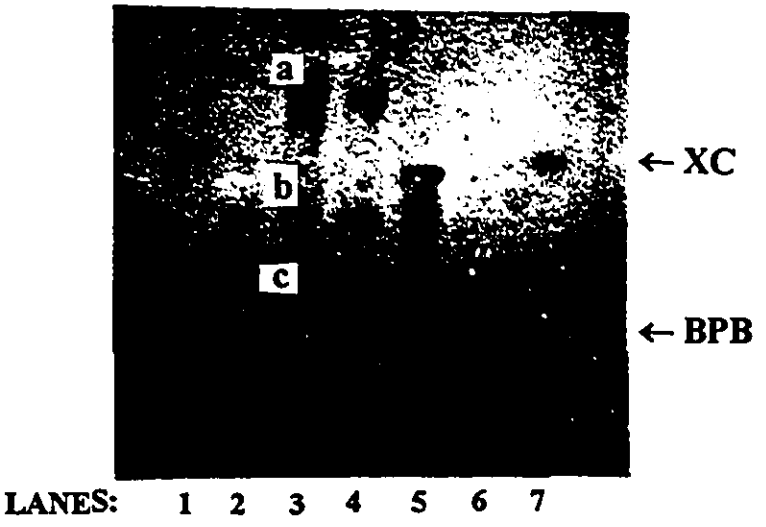

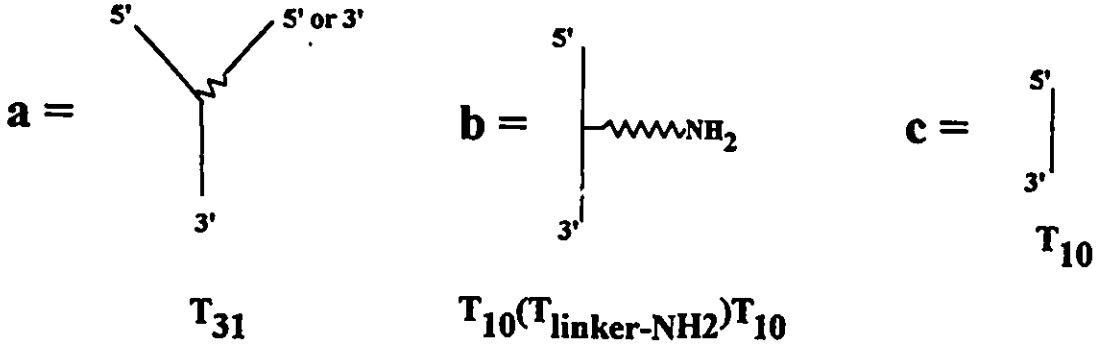

Figure 4.1 Electrophoresis of crude "Y"-shaped oligomers **III** and **IV** on 16% polyacrylamide/7M urea. *Lanes 1, and 7*; marker dyes, Xylene Cyanol (XC) and Bromophenol Blue (BPB); *lane 2*: linear 21-mer, $T_{10}AT_{10}$; *lane 3*: crude oligomer **III**; *lane 4*: crude oligomer **IV**: *lane 5*: linear 31-mer, $T_{10}AT_{20}$; *lane 6*: linear 13-mer, T_{13}.

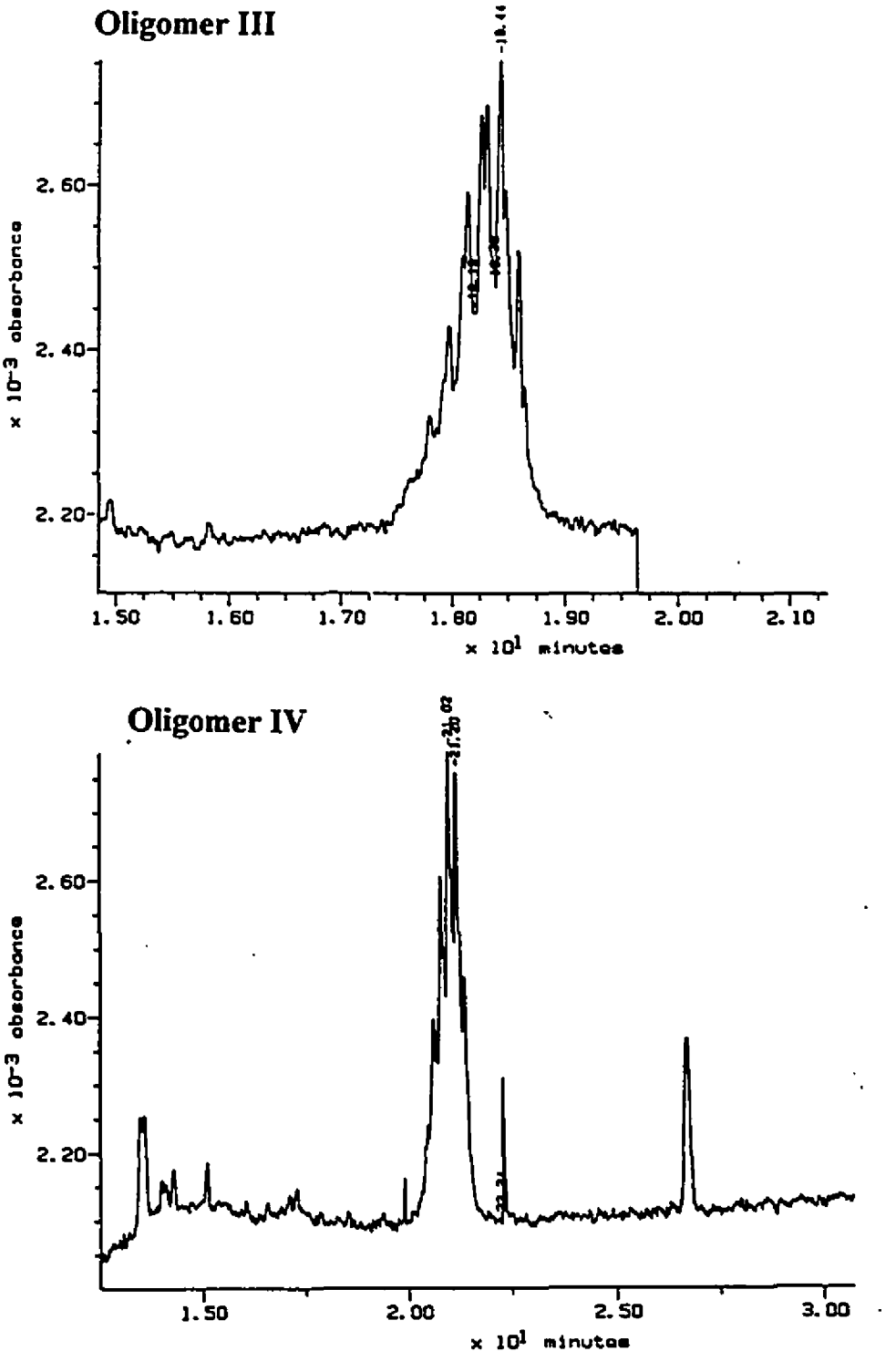

Figure 4.2 Capillary Gel Electrophoresis Analysis of "Y"-shaped Oligomers III and IV after PAGE Purification

4.3 Preliminary Binding Studies of Branched Oligomer III

A common technique used to study duplex and triplex formation is UV spectrophotometry. By virtue of their heterocyclic bases, which are flat aromatic chromophores, nucleic acids display UV absorption spectra. The stacking interactions of adjacent heterocyclic bases on a single strand of ribonucleic or deoxyribonucleic acid are responsible for lowering the UV absorption of the whole molecule relative to the sum of the individual nucleotide components. In addition, the UV absorption of double-helices is lower than that of the individual strands as result of chromophore:chromophore interactions.[113] This hypochromicity is usually measured at 260 nm and is calculated as a percentage, where $H\%=\{(A_{final}-A_{initial})/A_{final}\} \times 100\%$, where A_{final} = high temperature absorbance and $A_{initial}$ = low temperature absorbance.

When heating a solution of DNA, the hydrogen bonds between the paired bases on opposite strands of the double helix are disrupted, and the DNA is said to be denatured into two single strands. This dissociation from a double helix into single separated strands can be readily monitored by measuring the absorption of the "melting" process at 260 nm. A distinct *S*-shaped curve, known as the "melt" curve, is observed when absorption is plotted against temperature. The point at which the concavity of this thermal transition curve changes is known as the melting temperature, T_m, and is defined as the temperature at which half the double helical structure is lost.

The temperature melting curve for the complex formed between oligomer **III** and one mole-equivalent of dA_{10} (figure 4.3) at 260 nm shows a monophasic, cooperative transition at T = 48 °C with a hyperchromicity of 16 % (1M, 10mM PO_3^{-3}, pH = 7). The T_m observed is significantly higher than that observed for the T_{10}:dA_{10} duplex (T_m = 30 °C, under the same buffer conditions) and the complex formed between 5'-T10 $A^{T10\text{-}3'}{}_{T10\text{-}3'}$ and one mole-equivalent of dA_{10} (T_m = 39 °C, under the same conditions).[77] This observation suggests, perhaps, that the flexible linker separates the

two polypyrimidine "tails" enabling full hybridization or base pairing with complementary dA_{10}.

It has been shown that there is no change in absorbance when the dissociation of dA_{10}:dT_{10} to single stranded dA_{10} and dT_{10} is monitored at 284 nm[114]. However, at this same wavelength the transition tsDNA → dsDNA → ssDNA does exhibit an increase in UV absorption. Therefore, triple helix association/dissociation can be independently monitored at this wavelength. With this characteristic in mind, monitoring the dissociation of the complex formed between **III** and one mole-equivalent of dA_{10} at 284 nm showed a monophasic,cooperative transition at T = 48 °C with a hyperchromicity of 5%, consistent with triple helix formation (data not shown). However, with the addition of two mole-equivalents of dA_{10} no hyperchromicity increase was observed. How could this occur if the branched nucleic acid has an extra site available for the binding of an additional deoxyadenosine decamer (figure 4.4)? It was speculated (from the capillary gel electropherogram) that the second polypyrimidine "tail" may be shorter than the expected deoxythymidine decamer and, therefore, could not fully hybridize to a complement deoxyadenosine decamer. It should be noted that in figure 4.4 triplex formation is shown to precede duplex formation, assuming that the triplex is thermodynamically favored over duplex formation. However, the asymmetry in the lower temperature region of the melt curve (T ≈ 30 °C, figure 4.3) suggests the formation of a small amount of a duplex structure (with two T_{10} "arms" remaining as "spectators"). Studies are currently being pursued in our laboratory to further investigate the binding properties of oligomers **III** and **IV**.

Preliminary studies incorporating branching monomers **37** and **38** have also been carried out in our laboratory and show coupling yields >80% at the branching point and consistently >96% coupling yields beyond the branching point, depicting a normal synthesis. In addition to this promising result, the temperature melting curve for the complex formed between **II** and one equivalent of dA_{10} at 260 nm shows a monophasic,

cooperative transition at 49 °C with a hyperchromicity increase of 18% (1M, 10 mM PO^{-3}, pH = 7). In addition, a monophasic cooperative transition was observed for the complex formed between **II** and one mole- equivalent of dA_{10} at 284 nm, consistent with triple helix formation. The similar T_m's obtained for branched molecules **II** and **III** incorporating branching monomers **37** and **20**, respectively, suggests that both short and long linkers provide about the same stability to the triplex structure. Studies are currently continuing in our laboratory to fully investigate the binding properties of such systems.

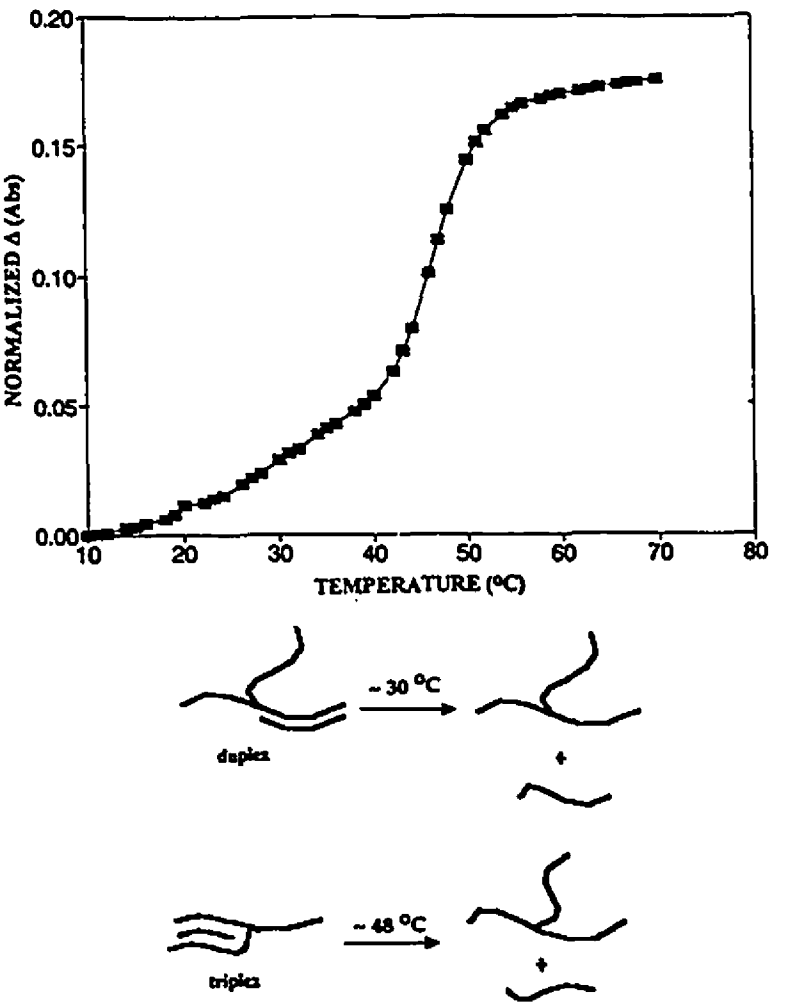

Figure 4.3 Thermal melt curve for dA_{10}:Oligomer **III** = 1:1, monitored at 260 nm. Normalized absorbances were calculated as $[(A_t - A_o)/A_f]$ where A_t = absorbance at any temperature, A_o = initial absorbance, and A_f = final absorbance. Conditions for melt curve were 1M NaCl, 10 mM PO_4^{-3}, pH = 7.0. ([dA_{10}] = [oligomer **III**] = .809 μM).

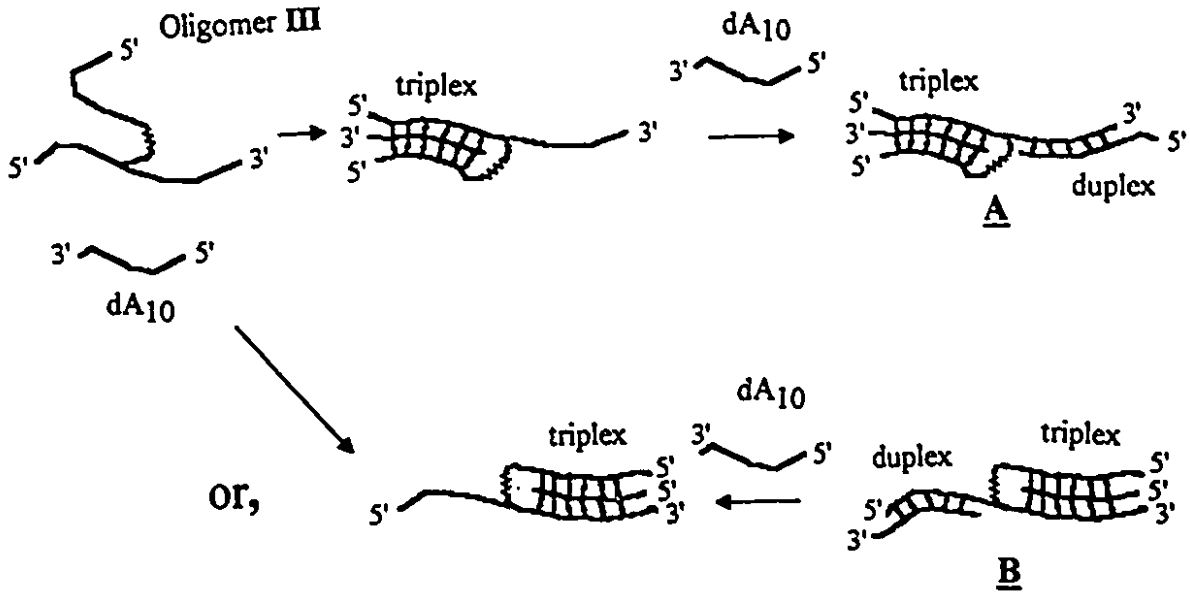

Figure 4.4 Association of Oligomer III and dA_{10}. Note different orientations for third (branch) strand. Configuration **B** corresponds to the more common Hoogsteen bonding motif with the third strand parallel to the purine strand of the duplex complex. Configuration **A** corresponds to the less favorble reverse-Hoogsteen bonding motif with a anti-parallel orientation of the third strand relative to the purine strand of the duplex.(Adapted from ref. # 115)

FUTURE WORK

In addition to employing branching monomer **20** bis(phosphoramidite) synthons **41** and **42** may also be incorporated at the branching point as described by Damha *et al.*[109] (scheme 16). The efficiency of this synthetic methodology is dependent on the distance between neighbouring 5'- hydroxy end groups of the immobilized thymidine chains on the surface of LCAA-CPG and on the concentration of the bis(phosphoramidite) employed. The lateral distance between neighbouring nucleoside units is dependent on the degree of derivatization of the solid support, with a highly substituted solid support providing closely spaced nucleosidic units and vice-versa. Therefore, the size of our flexible linkers should determine the degree of solid support derivatization and nucleoside "loadings" (μmol nucleoside / g of support) that will provide an efficient branching reaction. Studies using this approach are currently being pursued in our laboratory.

Scheme 16

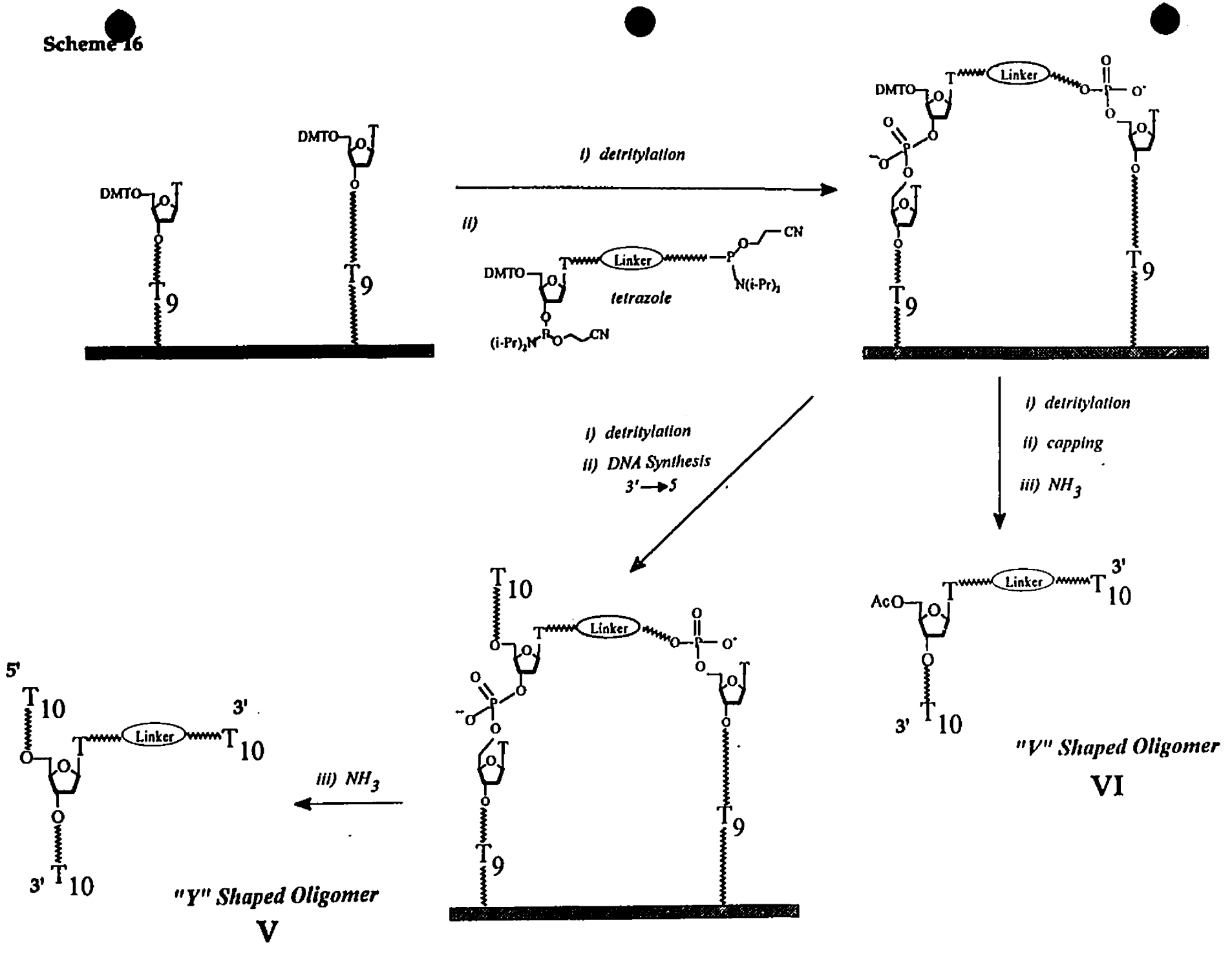
DMTO
T
9
i) detritylation
ii)
tetrazole
Linker
CN
N(i-Pr)2
(i-Pr)2N
i) detritylation
ii) capping
iii) NH3
i) detritylation
ii) DNA Synthesis
3'→5'
10
AcO
3'
5'
iii) NH3
"Y" Shaped Oligomer
V
"V" Shaped Oligomer
VI

CONCLUSIONS

We have demonstrated an efficient and simple method for functionalization of pyrimidine nucleobases with different sized aminoalkyl linkers. It was shown that alkylation occured exclusively at the N^3 position with no functionalization on the sugar ring. Cleavage of the phthalimido protected amino group with methylamine proved to be completely incompatible with the solid phase synthesis of our branched oligomers. However, protection of the end primary amino group as its levulinate and deprotection of the resulting N-levulinyl group with Letsinger's hydrazine solution proved to be more compatible, although not completely labile to hydrazinolysis. Itakura's methodology was successfully applied to incorporate a flexible linker moiety with a primary hydroxy group at the site of levulinic protection. Protection of the primary hydroxy moiety with a levulinyl group provided a levulinic ester which was much more labile to hydrazinolysis, rendering it completely compatible with the automated solid phase synthesis of our branched molecules.

Preliminary binding studies of our "V"- and "Y"-shaped oligomers **II** and **III** incorporating branching monomers **37** and **20**, respectively, indicated triple helix formation with one mole-equivalent of dA_{10}. Furthermore, the melting temperatures indicated a strong binding interaction between complementary strands with the size of the linker not being a critical factor in the stabilization of the triplex structure.

CHAPTER 5

EXPERIMENTAL

5.1 General Methods and Materials

Anhydrous tetrahydrofuran (THF): THF was dried overnight at room temperature over calcium hydride. The THF was decanted and continuously refluxed over sodium and benzophenone under nitrogen until a purple colour persisted. The THF was distilled prior to use and removed from the septum port of a collection bulb using a syringe. *N,N-dimethylformamide (DMF)*: DMF was dried overnight at room temperature over calcium hydride followed by fractional distillation under reduced pressure (8 mm torr). The dry distilled DMF was collected and stored over activated (400 °C) 4 Å molecular sieves. *Anhydrous pyridine*: pyridine was dried overnight at room temperature over calcium hydride followed by fractional distillation at atmospheric pressure. The dry distilled pyridine was collected and stored over activated (400 °C) 4 Å molecular sieves. *Imidazole and 4-dimethylaminopyridine* (Aldrich): were recrystallized from anhydrous THF and dried under vacuum over P_2O_5 prior to use. *Diisopropylethylamine* was dried overnight over calcium hydride with mild heating followed by distillation under reduced pressure. The distilled material was collected and stored over activated (400 °C) 4 Å molecular sieves. N,N-Diisopropyl(β-cyanoethyl)phosphonamidic chloride was purchased from Dalton Chemicals (Toronto) and stored at -5 °C. *N-(2-bromoethly)phthalimide, N-(3-bromopropyl)phthalimide and N-(4-bromobutyl)phthalimide* were purchased from Aldrich. *N-(5-bromopentyl)phthalimiae* was purchased from TransWorld Chemicals. *Triisopropylsilyl chloride* (stored at 0°C), *tert-butyldimethylsilyl chloride* (stored at °C), *trimethylsilyl chloride, benzoyl chloride, levulinic acid, methylamine* (40% aqueous), *succinic anhydride, pentachlorophenol, dicyclohexylcarbodiimide* (DCC), *hydrazine*

hydrate, *tert-butyl ammonium fluoride* (as a 1M solution in THF) and *5-amino-1-pentanol* were all purchased from Aldrich.

5.2 Chromatography

Silica Gel Column Chromatography: Merck Kieselgel 60 (200-400 mesh) silica gel was employed for gravity and flash columns. *Thin Layer Chromatography*: R_f values were obtained by using Merck Kieselgel 60F 254 silica analytical sheets (0.2 mm x 20 cm x 20 cm). Nucleosides and derivatives were detected by using a UV light source (*mineralite*, output *ca.* 254 nm). Trityl containing compounds were detected by passing silica gel sheet over concentrated hydrochloric acid vapour. *Preparation of C_{18} Reverse Phase Silica Gel*[116]: Merck silica gel (40 grams, Merck Kieselgel 60, 230-400 mesh) was placed in a dry, nitrogen-purged septum-capped 500 mL round bottom flask, and suspended in dry CCl_4 (300 mL, redistilled from P_2O_5). Octadecyltrichlorosilane (4 mL) was added to the suspension at room temperature and after two hours of stirring the mixture was filtered through a dry sintered (coarse) funnel. The silica gel was then washed with dry CCl_4 (3 x 100 mL) to remove any unreacted silane, followed by dry methanol (2 x 100 mL, redistilled over Mg metal) to convert residual chloride substituents to methoxy groups, and dry CH_2Cl_2 (2 x 100 mL, redistilled from P_2O_5). The silica gel, briefly dried under vacuum, was placed in a dry, nitrogen-purged, septum-capped 500 mL round bottom flask and suspended in dry CCl_4 (300 mL). Trimethylchlorosilane (4 mL) was added and after two hours of stirring the mixture was filtered, washed with dry CH_2Cl_2 (3 x 100 mL), and dried at 40 ^{o} C overnight and under vacuum for a day.

5.3 Spectra

Ultraviolet spectra were recorded on a Varian Cary 1 UV-VIS spectrophotometer. All nuclear magnetic resonance spectra (^{1}H, ^{13}C, and ^{31}P) were recorded on either a Unity-500 or XL-300 NMR spectrometer and all chemical shifts are quoted in parts per million (ppm). The residual proton signals of dimethylsulfoxide-d_6 (δ 2.49 ppm) and acetone-d_6 (δ 2.05 ppm) were used as references in these solvents. ^{31}P-NMR spectra were referenced with respect to 85% H_3PO_4 (external capillary standard). Low and high resolution FAB mass spectra were recorded on a VG-ZAB-HS Sector Mass Spectrometer in the direct inlet mode.

5.4 EXPERIMENTAL FOR CHAPTER 2

Synthesis of 5'-O-DMT-N^6-benzoyl-N'^6-(5-phthalimidopentyl)adenosine (3).

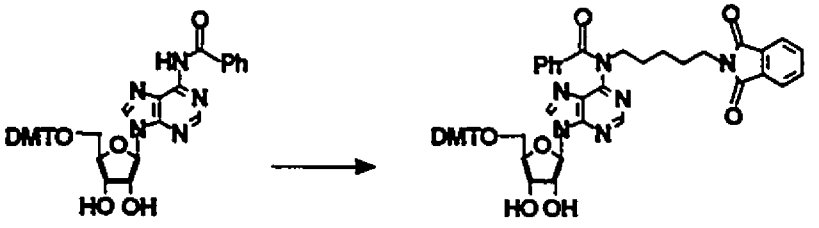

N^6-benzoyl-5'-(4,4'dimethoxytrityl)adenosine **1** (1.00 gr, 1.50 mmol) was dissolved in dry DMF (6 mL), and sodium hydride (72 mg, 1.80 mmol, 1.2 eq) was added at room temperature. After 30 min stirring, a 20% DMF solution (w/v) of N-(5-bromopentyl)phthalimide (710 mg, 2.40 mmol, 1.6 eq) was added dropwise to the reaction mixture and left to stir overnight. Water (1 mL) was added slowly and the reaction mixture was concentrated to an oily residue which was taken up in methylene chloride (35 mL) and washed with saturated brine (2 x 35 mL). The aqueous washes were back-extracted with methylene chloride (3 x 25 mL) and the combined organic layers were pooled, dried (Na_2SO_4) and evaporated *in vacuo* to give a yellow oil which was purified on a silica gel column, eluting with a gradient from 0-5% methanol in methylene chloride, to give the title compound **3** as a near colorless oil. The residue was taken up in CH_2Cl_2 (30 mL) and precipitated in hexanes (450 mL) to afford the desired compound **3** (1.32 mg, 28 %) as a white solid foam: TLC (ethyl acetate/acetone, 7:3, v/v) R_f = .63 (R_f **1** =.32), ^{1}H-NMR (500 MHz, acetone-d_6) δ: 1.26 (q^5, 2H, H10), 1.53 (q^5, 2H, H11), 1.61 (q^5, 2H, H9), 3.16 (m, 2H, H5'AB), 3.48 (t, 2H, H12), 3.70 (s, 6H, 2 x $PhOCH_3$), 4.04 (m, 1H, H4'), 4.18 (t, 1H, H8), 4.29 (m, 1H, H3'), 4.69 (m, 2H, H2'), 5.96 (d, 1H, H1'), 8.47 (s, 1H, H6), 8.53 (s, 1H, H7); MS (FAB-NBA, NaCl), m/z 895 ([M+Na^+]), 873 ([M+H^+]), 455 ([MH^++H^+-sugar]), 303 ([DMTr^+]).

Synthesis of 5'-O-DMT-N^3-(5-phthalimidopentyl)uridine (6).

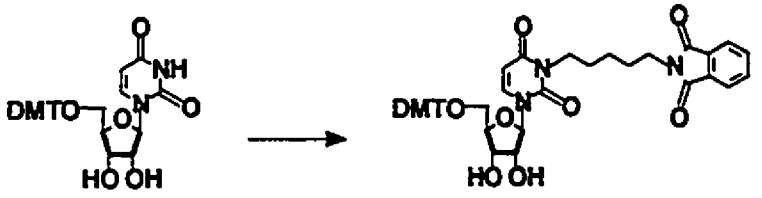

5'-O-(4,4'dimethoxytrityl)uridine 4 (819 gr, 1.50 mmol) was dissolved in dry DMF (6 mL), and sodium hydride (72 mg, 1.80 mmol, 1.2 eq) was added at room temperature. After 30 min stirring, a 20 % DMF solution (w/v) of N-(5-bromopentyl)phthalimide (710 mg, 2.40 mmol, 1.6 eq) was added dropwise to the reaction mixture and left to stir overnight. Water (1 mL) was added slowly and the reaction mixture was concentrated to an oily residue which was taken up in methylene chloride (35 mL) and washed with saturated brine (2 x 35 mL). The aqueous washes were back-extracted with methylene chloride (3 x 25 mL) and the combined organic layers were pooled, dried (Na_2SO_4) and evaporated *in vacuo* to give a yellow oil which was purified on a silica gel column, eluting with a gradient from 0-5% methanol in methylene chloride to give the title compound 3 as a near colorless oil. The residue was taken up in CH_2Cl_2 (30 mL) and precipitated in hexanes (450 mL) to afford the desired compound 6 (994 mg, 87 %) as a white solid foam: TLC (ethyl acetate/acetone, 65:25, v/v) R_f = .63 (R_f 4 =.31) MS (FAB-NBA, NaCl), m/z 785 ([M+Na^+]), 763 ([M+H^+]), 328 ([MH^++H^+-sugar]), 303 ([DMTr^+]).

Synthesis of 5'-O-DMT-N^3-(n-phthalimidoalkyl)-2'-deoxythymidine (7-10).

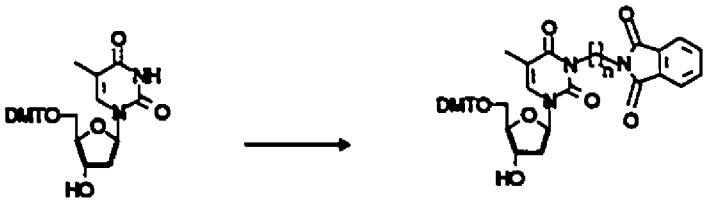

5'-O-DMT-(5-phthalimidopentyl)thymidine (7). 5'-O-(4,4'-dimethoxytrityl) thymidine 5 (816 mg, 1.50 mmol) was dissolved in dry DMF (6 mL), and sodium hydride (72 mg, 1.80 mmol, 1.2 eq) was added at room temperature. After 30 min stirring, a 20% DMF solution (w/v) of N-(5-bromopentyl)phthalimide (710 mg, 2.40 mmol, 1.6 eq) was added dropwise to the reaction mixture and left to stir overnight. Water (1 mL) was added slowly and the reaction mixture was concentrated to an oily residue which was taken up in methylene chloride (35 mL) and washed with saturated brine (2 x 35 mL). The aqueous washes were back-extracted with methylene chloride (3 x 25 mL) and the combined organic layers were pooled, dried (Na_2SO_4) and evaporated *in vacuo* to give a yellow oil which was purified on a silica gel column, eluting with a gradient from 0-5% methanol in methylene chloride, to give the title compound 7 as a near colorless oil. The residue was taken up in CH_2Cl_2 (30 mL) and precipitated in hexanes (450 mL) to afford the desired compound 7 (668 mg, 88%) as a white solid foam: TLC (7.5% MeOH/CH_2Cl_2) R_f = .63; ^{1}H-NMR and ^{13}C-NMR data are summarized in tables 1 and 2, respectively; MS (FAB-NBA, NaCl), m/z 782 ([M+Na^+]), 760 ([M+H^+]), 342 ([MH^++H^+-sugar]), 303 ([DMTr$^+$]).

5'-O-DMT-(2-phthalimidoethyl)thymidine (8). As for 7, nucleoside 5 (816 mg, 1.50 mmol) was dissolved in dry DMF (6 mL), and sodium hydride (72 mg, 1.80 mmol, 1.2 eq) was added at room temperature. After 30 min stirring, a 20% DMF solution (w/v) of N-(2-bromoethyl)phthalimide (610 mg, 2.40 mmol, 1.6 eq) was added dropwise to the

reaction mixture and left to stir overnight. Same work-up was employed as in case 7, and the title compound 8 was obtained in 52% yield (560 mg) as a white foam: TLC (7.5% MeOH/CH_2Cl_2) R_f = .60; ^{1}H-NMR and ^{13}C-NMR data are summarized in tables 1 and 2, respectively; MS (FAB-NBA, NaCl), m/z; 741 ([M+Na^+]), 718 ([M+H^+]), 300 ([MH^++H^+-sugar]), 303 ([$DMTr^+$]).

5'-DMT-3'-OH-(3-phthalimidopropyl)thymidine (9). As for 7, nucleoside 5 (816 mg, 1.50 mmol) was dissolved in dry DMF (6 mL), and sodium hydride (72 mg, 1.80 mmol, 1.2 eq) was added at room temperature. After 30 min stirring, a 20% DMF solution (w/v) of N-(2-bromopropyl)phthalimide (643 mg, 2.40 mmol, 1.6 eq) was added dropwise to the reaction mixture and left to stir overnight. Same work-up was employed as in case 7, affording the title compound 9 in 72% yield (789 mg) as a white foam: TLC (7.5% MeOH/CH_2Cl_2) R_f = .62; ^{1}H-NMR and ^{13}C-NMR data are summarized in tables 1 and 2, respectively; MS (FAB-NBA, NaCl), m/z 755 ([M+Na^+]), 732 ([M+H^+]), 315 ([MH^++H^+-sugar]), 303 ([$DMTr^+$]).

Synthesis of 5'-O-DMT-(4-phthalimidobutyl)thymidine (10). As for 7, nucleoside 5 (832mg, 1.50 mmol) was dissolved in dry DMF (6 mL), and sodium hydride (72 mg, 1.80 mmol, 1.2 eq) was added at room temperature. After 30 min stirring, a 20% DMF solution (w/v) of N-(4-bromobutyl)phthalimide (677 mg, 2.40 mmol, 1.6 eq) was added dropwise to the reaction mixture and left to stir overnight. Same work-up was employed as in case 7, affording the title compound 10 in 82% yield (916 mg) as a white foam: TLC (7.5% MeOH/CH_2Cl_2) R_f = .62; ^{1}H-NMR and ^{13}C-NMR data are summarized in tables 1 and 2, respectively; MS (FAB-NBA, NaCl), m/z 769 ([M+Na^+]), 746 ([M+H^+]), 328 ([MH^++H^+-sugar]), 303 ([$DMTr^+$]).

Synthesis of 5'-O-DMT-N^3-(5-aminopentyl)thymidine (12).

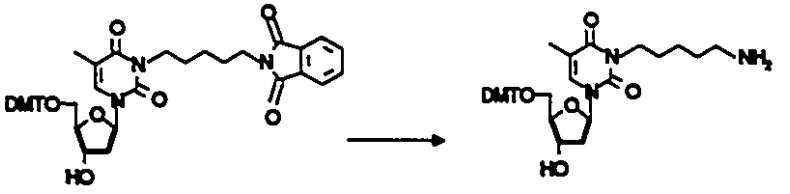

Phthalimide 7 (759 mg, 1.0 mmol) was dissolved in benzene (2.5 mL) and ethanol (5 mL) and 40% aqueous methylamine (862 μL, 10.0 mmol, 0.1 eq) were added at room temperature. After overnight stirring, the mixture was concentrated to a white foam. The solid was purified on a reverse-phase silica gel column to afford amino alcohol 12 (510 mg, 81%) as a white foam: TLC (CH_2CL_2/MeOH/TEA, 85:12:3, v/v) R_f = .18; ^{1}H-NMR (500 MHz, acetone-d_6) δ: 1.37 (m, 2H, H10), 1.49 (d, 3H, H7), 1.57 (d, 2H, H11), 1.58 (m, 2H, H9AB), 2.29-2.39 (m, 2H, H2'AB), 3.16 (t, 2H, H12), 3.36 (d, 2H, H5'AB), 3.78 (s, 6H, 2 x PhOCH_3), 3.87 (m, 2H, H8AB), 4.04 (m, 1H, H4'), 4.58 (m,1H, H3'), 6.39 (t, 1H, H1'), 7.63 (d, 1H, H6), coupling constants (Hertz): $J_{H1'-H2'AB}$ = 6.35, 7.23, $J_{H2'A-H2'B}$ = 13.43, $J_{H2'-H3'}$ = 3.42, 6.00, $^3J_{H6-H7}$ = 1.5, $J_{H8'A-H9XY}$ = 7.23, 7.50, $J_{H8'B-H9XY}$ = 6.49, 7.0, $J_{H8A'-H8'B}$ = 12.46; ^{13}C-NMR (DMSO-d_6) δ: 12.38 (C7), 23.81 (C10), 29.00 (C9), 32.99 (C11), 40.55 (C2' and C8), 41.37 (C12), 55.01 (PhOCH_3), 63.69 (C5'), 70.39 (C3'), 84.80 (C1'), 85.59 (C4'), 108.70 (C6), 134.29 (C5), 150.24 (C2), 162.52 (C4); MS (FAB-NBA, NaCl) m/z; 654 ([M+Na^+]), 631 ([M+H^+]), 212 ([MH^++H^+-sugar]), 303 ([$DMTr^+$]); UV(ethanol, nm) λ_{max} = 269.4, λ_{min} = 255.2.

Reverse-Phase Flash Column Chromatography of Amino Alcohol (12)

Freshly prepared reverse-phase silica gel (20 grams of C_{18} bonded reverse-phase silica gel per gram of crude product) was packed into a column as a methanolic slurry and then very slowly equilibrated with water by adding succesively increasing percentages (0-100% in increments of 10%) of water in methanol. The crude amino alcohol **12** was absorbed onto a small amount of C_{18} reverse-phase silica gel (1-2 gr) by dissolving in a minimum amount of an $H_2O/CH_3OH/CH_2Cl_2$ mixture and evaporating the organic solvents to an aqueous slurry (2-3 mL). The aqueous slurry was loaded onto the reverse-phase column and eluted with a gradient of 0-100% water in methanol, followed by a gradient of 0-100% methanol in methylene chloride.

Isolation and Characterization of Phthalimide Intermediate (11)

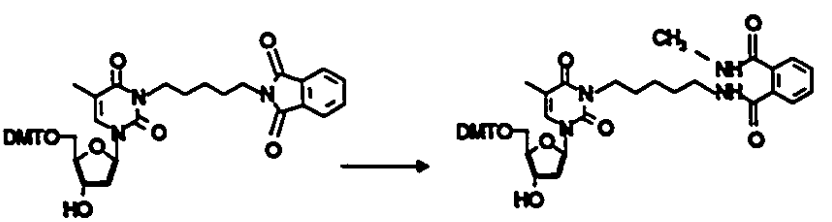

Phthalimide **7** (759 mg, 1.0 mmol) was dissolved in benzene (2.5 mL), and ethanol (5 mL) and 40% aqueous methylamine (862 µL, 10.0 mmol, 1.0 eq) were added at room temperature. After 45 min stirring, the mixture was concentrated to a white foam. The crude residue was purified on a silica gel column, eluting with a gradient from 0-5% methanol in methylene chloride to afford intermediate **11** as a white foam in quantitative yield: TLC (7.5% CH_2Cl_2/isopropanol) $R_f = 0.5$; ^{1}H-NMR (500 MHz, acentone-d_6) δ: 1.41 (m, 2H, H10), 1.48 (d, 3H, H7), 1.62 (m, 4H, H9 and H11), 2.28-2.39 (m, 2H, H2'), 2.86 (d, 3H, CH_3NH), 3.37 (aq, 2H, H12), 3.39 (d, 2H, H5'),

3.78 (s, 6H, 2 x $PhOCH_3$), 3.88 (AB of ABXY, m, 2H, H8), 4.05 (q, 1H, H4'), 4.58 (m, 1H, H3'), 6.38 (t, 1H, H1'), 7.55 (bq and exchangeable, 1H, CH_3NH), 7.65 (bt and exchangeable, 1H, CH_2NH) , coupling constants (Hertz): $J_{H1'\text{-}H2AB'}$ = 6.35, 7.24, $J_{H2'\text{-}H3'}$ = 3.42, 5.99, $J_{H2'A\text{-}H2'B}$ = 13.15, $^3J_{H6\text{-}H7}$ = 1.5, $J_{H8'A\text{-}H9XY}$ = 7.28, 7.59, $J_{H8'B\text{-}H9XY}$ = 6.348, 7.68, $J_{H8A'\text{-}H8'B}$ = 12.59; ^{13} C-NMR (acetone-d_6) δ: 12.89 (C7), 24.93 (C10), 26.76 (C15), 29.49 (C11), 29.76 (C9), 40.27 (C12), 41.27 (C8), 41.38 (C2'), 55.49 ($PhOCH_3$), 64.68 (C5'), 72.26 (C3'), 86.13 (C4'), 87.12 (C1'), 110.07 (C6), 134.85 (C5), 151.53 (C2), 163.68 (C4), 169.36 (C14), 169.97 (C15); MS (FAB-NBA, NaCl) m/z; 814 ([M+Na^+]), 792 ([M+H^+]), 373 ([MH^++H^+-sugar]), 303 ([$DMTr^+$]); UV(ethanol, nm) λ_{max} = 269.2, λ_{min} = 255.2.

Synthesis of 5'-O-DMT-N^3-(5-N-levulinylpentyl)thymidine (16)

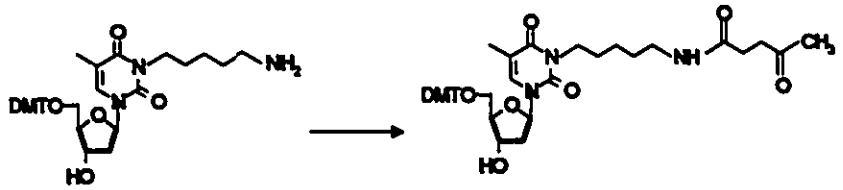

Amino alcohol **12** (945 mg, 1.50 mmol) was dissolved in dry DMF (7.5 mL) and freshly prepared levulinic anhydride (1.8 mmol, 1.2 eq) was added dropwise at room temperature. After stirring for 24 hr the mixture was concentrated to a yellow oil. The residue was taken up in CH_2Cl_2 (30 mL) and washed with 5% sodium bicarbonate (2 x 30 mL) and saturated brine (30 mL). The aqueous washes were back-extracted with CH_2Cl_2 (2 x 30mL) and the combined organic layers were washed with saturated brine (30 mL) and water (30 mL). The dried (Na_2SO_4) organic phase was concentrated *in vacuo* and the resulting yellow residue was purified on a silica gel column, eluting with a gradient of 0-5% methanol in methylene chloride, to afford the title compound **16**

(585 mg, 80%) as a white foam: TLC (CH_2Cl_2/EtOH, 9:1, v/v) R_f = 0.48; ^{1}H-NMR (500 MHz, acentone-d_6) δ: 1.318 (m, 2H, H10), 1.48 (d, 3H, H7), 1.49 (m, 2H, H11), 1.57 (m, 2H, H9), 2.09 (s, 3H, H17), 2.29-2.39 (m, 2H, H2'), 2.36 (t, 2H, H14), 2.67 (t, 2H, H15), 3.14 (aq, 2H, H12), 3.36 (d, 2H, H5' AB), 3.78 (s, 6H, 2 x PhOCH_3), 3.86 (AB of ABXY, m, 2H, H8), 4.04 (q, 1H, H4'), 4.578 (m, 1H, H3'), 6.382 (t, 1H, H1'), 6.98 (bs and exchangeable, 1H, CH_2NH), 7.63 (d, 1H, H6) coupling constants (Hertz): $J_{H1'-H2AB'}$ = 6.42, 7.20, $J_{H2'A-H2'B}$ = 13.26, $J_{H2'-H3'}$ = 3.35, 6.18, , $^3J_{H6-H7}$ = 1.0, $J_{H8'A-H9XY}$ = 7.13, 7.56, $J_{H8'B-H9XY}$ = 6.33, 7.05, $J_{H8A'-H8'B}$ = 12.59; ^{13} C-NMR (DMSO-d_6) δ: 12.68 (C7), 24.10 (C10), 27.12 (C11), 29.04 (C9), 38.68 (C12), 29.94 (C17), 29.35 (C15), 38.32 (C14), 40.42 (C8), 41.38 (C2'), 55.49 (PhOCH_3), 63.98 (C5'), 70.70 (C3'), 85.07 (C1'), 85.88 (C4'), 108.98 (C6), 134.60 (C5), 150.53 (C2), 162.81 (C4), 171.18 (C13), 207.71 (C16); MS(FAB-glycerol), m/z 820 ([MH^++ glycerol]), 728 ([M+H^+]), 426 ([MH^+-DMTrH]), 303 ([$DMTr^+$]); UV(ethanol, nm) λ_{max} = 269.4, λ_{min} = 254.8.

Levulinic Acid Synthesis: DCC (375 mg, 1.8 mmol) was dissolved in ether (7.8 mL) and levulinic acid (370 μL, 3.6 mmol, 2.0 eq) was added dropwise. A white solid appeared (N,N-dicyclohexylurea) after 30 seconds indicating the start of the desired reaction. After four hours stirring, the mixture was filtered through a dry fine sintered glass funnel and the organic solvent was concentrated *in vacuo* to yield levulinic anhydride quantitatively as near colorless oil.

Synthesis of 5'-DMT-N^3-(5-N-levulinylpentyl)thymidine-3'-(β-cyanoethyl)-N,N'-Di-isopropylphosphoramidite (20).

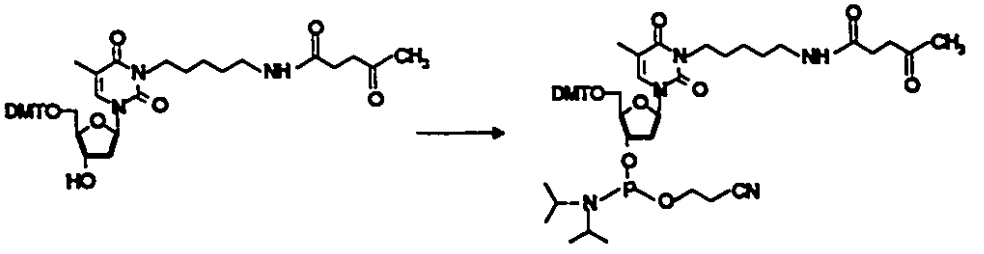

Levulinic amide **16** (500 mg, 685 μmol) was dissolved in a nitrogen-purged, septum-capped 10.0 mL hypovial containing anhydrous THF (2.50 mL). To the solution was added a catalytic amount of DMAP (16.7 mg, 137 μmol, .2 eq) followed by the slow (over 20 seconds) dropwise addition of N,N'-diisopropylethylamine (600 μL, 3.42 mmol, 5 eq) and N,N'-diisopropyl(β-cyanoethyl)phosphonamidic chloride (180 μL, 822 μmol, 1.2 eq). A white precipitate (diisopropylethylammonium hydrochloride) appeared after 5 min, indicating the start of the desired reaction. TLC (ether/CH_2Cl_2, 2:1, v/v) confirmed complete consumption of starting material. After 4 hr of stirring, the reaction mixture was added to ethyl acetate (75 mL, prewashed with 5% $NaHCO_3$) and the resulting diluted mixture was then washed with saturated brine (5 x 10 mL). The aqueous washes were back-extracted with 50 mL of prewashed ethyl acetate. The organic phases were pooled, dried (Na_2SO_4) and concentrated *in vacuo* to a white foam, which was purified on a silica gel column (4 cm, 40 gr) eluting with CH_2Cl_2/hexanes/TEA (45:50:5, v/v). After evaporating the desired pooled fractions, the product was first coevaporated with 95% ethanol (2 x 15 mL) and then with diethyl ether (3 x 10 mL) to afford amidite **20** (540 mg, 85%) as a white foam: TLC (CH_2Cl_2/ether, 2:1, v/v) R_f = .47 and .57 (2 diastereomers); ^{31}P-NMR (DMSO-d_6) δ: 147.695, 148.075 (2 diastereomers); ^{1}H-NMR (500 MHz, acetone-d_6) δ: 1.086-1.193 (d, 12H, [NHCH(CH_3)$_2$], diastereotopic methyls), 1.31 (m, 2H, H10), 1.56 (d, 3H, H7), 1.56 (m, 2H, H9), 1.58 (m, 2H, H11), 2.07 (s, 3H, H17), 2.37 (m, 2H, H14), 2.44-2.55 (m, 2H, H2'AB), 2.67 (t, 2H, H15),

3.42 (m, 2H, H12), 3.43 (d, 2H, H5'AB), 3.65 (m, 2H, $N[CH(CH_3)_2]_2$), 3.78 (s, 6H, 2 x $PhOCH_3$), 3.86 (m, 2H, H8AB); ***diastereomer I***: 2.62 (t, 2H, CH_2CN, 3.72 (t, 2H, $POCH_2$), 4.14 (q, 1H, H4'), 6.39 (t, 1H, H1'), 7.62 (s, H, H6), ***diastereomer II***: 2.76 (t, 2H, CH_2CN), 3.84 (t, 2H, $POCH_2$), 4.20 (q, 1H, H4'), 6.38 (t, 1H, H1'), 7.65 (s,1H, H6), MS(FAB-glycerol, resolution = 2000, both diastereomers) m/z; 928 ([M+H^+]), 710 ([MH^+-$iPr_2NP(OH)OCH_2CH_2CN$ or CEP]), 407 ([MH^+-CEP-DMTrH]), 312 ([MH^++H^+-sugar]), 303 ([$DMTr^+$]); UV(ethanol, nm) λ_{max} = 271.2 λ_{min} = 255.8.

5.5 EXPERIMENTAL FOR CHAPTER 3

Synthesis of 5'-O-(4,4'-dimethoxytrityl)-3'-O-silylated-N^3-(n-phthalimidoalkyl)-2'-deoxythymidine (21-22).

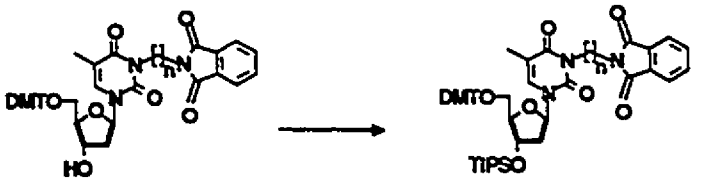

5'-O-DMT-3'-O-TIPS-N^3-(2-phthalimidoethyl)thymidine (21). Phthalimide **8** (718 mg, 1.0 mmol) was dissolved in DMF (1.0 mL) under a nitrogen atmosphere to which was added imidazole (272 mg, 4.0 mg, 4.0 eq) followed by triisopropylsilyl chloride (266 µL, 2.0 mmol, 2.0 eq) with stirring. TLC analysis in CH_2Cl_2/ether (2:1, v/v) showed complete reaction after 24 hr with a new spot of R_f = .75 (R_f **8** = .35). The reaction was quenched with 5% sodium bicarbonate and concentrated *in vacuo* to a yellow oil. The residue was taken up in CH_2Cl_2 (15 mL) and washed with 15 mL of saturated brine. The aqueous wash was extracted with CH_2Cl_2 (3 x 15 mL) and the combined organic layers were dried (Na_2SO_4) and concentrated *in vacuo*. The residual yellow oil was purified on a silica gel column, eluting with a gradient from 0-2% methanol in methylene chloride to afford silylated deoxynucleoside **21** (800 mg, 92%) as a white foam. ^{1}H-NMR and ^{13}C-NMR data are summarized in tables 3, 4, and 5: MS (FAB-NBA and NaCl) m/z; 897 ([M+Na^+]), 874 ([M+H^+]), 571 ([MH^+-DMTrH]), 300 ([MH^++H^+-sugar]), 303 ([$DMTr^+$]).

5'-O-DMT-3'-O-TIPS-N^3-(5-phthalimidopentyl)thymidine (22). As per **21**, nucleoside **7** (759 mg, 1.0 mmol) was dissolved in DMF (1.0 mL) under a nitrogen atmosphere to which was added imidazole (272 mg, 4.0 mg, 4.0 eq) followed by triisopropylsilyl chloride (266 µL, 2.0 mmol, 2.0 eq) with stirring. TLC analysis in CH_2Cl_2/ether (2:1, v/v) showed complete reaction after 24 hr with a new spot of R_f = .77

(R_f 7 = .36). The same work-up employed as in case **21**, and the title compound **22** was obtained in 92% yield as a white foam. ^{1}H-NMR and ^{13}C-NMR data are summarized in tables 3, 4, and 5: MS (FAB-NBA and NaCl) m/z; 933 ([M+Na$^+$]), 911 ([M+H$^+$]), 608 ([MH$^+$-DMTrH]), 342 ([MH$^+$+H$^+$-sugar]), 303 ([DMTr$^+$]).

Synthesis of 5'-(4,4'-dimethoxytrityl)-3'-O-(triisopropylsilyl)-N^3-(n-aminoalkyl)-2'-deoxythymidine (25-26).

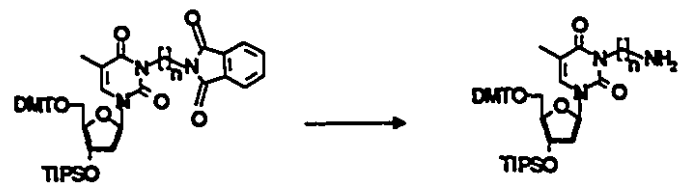

5'-O-DMT-3'-O-TIPS-N^3-(2-aminoethyl)thymidine (25). Nucleoside **21** (873 mg, 1.0 mmol) was dissolved in benzene (2.5 mL) and ethanol (5.0 mL) and 40% aqueous methylamine (862 µL, 10.0 mmol, 10.0 eq) were added at room temperature. After overnight stirring, TLC analysis in CH_2Cl_2/ether (9:1, v/v) showed complete disappearance of starting material with the formation of a major spot of R_f = .12 (ninhydrin positive) and a minor spot of R_f = .40 (ninhydrin negative). The mixture was concentrated *in vacuo* to a white foam and the crude material was purified on a silica gel column (50 gr), eluting first with a gradient of 0-10% isopropanol in methylene chloride to separate the phthalamide intermediate **23** and then with a gradient of 0-5% methanol *plus* 0-5% triethylamine in methylene chloride to recover the desired deoxynucleoside **25**. The fractions containing **25** were combined and evaporated *in vacuo*. The yellow residue was then coevaporated with 95% ethanol (2 x 20 mL), followed with CH_2Cl_2 (3 x 15 mL) to afford **25** (850 mg, 78%) as a white foam. ^{1}H-NMR and ^{13}C-NMR data are summarized in tables 3, 4, and 5: MS (FAB-NBA and NaCl) m/z; 768 ([M+Na$^+$]), 745 ([M+H$^+$]),

442 ([MH^+-DMTrH]), 172 ([MH^++H^+-sugar]), 303 ([$DMTr^+$]). UV (ethanol, nm), λ_{max} = 270.3, λ_{min} = 255.5.

5'-O-DMT-3'-O-TIPS-N^3-(2-aminopentyl)thymidine (26). As per **25**, nucleoside **22** (910 mg, 1.0 mmol) was dissolved in benzene (2.5 mL), and ethanol (5.0 mL) and 40% aqueous methylamine (862 μL, 10.0 mmol, 10.0 eq) were added at room temperature. After overnight stirring, TLC analysis in CH_2Cl_2/ether (9:1, v/v) showed complete disappearance of starting material with the formation of a major spot of R_f = .14 (ninhydrin positive) and minor spot of R_f = .40 (ninhydrine negative). The same work-up was employed as in case **25** and the title compound **26** was obtained in 80% yield as a white foam: ^{1}H-NMR and ^{13}C-NMR data are summarized in tables 3, 4, and 5: MS (FAB-NBA and NaCl) m/z; 804 ([M+Na^+]), 781 ([M+H^+]), 478 ([MH^+-DMTrH]), 212 ([MH^++H^+-sugar]), 303 ([$DMTr^+$]). UV (ethanol, nm), λ_{max} = 271.0, λ_{min} = 254.5.

Synthesis of 5'-O-(4,4'-dimethoxytrityl)-3'-O-(triisopropylsilyl)-N^3-[n-(succinyl) alkyl]-2'-deoxythymidine (27-28).

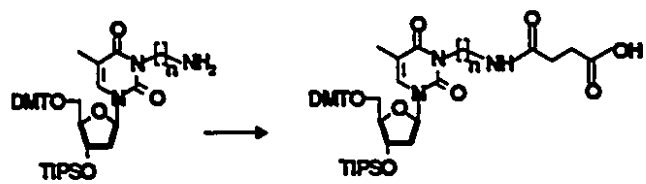

5'-O-DMT-3'-O-TIPS-N^3-[2-(succinyl)ethyl]thymidine (27). To a solution of amine **25** (1.488 gr, 2 mmol, coevaporated from three 10 mL portions of anhydrous pyridine) in anhydrous pyridine (10 mL) was added succinic anhydride (400 mg, 4.0 mmol, 2.0 eq) and a catalytic amount of DMAP (73 mg, 0.6 mmol, 0.3 eq). After 48 hr stirring, TLC analysis in 7.5% CH_2Cl_2/MeOH showed that succinylation was complete with the formation of a slightly less polar product of R_f = .24. Pyridine was then removed

in vacuo and the residue was coevaporated with three 50 mL portions of toluene. The yellow residue was then taken up in methylene chloride (50 mL) and washed with saturated brine (2 x 50 mL). The combined organic phases were dried (Na_2SO_4) and removed *in vacuo* to yield the crude product **27** in quantitative yield as a yellowish white foam: ^{1}H-NMR of crude **27** (500 MHz, acetone-d_6) δ: 1.03 (dd, 12H, SiCH(CH_3)$_2$, 1.10 (m, 3H, SiCH(CH_3)$_2$), 1.56 (d, 3H, H7), 2.25-2.32 (A of ABX, m, 1H, H2'A), 2.35-2.45 (B of ABX, m, 1H, H2'B), 2.41 (t, 2H, NHCOCH_2), 2.55 (t, 2H, CH_2COOH), 3.24 (m, 2H, H9AB), 3.37 (A of ABX, overlapping signals, H5'A), 3.46 (B of ABX, overlapping signals, H5'B), 3.78 (s, 6H, 2 x PhOCH_3), 4.04 (m, 2H, H8AB), 4.08 (m, 1H, H4'), 4.69(m, 1H, H3'), 6.34 (t, 1H, H1'), 7.67 (s, 1H, H6).

5'-O-DMT-3'-O-TIPS-N^3-[5-(succinyl)pentyl]thymidine (28). As per **27**, to a solution of amine **26** (1.560 gr, 2.0 mmol, coevaporated from three 10 mL portions of anhydrous pyridine) in anhydrous pyridine (10 mL) was added succinic anhydride (400 mg, 4.0 mmol, 2.0 eq) and a catalytic amount of DMAP (73 mg, 0.6 mmol, 0.3 eq). After 48 hr stirring, TLC analysis in 7.5% CH_2Cl_2/MeOH showed that succinylation was complete with the formation of a slightly less polar product of R_f = .24. The same work-up was employed as in case **27** and the title compound **28** was obtained in quantitative yield as a yellowish white foam: ^{1}H-NMR of crude **28** (500 MHz, acetone-d_6) δ: 1.00 (d, 12H, SiCH(CH_3)$_2$, 1.03-1.03 (m, 3H, SiCH(CH_3)$_2$, 1.34 (m, 2H, H10), 1.52 (m, 2H, H11), 1.56 (d, 1H, H7), 2.34-2.44 (m, 2H, H2'AB), 2.46 (t, 2H, NHCOCH_2), 2.56 (t, 2H, CH_2COOH), 3.18 (aq, 2H, H12), 3.34 (A of ABX, dd, 1H, H5'A), 3.46 (B of ABX, dd, 1H, H5'B), 3.78 (s, 6H, 2 x PhOCH_3), 3.86 (m, 2H, H8AB), 4.06 (q, 1H, H4'), 4.66 (m, 1H, H3'), 6.40 (dd, 1H, H1'), 7.68 (d, 1H, H6); coupling constants (Hertz), $J_{H1'-H2AB'}$ = 3.0, 5.68, $J_{H2'-H3'}$ = 7.99, 3.0, $J_{H4'-H5'A}$ = 2.93, $J_{H4'-H5'B}$ = 3.42, $J_{H5'A-H5'B}$ = 10.74, $J_{H8-H9XY}$ = 5.25, 6.31, $J_{H8A-H8B}$ = 12.83, $^3J_{H6-H7}$ = 1.0.

Synthesis of 5'-O-(4,4'-dimethoxytrityl)-3'-O-(triisopropylsilyl)-N^3-{n-[(pentachlorophenyl)succinyl]alkyl}-2'-deoxythymidine (29-30).

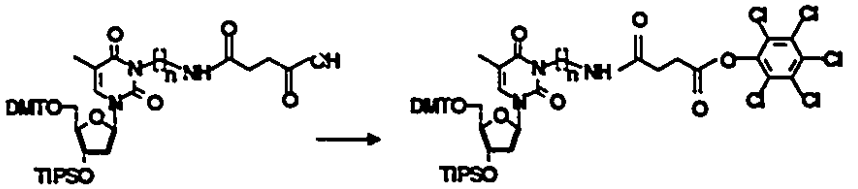

5'-O-DMT-3'-O-TIPS-N^3-{2-[(pentachlorophenyl)succinyl]ethyl}thymidine (29). To succinate 27 (422 mg, 0.50 mmol), pentachlorophenol (200 mg, 0.75 mmol, 1.5 eq), DMAP (15.3 mg, 0.125 mmol, 0.25 eq), and DCC (206 mg, 1.0 mmol, 2 eq) was added DMF (3.75 mL). A white solid (N,N-dicyclohexylurea) appeared after 30 min stirring indicative of the desired reaction. TLC analysis in CH_2Cl_2/MeOH (9:1, v/v), showed complete reaction after 48 hr with the formation of a single nonpolar compound of $R_f = 0.75$. The reaction was quenched with 95% ethanol and evaporated *in vacuo* to a dark yellow residue. After coevaporation with toluene (3 x 6.5 mL) the residue was taken up in methylene chloride (20 mL) and washed with saturated brine (2 x 20 mL). After drying the organic layer (Na_2SO_4) and removal of the solvent *in vacuo*, the residue was dissolved in methylene chloride (3.75 mL) and filtered through a fine sintered glass funnel. The solvent was then removed *in vacuo* and the filtration procedure was repeated twice more. The residue was taken up in methylene chloride (2.0 mL) and precipitated in 25 mL of hexanes to yield the desired crude ester 29 (500 mg, 92%) as a yellow gummy foam: ^{1}H-NMR of crude 29 (500 MHz, acetone-d_6) δ: .023 (d, 18H, SiCH(CH_3)$_2$), .083 (m, 3H, SiCH(CH_3)$_2$), 1.56 (d, 3H, H7), 2.40 (t, 2H, $CH_2CO\phi5C$;), 2.34-2.36 (m, 2H, H2'AB), 2.54 (t, 2H, NHCOCH_2), 3.35-3.46 (m, 2H, H5'AB), 3.46 (m, 2H, H9AB), 3.80 (s, 6H, 2 x PhOCH_3), 4.04 (m, 2H, H8AB), 4.65 (m, 1H, H3'), 4.67 (m, 2H, H4'), 6.38 (dd, 1H, H1'), 7.67 (s, 1H, H6).

5'-O-DMT-3'-O-TIPS-N^3-{5-[(pentachlorophenyl)succinyl]pentyl}thymidine (30). As per **29**, to succinate **28** (440 mg, 0.50 mmol), pentachlorophenol (200 mg, 0.75 mmol, 1.5 eq), DMAP (15.3 mg, 0.125 mmol, 0.25 eq), and DCC (206 mg, 1.0 mmol, 2 eq) was added DMF (3.75 mL). A white solid (N,N-dicyclohexylurea) appeared after 30 min stirring indicative of the desired reaction. TLC analysis in CH_2Cl_2/MeOH (9:1, v/v), showed complete reaction after 48 hr with the formation of a single nonpolar compound of $R_f = .77$. The same work-up was employed as in case **29** to afford the crude ester **30** (510 mg, 90%) as a yellow gummy foam: ^{1}H-NMR of crude **30** (500 MHz, acetone-d_6) δ: 1.023 (d, 18H, SiCH(CH_3)$_2$), 1.029-1.033 (m, 3H, SiCH(CH_3)$_2$), 1.40 (m, 2H, H10), 1.54 (m, 2H, H11), 1.56 (d, 1H, H7), 1.57 (m, 2H, H9), 2.33-2.44 (m, 2H, H2'AB), 2.63 (t, 2H, NHCOCH_2), 3.04 (t, 2H, CH_2COϕ5Cl), 3.20 (aq, 2H, H12), 3.34 (A of ABX, 1H, H5'A), 3.45 (B of ABX, 1H, H5'B), 3.78 (s, 6H, 2 x PhOCH_3), 3.84 (m, 2H, H8AB), 4.06 (q, 1H, H4'), 4.66 (q^5, 1H, H3'), 6.39 (t, 1H, H1'), 7.66 (s, 1H, H6); coupling constants (Hertz), $J_{H1'-H2AB'}$ = 3.23, 5.62, $J_{H2'-H3'}$ = 7.98, 3.52, $J_{H4'-H5'A}$ = 2.93, $J_{H4'-H5'B}$ = 3.42, $J_{H5'A-H5'B}$ = 10.25, $J_{H8A-H9XY}$ = 6.997, 7.039, $J_{H8B-H9XY}$ = 5.00, 6.28, $^3J_{H6-H7}$ = 1.0, $J_{H8A-H8B}$ = 12.68.

Synthesis of 5'-O-(4,4'-dimethoxytrityl)-3'-O-(triisopropylsilyl)-N^3-{n-[(5-hydroxypentyl)succinyl]alkyl}-2'-deoxythymidine (31-32)

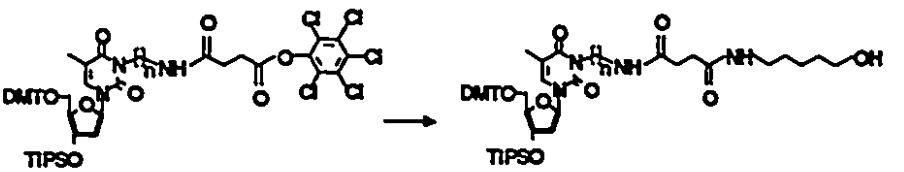

5'-O-DMT-O-TIPS-N^3-{2-[(5-hydroxypentyl)succinyl]ethyl}thymidine (31). Pentachlorophenyl ester **29** (490 mg, 0.450 mmol), dried by coevaporating with anhydrous pyridine (3 x 5 mL), was taken up in anhydrous pyridine (1.0 mL). The resulting solution was added, over a 15 min period, to a solution of 5-amino-1-pentanol (60 μL, 0.54 mmol, 1.2 eq), and triethylamine (122 μL) in anhydrous pyridine (5 mL). TLC analysis in 7.5% CH_2Cl_2/MeOH showed complete reaction after 24 hr with the formation of a single more polar product of $R_f = 0.32$. The mixture was concentrated *in vacuo* and coevaporated with toluene (3 x 10 mL). The dark yellow residue was taken up in methylene chloride (12 mL) and washed with saturated brine (2 x 12 mL). The aqueous layer was extracted with methylene chloride (2 x 12 mL) and the combined organic layers were dried (Na_2SO_4) and concentrated *in vacuo*. The crude product was purified on a silica gel column, eluting with a gradient from 0-5% methanol in methylene chloride, to afford **31** (315 mg, 76%) as a white foam: ^{1}H-NMR and ^{13}C-NMR data are summarized in tables 3, 4 and 6: MS (FAB-NBA and NaCl) m/z: 951 ([M+Na^+]), 929 ([M+H^+]), 625 ([MH^+-DMTrH]), 355 ([MH^++H^+-sugar]), 303 ([$DMTr^+$]). UV (ethanol, nm), $\lambda_{max} = 267.7$, $\lambda_{min} = 255.2$.

5'-O-DMT-O-TIPS-N^3-{5-[(5-hydroxypentyl)succinyl]pentyl}thymidine (32). As per **31**, pentachlorophenyl ester **30** (510 mg, 0.450 mmol), dried by coevaporating with anhydrous pyridine (3 x 5 mL), was taken up in anhydrous pyridine (1.0 mL). The resulting solution was added, over a 15 min period, to a solution of 5-amino-1-pentanol (60 μL, 0.54 mmol, 1.2 eq), and triethylamine (122 μL) in anhydrous pyridine (5 mL).

TLC analysis in 7.5% CH_2Cl_2/MeOH showed complete reaction after 24 hr with the formation of a single more polar product of $R_f = 0.34$. The same work-up was employed as in case **31** to afford alcohol **32** (315 mg, 72%) as a white foam: ^{1}H-NMR and ^{13}C-NMR data are summarized in tables 3, 4 and 6: MS (FAB-NBA and NaCl) m/z: MS (FAB-NBA and NaCl) m/z; 993 ([M+Na^+), 970 ([M+H^+]), 667 ([MH^+-DMTrH]), 397 ([MH^++H^+-sugar]), 303 ([$DMTr^+$]). UV (ethanol, nm), $\lambda_{max} = 268.3$, $\lambda_{min} = 254.8$.

Synthesis of 5'-O-(4,4'-dimethoxytrityl)-3'-O-(triisopropylsilyl)-N^3-{n-[(5-O-levulinylpentyl)succinyl]alkyl}-2'-deoxythymidine (33-34).

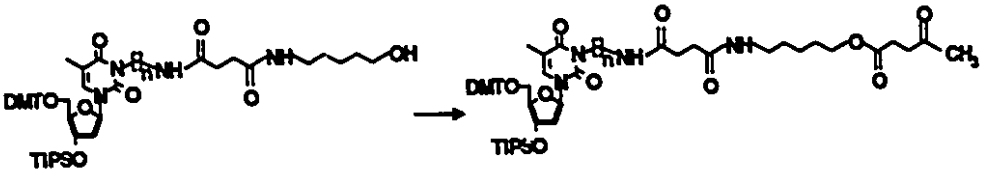

5'-O-DMT-3'-O-TIPS-N^3-{2-[(5-O-levulinylpentyl)succinyl]ethyl}thymidine (33). Freshly prepared levulinic anhydride (3.0 mol, 3 eq, see section 5.2) in anhydrous pyridine (1.5 mL) was added dropwise to a solution of alcohol **31** (929 mg, 1.0 mmol) in 4.5 mL of anhydrous pyridine. After 24 hr stirring, TLC in 7.5% CH_2Cl_2/MeOH showed complete disappearance of starting material with the formation of a less polar compound of $R_f = 0.40$. The dark red solution was concentrated *in vacuo* and coevaporated with toluene (3 x 3 mL). The residue was taken up in methylene chloride (15 mL) and washed with 5% sodium bicarbonate (2 x 15 mL) followed by saturated brine (15 mL). The aqueous washes were back-extracted with methylene chloride (2 x 15 mL) and the combined organic layers were dried (Na_2SO_4) and concentrated *in vacuo* to an oily residue. The crude material was purified on a silica gel column, eluting with a gradient of

0-5% methanol in methylene chloride to afford levulinic ester **33** (822 mg, 80%) as a white foam: ^{1}H-NMR and ^{13}C-NMR data are summarized in tables 3, 4 and 6: MS (FAB-NBA and NaCl) m/z: 1051 ([M+Na$^+$]), 1028 ([M+H$^+$]), 725 ([MH$^+$-DMTrH]), 455 ([MH$^+$+H$^+$-sugar]), 303 ([DMTr$^+$]). UV (ethanol, nm), λ_{max} = 267.7, λ_{min} = 255.8.

5'-O-DMT-3'-O-TIPS-N^3-{5-[(5-O-levulinylpentyl)succinyl]pentyl}thymidine (34). As per **33**, freshly prepared levulinic anhydride (3.0 mol, 3 eq) in anhydrous pyridine (1.5 mL) was added dropwise to a solution of alcohol **32** (970 mg, 1.0 mmol) in 4.5 mL of anhydrous pyridine. After 24 hr stirring, TLC analysis in 7.5% CH_2Cl_2/MeOH showed complete disappearance of starting material with the formation of a less polar compound of R_f = .45. The same work-up was employed as in case **33** to afford levulinic ester **34** (877 mg, 82%) as a white foam: ^{1}H-NMR and ^{13}C-NMR data are summarized in tables 3, 4 and 6: MS (FAB-NBA and NaCl) m/z: 1093 ([M+Na$^+$]), 1070 ([M+H$^+$]), 767 ([MH$^+$-DMTrH]), 495 ([MH$^+$+H$^+$-sugar]), 303 ([DMTr$^+$]). UV (ethanol, nm), λ_{max} = 268.8, λ_{min} = 255.2.

Synthesis of 5'-O-(4,4'-dimethoxytrity)-N^3-{n-[(5-O-levulinylpentyl)succinyl] alkyl}-2'-deoxythymidine (35-36).

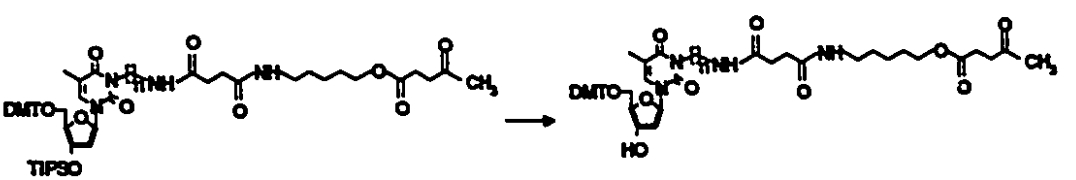

5'-O-DMT-N^3-{2-[(5-levulinylpentyl)succinyl]ethyl}thymidine (35). Levulinic ester **33** (745 mg, 725 μmol) was coevaporated from anhydrous pyridine (5 mL) followed by coevaporation from anhydrous THF/toluene (2 x 5 mL, 3:2, v/v). A solution of tetra-*n*-butylammonium fluoride in THF (1 M, 2.2 mL, 2.2 mmol, 3 eq) was added to a stirred

solution of dry nucleoside **33** in 2.50 mL of anhydrous THF. TLC analysis in ether/CH_2Cl_2/MeOH (85:5:10, v/v) showed complete disappearance of starting material (R_f = 0.38) with the formation of a single more polar compound of R_f = 0.12. The reaction mixture was diluted with 50 mL of methylene chloride and washed with saturated brine (5 x 50 mL). The organic layer was dried (Na_2SO_4) and evaporated *in vacuo* to a yellow residue. The crude material was purified on a short (3 x 6 cm) column of silica gel, eluting with 2.5% CH_2Cl_2/MeOH, to afford alcohol **35** in quantitative yield (630 mg) as a white foam. ^{1}H-NMR and ^{13}C-NMR data are summarized in tables 3, 4 and 6: MS (FAB-NBA and NaCl) m/z: 894 ([M+Na^+]), 871 ([M+H^+]), 568 ([MH^+-DMTrH]), 455 ([MH^++H^+-sugar]), 303 ([$DMTr^+$]).

5'-O-DMT-N^3-{5-[(5-levulinylpentyl)succinyl]pentyl}thymidine(36). Levulinic ester **34** (775 mg, 725 µmol) was coevaporated from anhydrous pyridine (5 mL) followed by coevaporation from anhydrous THF/toluene (2 x 5 mL, 3:2, v/v). A solution of tetra-*n*-butylammonium fluoride in THF (1 M, 2.2 mL, 2.2 mmol, 3 eq) was added to a stirred solution of dry nucleoside **34** in 2.50 mL of anhydrous THF. TLC analysis in ether/CH_2Cl_2/MeOH (85:5:10, v/v) showed complete disappearance of starting material (R_f = .36) with the formation of a single more polar compound of R_f = .18. The same work-up was employed as in case **35** to yield the desired alcohol **36** in quantitative yield (660 mg) as a white foam. ^{1}H-NMR and ^{13}C-NMR data are summarized in tables 3, 4 and 6: MS (FAB-NBA and NaCl) m/z: 936 ([M+Na^+]), 913 ([M+H^+]), 610 ([MH^+-DMTrH]), 495 ([MH^++H^+-sugar]), 303 ([$DMTr^+$]).

Synthesis of 5'-O-(4,4'-dimethoxytrityl)-N^3-{n-[(5-hydroxypentyl)succinyl] alkyl}-2'-deoxythymidine (39-40).

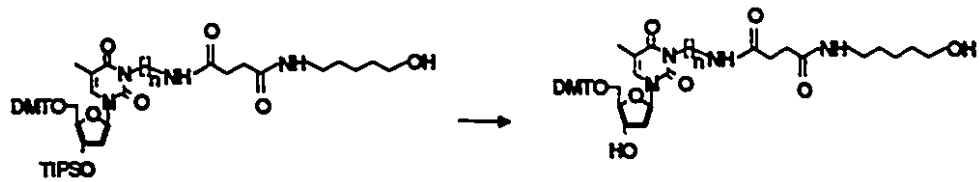

5'-O-DMT-N^3-{2-[(5-hydroxypentyl)succinyl]ethyl}thymidine (39). Alcohol **31** (928 mg, 1.0 mmol) was coevaporated from anhydrous pyridine (7 mL) followed by coevaporation from anhydrous THF/toluene (2 x 7 mL, 3:2, v/v). A solution of tetra-*n*-butylammonium fluoride in THF (1 M, 3.0 mL, 3.0 mmol, 3.0 eq) was added to a stirred solution of dry nucleoside **31** in 3.50 mL of anhydrous tetrahydrofuran. After 30 min stirring, TLC analysis in ether/CH_2Cl_2/MeOH (80:5:15, v/v) showed complete disappearance of starting material (R_f = 0.50) with the formation of a single more polar compound of R_f = 0.16. The same work-up was employed as in case **35** to afford the diol **39** (696 mg, 90%) as a white foam. ^{1}H-NMR and ^{13}C-NMR data are summarized in tables 3, 4 and 6: MS (FAB-NBA and NaCl) m/z: 796 ([M+Na^+]), 773 ([M+H^+]), 470 ([MH^+-DMTrH]), 355 ([MH^++H^+-sugar]), 303 ([$DMTr^+$]).

5'-O-DMT-N^3-{5-[(5-hydroxypentyl)succinyl]pentyl}thymidine (40). Alcohol **32** (969 mg, 1.0 mmol) was coevaporated from anhydrous pyridine (7 mL) followed by coevaporation from anhydrous THF/toluene (2 x 7 mL, 3:2, v/v). A solution of tetra-*n*-butylammonium fluoride in THF (1 M, 3.0 mL, 3.0 mmol, 3 eq) was added to a stirred solution of dry nucleoside **32** in 3.50 mL of anhydrous tetrahydrofuran. After 30 min stirring, TLC analysis in ether/CH_2Cl_2/MeOH (80:5:15, v/v) showed complete disappearance of starting material (R_f = 0.52) with the formation of a single more polar compound of R_f = 0.18. The same work-up was employed as in case **35** to afford the diol **40** (750 mg, 92%) as a white foam. ^{1}H-NMR and ^{13}C-NMR data are summarized in

tables 3, 4 and 6: MS (FAB-NBA and NaCl) m/z: 839 ([M+Na$^+$]), 816 ([M+H$^+$]), 513 ([MH$^+$-DMTrH]), 397 ([MH$^+$+H$^+$-sugar]), 303 ([DMTr$^+$]).

Synthesis of 5'-O-(4,4'-dimethoxytrityl)-N^3-{n-[(5-hydroxypentyl)succinyl]alkyl} thymidine-3'-O-(β-cyanoethyl)-N,N'-diisopropylphosphoramidites (37-38).

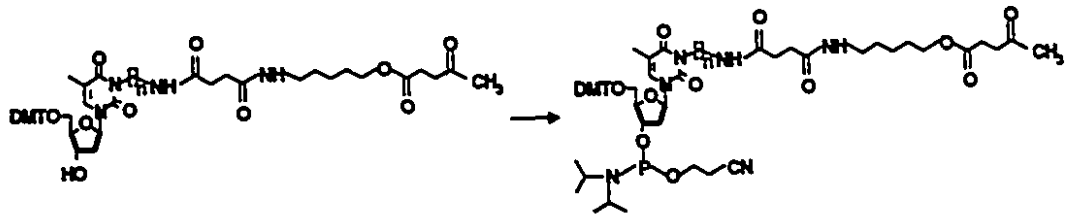

5'-O-DMT-N^3-{2-[(5-hydroxypentyl)succinyl]ethyl}thymidine-3'-O-(β-cyanoethyl)-N,N'-diisopropylphosphoramidite (37). Alcohol 35 (248 mg, 285 mmol), dried by coevaporation from anhydrous pyridine (2 x 50 mL) followed by THF/toluene (2 x 50 mL, 3:2, v/v), was dissolved in a nitrogen-purged, septum-sealed 10 mL hypovial containing dry THF (890 μL). To the solution was added a catalytic amount of DMAP (7 mg, 57 μmol, 0.2 eq), followed by the slow (over 20 seconds) dropwise addition of N,N'-diisopropylethylamine (250 μL, 1.425 mmol, 5 eq) and N,N'-diisopropyl(β-cyanoethyl)phosphonamidic chloride (765 μL, 342 mmol, 1.2 eq). A white precipitate (diisopropylethylammonium hydrochloride) appeared after 2 min, indicating the start of the desired reaction. After 4 hr stirring, TLC analysis in CH_2Cl_2/isopropanol (9:1, v/v) showed complete consumption of starting material (R_f = 0.20) with the formation of two nonpolar products (R_f = 0.44 and 0.48, diastereomers). The reaction mixture was added to ethyl acetate (35 ml, prewashed with 5% sodium bicarbonate) and washed with saturated brine (5 x 20 mL). The aqueous washes were back-extracted with 20 mL of prewashed ethyl acetate and the organic phases were pooled, dried (Na_2SO_4) and concentrated *in vacuo* to a white gum. The crude material was purified on a silica gel

column (4 cm, 20 gr), eluting with CH_2Cl_2/hexanes/TEA (65:25:10, v/v). After evaporating the desired (pooled) fractions, the product was coevaporated with 95% ethanol (2 x 6.7 mL) followed by ether (3 x 5 mL) to afford phosphoramidite **37** (210 mg, 72%) as a white foam: ^{1}H-NMR (500 MHz, acetone-d_6) δ; 1.096-1.289 (d, 12H, $NH[CH(CH_3)_2]_2$, diastereotopic methyls), 1.37 (m, 2H, H16), 1.51 (d, 3H, H7), 1.61 (m, 2H, H17), 2.12 (s, 3H, overlapping ABCD of H11AB and H12CD), 2.74 (t, 2H, H21AB), 3.16 (aq, 2H, H14), 3.42 (m, 2H, H5'AB), 3.43 (m, 2H, H9AB), 3.63 (m, 2H, $N[CH(CH_3)_2]_2$), 3.79 (s, 6H, 2 x $PhOCH_3$), 4.02 (m, 2H, H8AB), 4.21 (t, 1H, H18); ***diastereomer I***, 2.74 (t, 2H, CH_2CN), 3.88 (m, 2H, $POCH_2$), 4.21 (m, 1H, H4'), 4.74 (m, 2H, H3'), 6.38 (m, 1H, H1'), 7.64 (s, 1H, H6); ***distereomer II***, 2.49 (t, 2H, CH_2CN), 3.72 (m, 2H, $POCH_2$), 4.15 (m, 1H, H4'), 4.59 (m, 1H, H3'), 6.37 (m, 1H, H1'), 7.63 (s, 1H, H6): ^{31}P-NMR (acetone-d_6) δ; 148.667 and 148.614 (two diastereomers); ^{1}H-NMR and ^{13}C-NMR data are summarized in tables 3, 4 and 6: MS (FAB-NBA and NaCl) m/z: 1051 ([M+Na^+]), 1028 ([M+H^+]), 957 ([MH^+-$HOCH_2CH_2CN$]), 927 ([MH^+-iPr_2NH]), 810 ([MH^+-$iPr_2NP(OH)OCH_2CH_2CN$]), 725 ([MH^+-DMTrH]), 455 ([MH^++H^+-sugar]), 303 ([$DMTr^+$]).

5'-O-DMT-N^3-{5-[(5-hydroxypentyl)succinyl]pentyl}thymidine-3'-O-(β-cyanoethyl)-N,N'-diisopropylphosphoramidite (38). Alcohol **36** was phosphitylated by a procedure similar to that used for the preparation of phosphoramidite **37** and amidite **38** was obtained in 80% yield as a white gum: ^{1}H-NMR (500 MHz, acetone-d_6) δ: 1.062-1.155 (d, 12H, $N[CH(CH_3)_2]_2$, diastereotopic methyls), 1.32 (m, 2H, H10), 1.35 (m,2H, H19), 1.48 (m, 2H, H11), 1.49 (m, 2H, H18), 1.56 (m, 2H, H9), 1.57 (m, 2H, H20), 1.57 (d, 1H, H7), 2.09 (s, 3H, H26), 2.36 (m, 4H, ABCD of H14AB and H15CD), 2.41-2.53 (m, 2H, H2'AB), 2.46 (t, 2H, H23), 2.73 (t, 2H, H24), 3.14 (two overlapping aq, 4H, H12 and H17), 3.40 (m, 2H, H5'AB), 3.63 (m, 2H, $N[CH(CH_3)_2]_2$), 3.78 (s, 6H, 2 x $PhOCH_3$), 3.83 (m, 2H, H8AB), 3.99 (t, 2H, H21); ***diastereomer I***, 2.60 (t, 2H, CH_2CN), 3.70 (t, 2H, $POCH_2$), 4.12 (m, 1H, H4'), 4.69

(m, 1H, H3'), 6.36 (m, 1H, H1'); ***diastereomer II***, 2.86 (t, 2H, CH_2CN), 3.88 (m, 2H, $POCH_2$), 4.18 (m, 1H, H4'), 4.71 (m, 1H, H3'), 6.37 (m, 2H, H1'), 7.54 (d, 1H, H6); ^{31}P-NMR (acetone-d_6) δ: 148.677 and 148.603 (two diastereomers); MS (FAB-NBA and NaCl) m/z: 1135 ([M+Na^+]), 1113 ([M+H^+]), 895 ([MH^+-$iPr_2NP(OH)OCH_2CH_2CN$]), 810 ([MH^+-DMTrH]), 740 ([MH^+-DMTrH-$HOCH_2CH_2CN$]), 592 ([MH^+-DMTrH-$iPr_2NP(OH)OCH_2CH_2CN$]), 303 ([$DMTr^+$]).

Synthesis of Bis(phosphoramidites) (41-42)

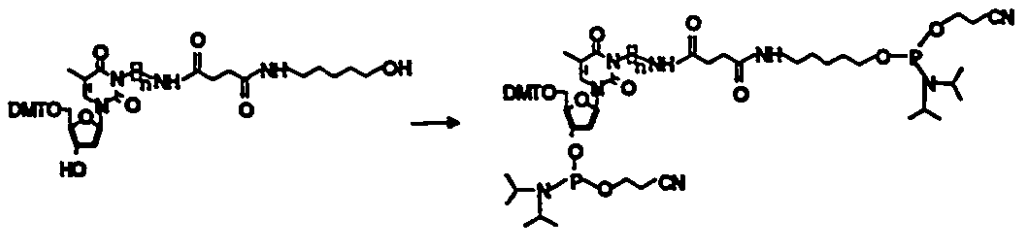

Bis(phosphosphoramidite) (41). Diol **39** (300 mg, 388 mmol) was dried according to the procedure used in case **37** and dissolved in a nitrogen-purged, septum-capped 10 mL hypovial containing dry THF (1.40 mL). To the solution was added a catalytic amount of DMAP (14.2 mg, 116 μmol, 0.3 eq) followed by the slow (over 20 seconds) dropwise addition of N,N'-diisopropylethylamine (676 μL, 3.88 mmol, 10eq) and N,N'-diisopropyl(β-cyanoethyl)phosphonamidic chloride (200 μL, 892 mmol, 2.3 eq). After 2 hr stirring TLC analysis in CH_2Cl_2/isopropanol (9:1, v/v) showed complete disappearance of starting material and the formation of two products of R_f = 0.48 and 0.50. The same work-up was employed as in case **37** using CH_2Cl_2/hexanes/TEA (75:15:10, v/v) as the solvent system for silica gel purification to afford **41** as a white viscous oil. The purified oil was taken up in methylene chloride (900 μL, 20% solution) and rapidly precipitated from stirring cold (dry ice/acetone bath) hexanes to afford **41** (234 mg, 52%) as a white gum. ^{31}P-NMR (acetone-d_6) δ; 148.625, 148.542, and 147.348

ppm: MS (FAB-NBA and NaCl) m/z: 1185 ([M+Na$^+$]), 1161 ([M+H$^+$]), 1060 ([MH$^+$-*i*Pr$_2$NH]), 959 ([MH$^+$-2 x *i*Pr$_2$NH]), 872 ([MH$^+$-*i*Pr$_2$NP(OH)OCH$_2$CH$_2$CN-*i*Pr$_2$NH]), 725 ([MH$^+$-2 x *i*Pr$_2$NH(OH)OCH$_2$CH$_2$CN]), 640 ([MH$^+$-DMTrH-*i*Pr$_2$NP(OH)OCH$_2$CH$_2$CN]), 303 ([DMTr$^+$)].

Bis(phosphoramidite) (42). Diol **40** was phosphitylated by a procedure similar to that used for the preparation of bis(phosphoramidite) **41** and bis(amidite) **42** was obtained in 68% yield as a white gum: ^{31}P-NMR (acetone-d$_6$) δ; 148.667, 148.582, and 147.372 ppm: MS (FAB-NBA and NaCl) m/z: 1239 ([M+Na$^+$]), 1215 ([M+H$^+$]), 1114 ([MH$^+$-*i*Pr$_2$NH]), 1013 ([MH$^+$-2x*i*Pr$_2$NH]) 895 ([MH$^+$-*i*Pr$_2$NP(OH)OCH$_2$CH$_2$CN-*i*Pr$_2$NH]), 779 ([MH$^+$-2x*i*Pr$_2$NHP(OH)OCH$_2$CH$_2$CN]), 303 ([DMTr$^+$]).

Synthesis of 3'-O-(4,4'-dimethoxytrityl)-5'-OH thymidine (45).

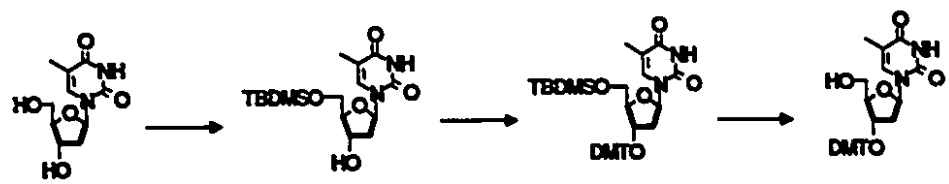

5'-O-TBDMS-3'-OH-thymidine (43). Thymidine (727 mg, 3.0 mmol) was dried by coevaporating from anhydrous pyridine (2 x 20 mL) followed by coevaporation from anhydrous DMF/toluene (2 x 50 mL, 1:5, v/v). The dried thymidine was then dissolved in a nitrogen-purged, septum-sealed 10 mL hypovial containing dry DMF (3.6 mL). To the solution was added imidazole (450 mg, 6.6 mmol, 2.2 eq) and *tert*-butyldimethylsilyl chloride (500 mg, 3.3 mmol, 1.1 eq). After overnight stirring, TLC analysis in CH_2Cl_2/ether (1:1, v/v) showed near complete disappearance of starting material with the formation of two nonpolar compounds (R_f = 0.41, major component- 5' monosilylated derivative, and R_f = 0.75, minor component- 5' and 3' disilylated derivative). The mixture

was evaporated *in vacuo*, taken up in methylene chloride (20 mL) and washed with saturated brine (2 x 35 mL). The organic layer was dried (Na_2SO_4) and evaporated to dryness. The crude product **43** was used for the next step without further purification.

5'-O-TBDMS-3'-O-DMT-thymidine (44). Assuming 90% yield from the silylation reaction, crude nucleoside **43** (2.7 mmol) was dried by coevaporating with three 20 mL portions of anhydrous pyridine and then dissolved in a nitrogen-purged, septum-sealed 25 mL round bottom flask containing anhydrous pyridine (3.5 mL). To the solution was added a catalytic amount of DMAP (66 mg, 0.54 mmol, 0.2 eq) and dimethoxytrityl chloride (1.20 gr, 3.50 mmol, 1.3 eq). After stirring 24 hr, TLC analysis in CH_2Cl_2/MeOH (95:5, v/v) showed complete disappearance of starting material with the formation of two less polar compounds (R_f = 0.54, major component, and R_f = 0.30, minor component). The reaction was then stopped by the addition of methanol (5 mL), concentrated *in vacuo*, and coevaporated with three 5 mL portions of toluene. The resulting oily residue was taken up in methylene chloride (20 mL) and washed with 5% sodium bicarbonate (3 x 20 mL) and water (20 mL). The organic layer was dried (Na_2SO_4) and evaporated to an oily residue. The crude product **44** (R_f = .54) was used for the next step without further purification.

3'-O-DMT-5'-OH thymidine (44). Assuming 90% tritylation of **43**, crude nucleoside **44** (2.43 mmol) was dried by coevaporating from anhydrous pyridine (2 x 15 mL) followed by coevaporation from anhydrous THF/toluene mixture (2 x 40 mL, 3:2, v/v). A solution of tetra-*n*-butylammonium fluoride in tetrahydrofuran (1 M, 12.2 mL, 12.2 mmol, 5 eq) was added to a stirred solution of crude **44** in 8.5 mL of anhydrous tetrahydrofuran. After 30 min stirring, TLC analysis in CH_2Cl_2/ether (1:2, v/v) showed complete disappearance of starting material (R_f = 0.64) with the formation of a major more polar compound of R_f = 0.29. The reaction mixture was diluted with 150 mL of methylene chloride and washed with saturated brine (5 x 150 mL). The organic layer was dried (Na_2SO_4) and evaporated *in vacuo* to a yellow oil. The residue was then purified

on a silica gel column, eluting with a gradient of 0-5% methanol in methylene chloride to afford the title compound **45** (1.20 gr, 75% overall) as a faint yellow foam: ^{1}H-NMR (500 MHz, acetone-d_6) δ; 1.72 (A of ABX, 1H, H2'A), 1.75 (s, 3H, CH_3), 1.86 (B of ABX, 1H, H2'B), 3.39 (A of ABX, 1H, H5'), 3.54 (B of ABX, 1H, H5'B), 3.90 (m, 1H, H4'), 4.42 (m, 1H, H3'), 6.91 (dd, 1H, H1'), 9.89 (bs and exchangeable, 1H, NH); MS (FAB-NBA) m/z: 545 ([M+H$^+$]), 242 ([MH$^+$-DMTrH]), 127 ([MH$^+$+H$^+$-sugar]), 303 ([DMTr$^+$]).

Synthesis of 3'-DMT-DMT thymidine-5'-O-(β-cyanoethyl) N,N'-diisopropyl-phosphoramidite (46).

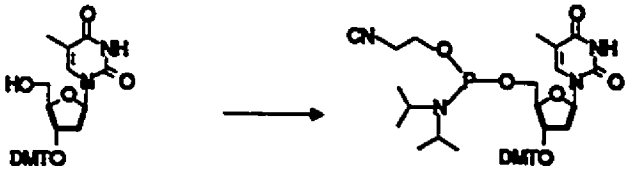

Nucleoside **45** (1.632 gr, 3 mmol) was dissolved in a nitrogen-purged, septum-sealed 25 mL round bottom flask containing dry THF (10.7 mL). To the solution was added a catalytic amount of DMAP (73.3 mg, 0.6 mmol, 0.2 eq) followed by the slow, over 20 seconds, dropwise addition of N,N'-diisopropylethylamine (2.60 mL, 15 mmol, 5 eq) and N,N'-diisopropyl(β-cyanoethyl)phosphonamidic chloride (803 μL, 3.6 mmol, 1.2 eq). A white precipitate (diisopropylethylammonium hydrochloride) appeared after 2 min, indicating the start of the desired reaction. After 4 hr stirring, TLC analysis in CH_2Cl_2/ether (2:1, v/v) showed the complete consumption of starting material. The same work-up was employed as in the case **37** using CH_2Cl_2/hexanes/TEA (45:50:5, v/v) as the solvent system for silica gel purification to afford phosphoramidite **46** (2.05 gr, 92%) as a white foam. ^{31}P-NMR (acetone-d_6) δ: 149.079 and 148.820 ppm (two diastereomers).

5.6 EXPERIMENTAL FOR CHAPTER 4

Solid Phase Synthesis of Branched Oligonucleotides

Branched "Y"-shaped oligomers were synthesized on an Applied Biosystems 381A Synthesizer by Rob Hudson of the University of Toronto. Both sequences were prepared in the "trityl off" mode on a 0.2 μmole scale employing the standard DNA synthesis cycle provided by Applied Biosystems. Long-chain alkylamine control-pore-glass supports (LCAA-CPG, 500 Å Pierce Rockford, IL, or CPG, Inc., N.J.) were derivatized with 5'-O-DMT thymidine 3'-N,N'-diisopropyl(β-cyanoethyl)phosphoramidites (purchased from Dalton Chemicals or prepared according to literature[117]). 3'-O-DMT thymidine 5'-N,N'-diisopropyl(β-cyanoethyl)phosphoramidites were prepared as described in section in 5.5. All reagants required for the solid phase synthesis of our branched oligomers were obtained from Applied Biosystems.

DNA Cleavage From the Solid Support

To a capped eppendorf containing the CPG bound oligomer was added 29% ammonia solution (1 mL). The mixture was shaken slowly on a "wrist action" shaker for 24 hr. The ammonia solution containing the desired unbound oligonucleotide was slowly decanted off into a 1 mL capped eppendorf, and the eppendorf containing the residue or CPG was washed several times with ethanol (4 x 250 μL) and transferred to a clean 1 mL eppendorf. The eppendorfs were then placed in Speed-Vac concentrator and lyopholized to dryness.

OLIGONUCLEOTIDE ANALYSIS AND PURIFICATION

Analytical Polyacrylamide Gel Electrophoresis (PAGE).

All reagents for gel electrophoresis: urea, BIS, TEMED, ammonium persulphate, acrylamide, xylene cyanol, bromophenol blue, boric acid and EDTA were purchased from BioRad.

The purity of the crude oligomer was checked by analytical PAGE prior to purification by preparative gel electrophoresis. The following stock solutions were prepared and stored at 4 °C.

i) *50% BIS/Acrylamide*: Acrylamide (200 gr) and BIS (10 gr) were dissolved in water and diluted to 400 mL.

ii) *10 x TBE Buffer:* prepared by dissoving EDTA (3.72 gr), Boric acid (55.65 gr) and TRIS-HCL (109 gr) in 1 L total water volume.

iii) *24% Denaturing Gel:* Urea (168 gr) was dissolved in 50% stock BIS/Acrylamide (192 mL) and 10 x TBE buffer (208 mL).

iv) *10% ammonium persulfate solution*: prepared by dissolving, for example 70 µg of ammonium persulfate in 700 µL of water.

An analytical gel electrophoresis was performed using 0.8 mm thick plate spacers and 16% denaturing gel, prepared by diluting the 24% denaturing gel stock solution (33.3mL) with the 10 x TBE buffer solution (16.7 mL). To the diluted solution was added 200 µL of 10% ammonium persulfate and 30 µL of TEMED. The gel was quickly poured in between the glass plates and a slot former or comb for analytical gels was inserted into the apparatus. After gel polymerization (30-45 min) the wells were washed with buffer to remove any urea/contaminants present which may affect resolution. The crude oligomer samples (0.2 O.D. units) in 8 µL of 80% formamide buffer were loaded into separate wells. The electrophoretic run was monitored by loading, in each of the end

wells, a 10 µL mixture of ionizable tracking dyes, xylene cyanol and bromophenol blue. The electrophoresis was started with a current of 10 mA for about 1/2 hr to allow the samples to slowly enter the gel. It was then increased to 50 mA for 3-4 hr.

After migration of the tracking dye to the bottom of the gel, the power was turned off. The gel containing the separated oligonucleotide mixture was removed from its glass plated, and visualized by UV shadowing by placing the gel on a clear plastic film (Saran wrap), on top of a fluorescent TLC plate. The gel was subsequently photographed on a 4 x 5 Polaroid Polaplan Instant Sheet Film (52, medium contrast, ISO 400/270).

Preparative Denaturing Gel Electrophorsesis

Preparative gel electrophoresis on a 16% denaturing gel was carried out similarly except that thicker (1.5 mm) plate spacers and a comb containing larger slots or wells were used. In addition, 25 O.D. units of the crude oligomer mixture was loaded using 200 µL of 80% formamide loading buffer. The separated bands were excised with a razor blade (rinsed with 95% ethanol to remove any nucleases) and placed in a properly labeled 10 mL polypropylene test tube. To each tube was added 5 mL of doubly-distilled and autoclaved water and incubated at 37 ^{o}C for 24 hr in order to "soak out" the oligonucleotides from the gel matrix. The polypropylene test tubes were placed in a speed-vac concentrator and concentrated to 3 mL.

C18 SEP-PAK ™ Reverse Phase Chromatography

The oligonucleotides, separated by gel electrophoresis, were desalted using C18 SEP-PAK™ cartridges. A C18 SEP-PAK™ cartridge was attached to a 20 mL syringe and conditioned with 10 mL of HPLC grade methanol followed by 10 mL of doubly-distilled and autoclaved water. The DNA sample was then suspended in 3 mL of 50 mM

TEAA and slowly injected into the cartridge. The salts were eluted by flushing the cartridge with 10 mL of doubly-distilled and autoclaved water and collected as eluant (A). Next, 10 mL of 50 mM TEAA was slowly flushed through and collected as eluant (B). The desired DNA sample was eluted from the cartridge with 10 mL of 7:3 (v/v) 50 mM TEAA:methanol, collected as 10 x 1 mL fractions. The 1 mL fractions containing the desalted oligonucleotides were lyophilized to dryness. The oligonucleotides were then quantified at 260 nm and values ranged from 2-3 O.D. units. Absorbances measured for eluants (A) and (B) indicated no oligonucleotide present.

Thermal Denaturation Curves

Thermal denaturation measurements were performed on a Varian-Cary UV/VIS spectrophotometer equipped with the Peltier thermal unit accesory and a six cell transport system. The cuvettes were 1 cm pathlength quartz cells and nitrogen was continuously circulated at low temperatures (10 ^{o}C) through the cuvette compartment to prevent moisture condensation. Extinction coefficients for oligomers **III** and **IV** were calculated to be 2.47 x 10^{5} L mol^{-1} cm^{-1} according to the nearest neighbour approximation.[117] Thermal denaturation samples were prepared by mixing oligomer solutions containing 0.809 μM of oligomer **III** or **IV** and the complementary dA_{10} oligomer. The combined solution was lypholyzed to dryness and dissolved in 1 mL of the thermal denaturation sodium phosphate buffer - 1M NaCl, 10mM PO_4^{3-}, pH = 7.0; prepared as a 100 mL stock solution of 1 M NaCl, dissolving 85.7 mg of NaH_2PO_4 and 53.7 mg of Na_2HPO_4 in doubly distilled and autoclaved water diluted to 100 mL, and adjusting the pH to 7. Prior to the actual experiment, the temperature was increased to 80^{o}C and slowly cooled down to 20 ^{o}C in 10 ^{o}C increments. For each thermal denaturing experiment, the temperature was ramped to 80 ^{o}C with a variation of 0.5^{o}C/min. Absorbances at 260 nm were recorded every minute, with 30 readings being averaged to improve the signal-to-

noise ratio. Digitized absorbance and temperature values were automatically displayed and stored for future data plotting and analysis. T*m* values were obtained as the midpoint of the line intersecting both the upper and lower slopping baselines of the absorbance *vs* temperature curve. Thermal denaturation data was also exported from the Cary program to the spreadsheet program Quattro™ for visualization purposes and presented as a normalized absorbance *vs* temperature curve.

REFERENCES

1. A. M. Belikova, V. F. Zarytova, N. I. Grineva, *Tetrahedron Lett.*, 37, 3557-3560 (1967)

2. P. S. Miller, S. Chandrasegaran, D.L. Dow, S.M. Pulford & L. S. Kan, *Biochemistry*, 21, 5468-5474 (1981)

3. B. M. Paterson, B. E. Roberts, E.L. Kuff, *Proc. Natl. Acad. Sci. U.S.A.*, 74, 4370-4374 (1977)

4. E. Uhlmann, A. Peyman, *Chem. Rev.*, 90, 543-584 (1990)

5. U. English, D.H. Gauss, *Angew. Chem.*, 103, 629-646 (1991); *Angew. Chem. Int. Ed. Engl.*, 30, 613-629 (1991)

6. G. Zon, *Pharmaceutical Research.* 5, 539-549, (1988)

7. C. A. Stein, J.S. Cohen, *Cancer Research*, 48, 2659-2668 (1988)

8. D.R. Burger, *Journal of Clinical Immunoassay*, 16, 224-230 (1993)

9. P.D. Cook, *Anti-Cancer Drug Des.*, 6, 585 (1991)

10. C. Hèléne, *Anti-Cancer Drug Des.*, 6, 569-584, (1991)

11. C. Hèléne, J.J. Toulme, *Biochim. et Biophys. Acta*, 1049, 99-125 (1990)

12. Nguyen T. Thuong, C.Helene, *Angew. Chem. Int. Ed. Engl.*, 32, 666-690 (1993)

13. L.J. Maher III, P.B. Dervan, B. Wold, *Inhibition of DNA/Protein Interactions by Oligonucleotide-Directed DNA Triple Helix Formation: Progress and Prospects*; Editor, E. Wickstrom in Prospects for Antisense Nucleic Acid Therapy of Cancer and Aids; pp. 227-242, Wiley-Liss, Inc., NY.

14. J.E. Gee, D.M. Miller, *Med. Sci.*, 304, 366 (1992)

15. L. J. Maher III, *BioEssays*, 14, 807 (1992)

16. S.T. Crooke, *Annu. Rev. Pharmacol. Toxicol.*, 32, 329 (1992)

17. P. Zamecnic, M. Stephenson, *Proc. Nat. Acad. Sci. USA*, 75, 280-284 (1978)

18. J. N. M. Mol & A. R. Van der Knot (Editors). Antisense Nucleic Acids and Proteins, Fundamentals and Applications, Marcel Dekker Inc., NY, 22, 50 (1991)

19. Cazenave,M. Chevrier, N.T. Thuong, C. Helene, *Nucleic Acid Research*, 10507-10521 (1987)

20. J. Minshull, T. Hunt, *Nucleic Acid Research*, **14**, 6433-6451 (1986)

21. R.Y. Walder, J.A. Walder, *Natl. Acad. Sci. USA*, **85**, 5011-5015 (1988)

22. P.S. Miller, K.B. McParland, K. Jayaraman, Paul On Pong Ts'O, *Biochemistry*, **20**, 1874-1880 (1981)

23. P.S. Miller, Paul On Pong Ts'O, *Anti Cancer Drug Design*, **2**, 117-128 (1987)

24. R. Heikkila, G. Schuab, E. Wickstrom. S.L, Loke, D.H. Pluznik, R. Watt, L.M. Neckers, *Nature*, **328**, 445-449 (1987)

25. M. Matsukura, K. Shinozuka, G. Zon, H. Mitsuya, M. Reitz, J.S. Cohen, S. Broder, *Proc. Natl. Acad. Sci. USA*, **84**, 7706-7710 (1987)

26. M. Matsukura, Antisense RNA and DNA, Wiley-Liss, NY, 1992, pp 285-304

27. P. J. Furdon, Z. Dominski, R. Kole, *Nucleic Acid Research*, **17**, 9193 (1989)

28. S.S. Yogesh, and P.D. Cook, *Towards Second-Generation Synthetic Backbones for Antisense Oligonucleotides*; Editors C.K. Chu, D.C. Baker, *In* Nucleosides and Nucleotides as Antitumor and Antiviral Agents, Plenum Publishing, NY, 1993.

29. J.P. Leonetti, B. Rayner, M. Lemaitre, C. Gaynor, P.G. Milhared, J.L. Imbach, B. Leblew, *Gene* , **72**, 323-332 (1988)

30. R. L. Letsinger, G. Zhang, D. K. Sun, T. Ikeuchi, P.S. Sarin, *Proc. Natl. Acad. Sci. U.S.A.*, **86**, 6553-6556 (1989)

31. C. Hèléne, J.J. Toulme, *In* J.S. Cohen (ed): Oligonucleotides-Antisense Inhibitors of Gene Expression, MacMillan Press Ltd, London, pp.137-172

32. U. Asseline, M. Delaire, G. Lancelot. J.J. Toulme, N.T. Thuong, T. Monteray-Garestier, C. Helene, *Proc. Natl. Acad Sci. USA*, **81**, 3297-3303 (1984)

33. A. Chollet, E. Kawasshima, *Nucleic Acid Research*, **16**, 305 (1988)

34. F. Seela, U. Bindig, H. Driller, W. Herdering, K. Kaiser, A. Kehne, H. Rosemeyer, H. Steker, *Nucleosides Nucleotides*, **6**, 11 (1987)

35. F. Seela, H. Driller, *Nucleic Acid Research*, **14**, 2319 (1986)

36. F. Seela, H. Driller, *Nucleic Acid Research*, 13, 911 (1985)

37. H. Inoue, A. Imaru, E. Ohtsuka, *Nucleic Acid Research*, 13, 7119, (1985)

38. E. Uhlmann, A. Peyman, *Chem. Rev.*, 90, pp. 556 (1990)

39. M. Robins, K.K. Robins, *J. Org. Chem.* 34, 2160 (1969)

40. J.K. Setlow (ed.), *Genetic Engineering*, NY: Plenum Press, 12, 37-52 (1990)

41. F. Morvan, B. Rayner, J.L. Imbach, D.K. Chang, J.W., *Nucleosides Nucleotides*, 6, 471 (1987)

42. C.A. Stein, C. Subasinghe C., K. Shinazuka K., J.S. Cohen, *Nucleic Acid Research*, 16, 3209 (1988)

43. C.G.B. Jennings, T.M. Woolf, D.A. Melton. *In* Conference on Antisense RNA and DNA, St. John's College, March 29-30, 1989, Cambridge, U.K.

44. Y. Furukawa, K. Kobayashi, Y. Kanai, M. Honjo, *Chem. Pharm. Bull.*, 12, 1273 (1965)

45. H. Inoue, Y. Hayase, A. Imura, S. Iwai, K. Miura, E. Ohtsuka, *Nucleic Acid Research*, 15, 6131 (1987)

46. A.M. Iribarren, B.S. Sproat, P. Nevner, I. Sulston, U. Ryder, adn A.I. Lamond, *Proc. Natl. Acad. Sci. USA* ,187, 7741 (1990)

47. M.J. Damha, P.A. Giannaris, P. Marfey, *Biochemistry*, 33, 7877-7885 (1993)

48. K.K. Oglivie, N. Nguyen, M.F. Gillen, B.K, Radatus, V.O. Cheryan, H.R. Hanna, S.M. Smith, adn K.S. Galloway, *Can. J. Chem.* 62, 241, (1984)

49. K.C. Schneider, S.A. Benner, *J. Amer. Chem. Soc.*, 112, 453 (1990)

50. P.E. Nielson, M. Egholm, R.H. Berg, O. Buchardt, *Science*, 254, 1497 (1991)

51. M. Egholm, O. Buchardt, P.E. Nielson, R.H. Berg, *J. Amer. Chem. Soc.*, 114, 1895 (1992)

52. E.P. Stirehak, J.E. Summerton, and D.D. Weller, *Nucleic Acid Research*, 17, 6129 (1989)

53. G. Felsenfeld, A. Rich, *Biochimica et Biophysica Acta*, 26, 457 (1957)

54. G. Felsenfeld, H.T. Miles, *Annual Review of Biochemistry*, **36**, 407 (1967)

55. A.M. Michelson, J. Massoulie, W. Guschlbauer, *Progress in Nucleic Acid Research and Molecular Biology*, **6**, 83 (1967)

56. R.D. Wells, D.A. Collier, J.C. Harvey, S. Shimizu, F. Wohlrab, *FASEB Journal*, **2**, 2939 (1988)

57. E.H. Moser, P.B. Dervan, *Science*, **238**, 645-650 (1987)

58. P. Rajagopal, J. Feignon, *Nature*, **339**, 637-640 (1989)

59. I. Radhadrishnan, C. de los Santos, D.J. Patel. *J. Mol. Biol.*, **221**, 1403-1418 (1991)

60. K. Hoogsteen, *Acta Crystallographica*, **12**, 822 (1959)

61. S.L. Broitman, D.D. In, J.R. Fersco, *Proc. Natl. Acad. Sci. USA*, **84**, 5120-5124 (1987)

62. A.E. Letai, M.A. Palladino, E. Fromme, V. Rizzo, J.R. Fresco, *Biochemistry*, **27**, 9108-9112 (1988)

63. P.A. Beal, P.B. Dervan , *Science*, **251**, 1360-1363 (1991)

64. C. Hèlène, *Anti-Cancer Drug Design*, **6**, 569-584 (1991)

65. D.A. Horvan, P.B. Dervan, *J. Amer. Chem. Soc.*, **112**, 2435-2437 (1990)

66. U. Asseline, N.T. Thuong, *Tetrahedron Letters*, **34**, 4173-4176 (1993)

67. A. Ono, C.N. Chen, L.S. Kan, *Biochemistry*, **30**, 9914-9921 (1991)

68. B.C. Froehler, T. Terhorst, J.P. Shaw, S.N. McCurdy, *Biochemistry*, **31**, 1603-1609 (1992); S. McCurdy, C. Moulds, B. Froehler, *Nucleosides Nucleotides*, **10**, 287-290 (1991)

69. R.L. Letsinger, S.K. Chaturvedi, F. Farooqui, M. Salunkhe, *J. Amer. Chem. Soc.*, **115**, 7535 (1993)

70. M. Salunkhe, T. Wu, R.L. Letsinger, *J. Amer. Chem. Soc.*, **114**, 8768 (1992)

71. C. Giovannangeli, N.T. Thuong, C. Helene, *Proc. Natl. Acad. Sci. USA*, **90**, 10013 (1993)

72. C. Giovannangeli, T. Montenay-Garestier, M. Rougee, N.T. Thuong, C. Helene, *Proc. Natl. Acad. Sci. USA*, 113, 7775 (1991)

73. M.J. Damha, G. Kanjana, R.H.E. Hudson and S.V. Zabarylo, *Nucleic Acid Research* 20, 6565-6573, (1992)

74. G. Prakash, E.T. Kool, *J. Chem. Soc. Chem. Commun.*, 1161 (1991)

75. E.T. Kool, *J. Amer. Chem. Soc.*, **113**, 6265 (1991)

76 D.J. D'Souza, E.T. Kool, *J. Biomol. Struct. Dyn.*, 10, 141 (1992)

77. R.H.E. Hudson, K. Ganeshan, & M.J. Damha, *Branched Nucleic Acids, Synthesis and Biological Applications*. American Chemical Society, 1994, Chapter 9. *In* Carbohydrate Modifications in Antisense Research, Y.S. Sanghivi and P.D. Cook (Editors), ACS Sympsium Series, 580, 1994.

78. A. Hovinen, A. Azhayev, H. Lonnberg, *J. Chem. Soc., Perkin Trans I*, 1994, 930-938

79. Y. Hisanaga, T. Tanabe, K. Yamauchi, M. Kinoshita, *Bull. Chem. Soc. Jpn.*, 54, 1569-1570 (1981)

80. D. Wagner, J.P.H. Verheyden, J.G. Moffatt, *J. Org. Chem.*, 39, 24 (1974)

81. J. Yamauchi, T. Nakagima, and M. Kinoshita, *Bull. Chem. Soc. Jpn.*, 53, 3865-3868 (1980)

82. M. Manoharan, C.J. Guinosso, P.D. Cook, *Tetrahedron Letters*, 49, 7171-7174 (1991)

83. R.A. Jones in M.J. Gait (Ed): Oligonucleotide Synthesis: A Practical Approach, IRL Press, Oxford, UK, 1984, pp 23-24

84. R. Izatt, M. Hansen, L.D. Rytting, J.J. Christensen, *J. Amer. Chem. Soc.*, 87, 2760-2761 (1965)

85. R. Haner, T.H. Keller, *Helvetica Chimica Acta*, 76, 884-892 (1993)

86. A. Albert, *Ionization Constants of Pyrimidines and Purines. Synthetic Procedures in Nucleic Acid Chemistry*, **vol. 2** of Physical and Physicochemical Aids in Determination of Structure, Wiley-Interscience, NY, pp 1-46

87. T. Kamimura, T. Masegu, M. Sekine, T. Hata, *Tetrahedron Letters*, 25, 4241 (1984)

88. M.S. Gibson, R.W. Bradshaw, *Angew. Chem. Internat. Edit.*, 7, 919-930 (1968)

89. S. Kukohga, N.D. Jones, M.O. Chaney, T.K. Elzey, J.W. Paschal, D.E. Dorman, *Journal Org. Chem.*, **40**, 2388 (1975)

90. R.A. Boissannas, *Adv. Org. Chem.*, 3, 1979 (1969): B.G. Ramsay, R.J. Stoodley, *J. Chem. Soc.*, 1319 (1969)

91. H.R. Ing, and R.F.H. Manske, *J. Chem. Soc.*, 2348 (1926)

92. E. Schroder and K. Lubke. The peptides, Vol. 1. Academic Press, New York, 1965, Chapter I. J.F.S. McOmie. *In* Advances in organic chemistry, Vol. 3 R.A. Raphael, (Editor). Interscience, New York.

93. F.S. Spring and J.C. Woods, *J. Chem. Soc.*, 625 (1945)

94. S. Wolfe, S.K. Hasan, *Can. J. Chem.*, **48**, 3572-3579 (1970)

95. A. Bax and M.F. Summers, *J. Amer. Chem. Soc.*, **108**, 2093 (1986)

96. M. F. Summers, L. G. Marzilli, A. Bax, *J. Amer. Chem Soc.*, **108**, 4285 (1986)

97. A. Hassner, E. Strand, M. Rubinstein, and A. Patchornik, *J. Amer. Chem. Soc.*, 97, 1614 (1975)

98. J.H. Van Boom, P.M.J. Burgers, *Tetrahedron Letters*, 52, 4875-78 (1976)

99. R.L. Letsinger, M.H. Caruther, P.S. Miller, K.K. Ogilvie, *J. Amer. Chem. Soc.*, **89**, 7146 (1967)

100. R.L. Letsinger, P.S. Miller, *J. Amer. Chem. Soc.*, **91**, 3356 (1969)

101. B.G. Ugarkar, V. Bhat, V.A. Sageed, K. Grimm, N. Kosora, P.A. Domenico, E. Stocker, *Nucleosides Nucleotides*, 2, 179-183 (1989)

102. K.K. Ogilvie, M.J. Nemer, H. Gholam, G.H. Hakimelahi, A. Zbigniew, P.M. Lucas, *Tetrahedron Letters*, 23, 2615-2618 (1982)

103. K. Miyoshi, T. Miyake, T. Hozumi, K. Itakura, *Nucleic Acid Research*, 8, 5473-5489 (1980)

104. N. Usman, K.K. Ogilvie, M.Y. Jiang, R.J. Cedergren, J.*Amer. Chem. Soc.* **109**, 7845-7854 (1987)

105. R.F. Cunico, L. Bedell, *J. Org. Chem.*, 45, 4797-4798 (1980)

106. K.K. Ogilvie, *Can. J. Chem.*, **51**, 3799-3807 (1973)

107. Thomas D. McClure and K.H. Schram, *Mass Spectrometry of Nucleotides and Oligonucleotides*. In S. Agrawal (ed.) Methods in Molecular Biology, **26**, Protocols for Oligonucleotide Conjugates, Humana Press, NY, 1994, pp. 319-345.

108. K. Masakazu, M.F. Moore, S.L. Beaucage, *J. Org. Chem.*, **56**, 3757 (1991)

109. R.H.E. Hudson, M.J. Damha, *J. Amer. Chem. Soc.*, **115**, 2119 (1993)

110. M.J. Damha, P.A. Giannaris, S.V. Zabarylo, *Nucleic Acids Res.*, **13**, 3813 (1990)

111. M.J. Damha, K.K. Ogilvie, *Oligoribonucleotide Synthesis: The Silyl-Phosphoramidite Method. In* S. Agrwal (ed.) Methods in Molecular Biology, **20**: Protocols for Oligonucletides and Analogs, Humana Press, NY, 1993, pp. 431-463

112. A. Andrus, *Gel-Capillary Electrophoresis Analysis of Oligonucleotides. In* S. Agrawal (ed.) Methods in Molecular Biology, **26**. Protocols for Oligonucleotide Conjugates, Synthesis and Analytical Techniques, Humana Press, NY, 1994, pp. 277-300

113. A. Rich, I. Jr. Tinoco, *J. Amer. Chem. Soc.*, **82**, 6409 (1960)

114. D.S. Pilch, C. Levenson, R.H. Shafer, *Proc Natl. Acad. Sci. U.S.A.*, **87**, 1942 (1190)

115. P. A. Beal, P.B. Dervan, *Science*, **251**, 7360 (1991)

116. M.B. Evans, A.D. Dale, C.J. Little, *Chromatographia*, **13**, 510 (1980)

117. J.D. Puglisi, I. Jr. Tinoco, *Methods in Enzymology*, **180**, 304 (1989)

APPENDIX

SELECTED 1-D and 2-D NMR SPECTRA

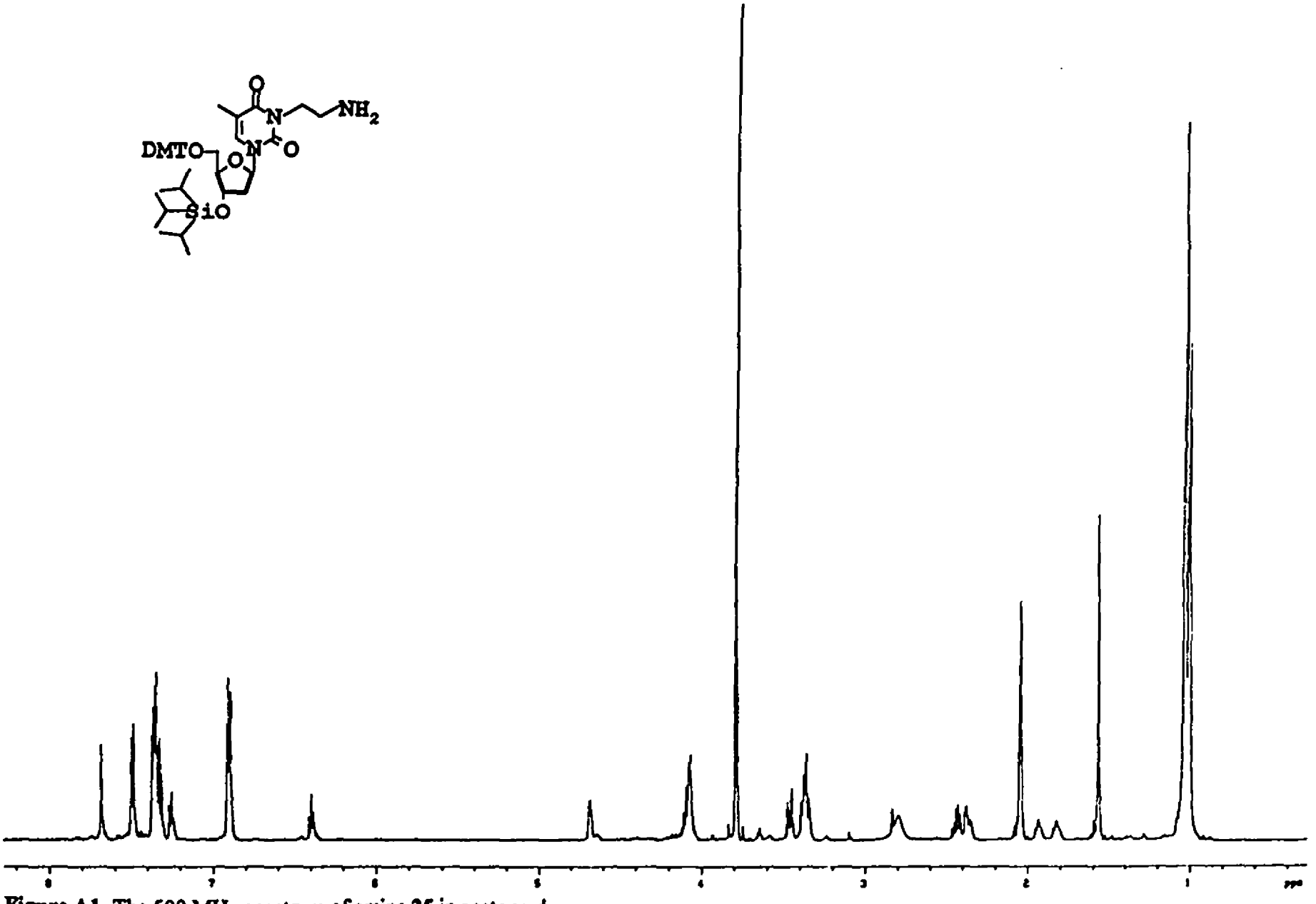

Figure A1 The 500 MHz spectrum of amine 25 in acetone-d_6

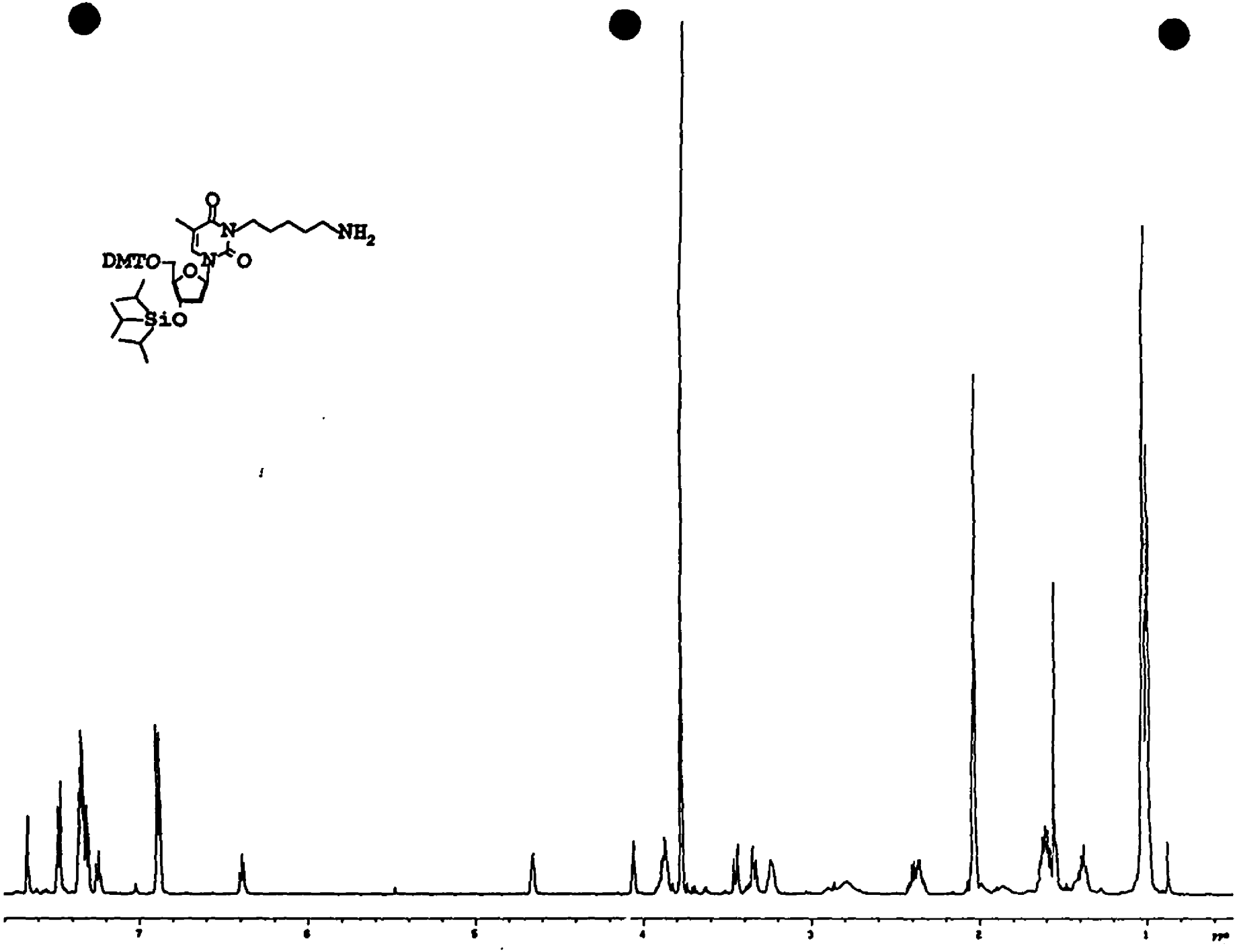

Figure A2 The 500 MHz spectrum of amine 26 in acetone-d_6

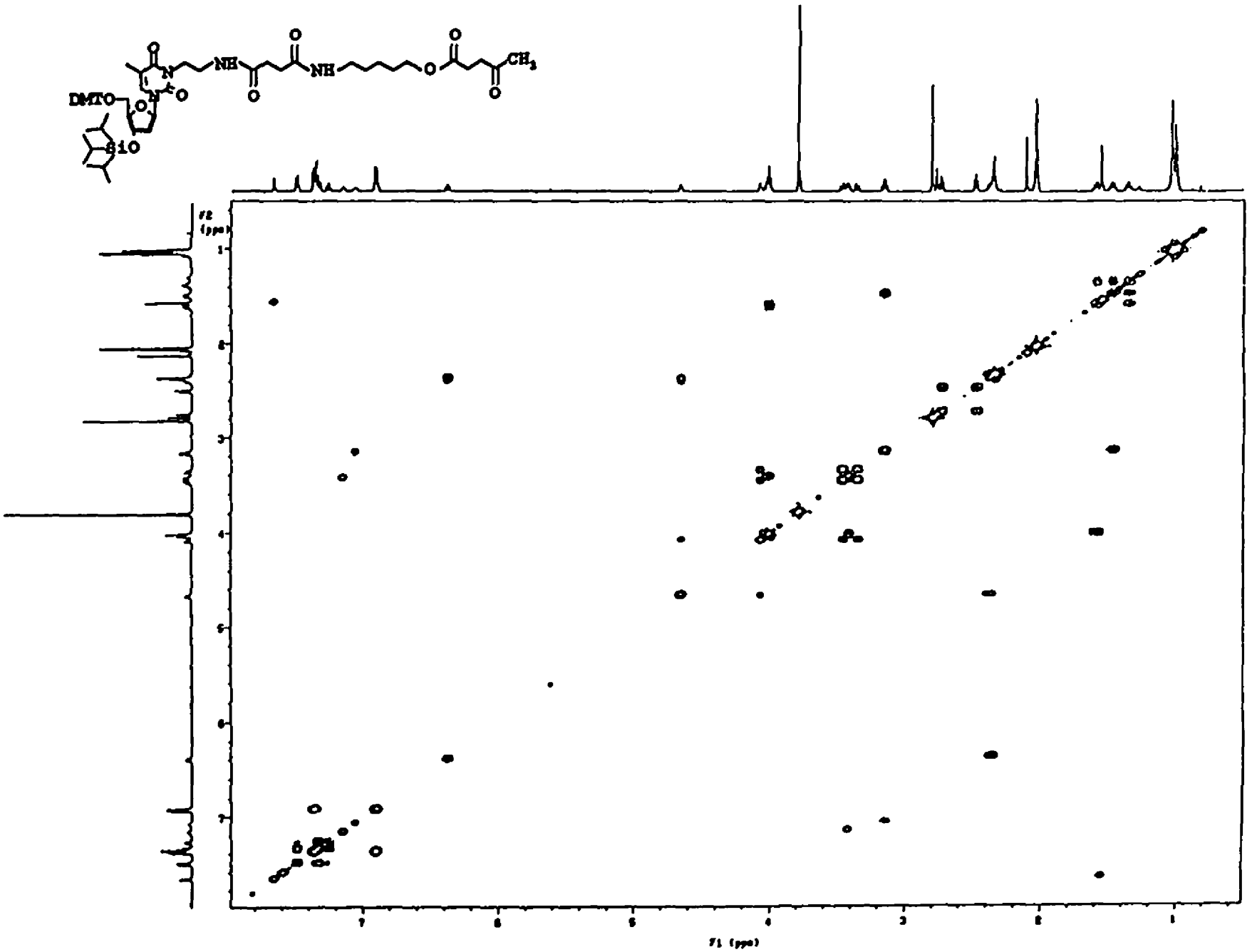

Figure A3 The 500 MHz COSY spectrum of levulinic ester 33 in acetone-d_6

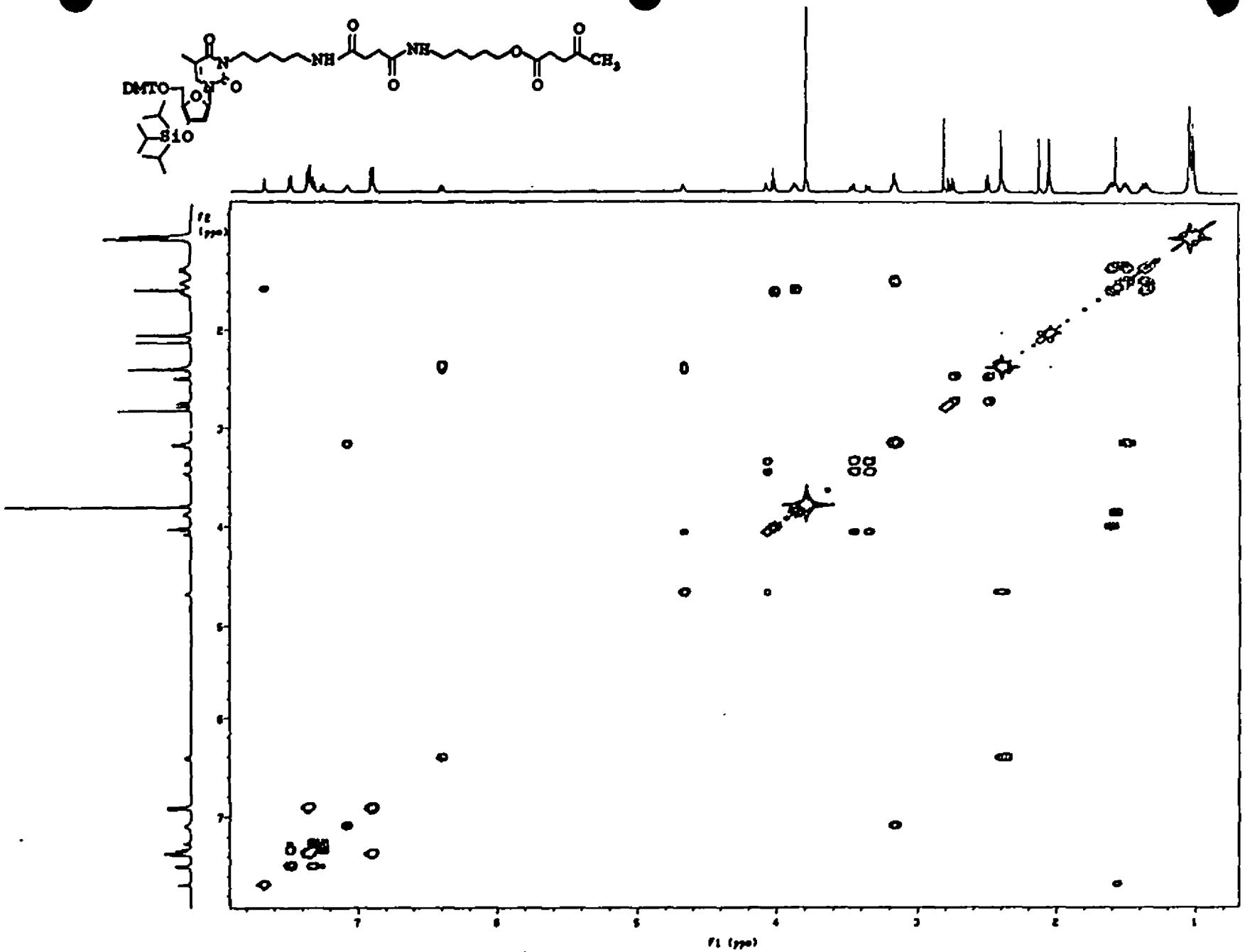

Figure A4 The 500 MHz COSY spectrum of levulinic ester **34** in acetone-d_6

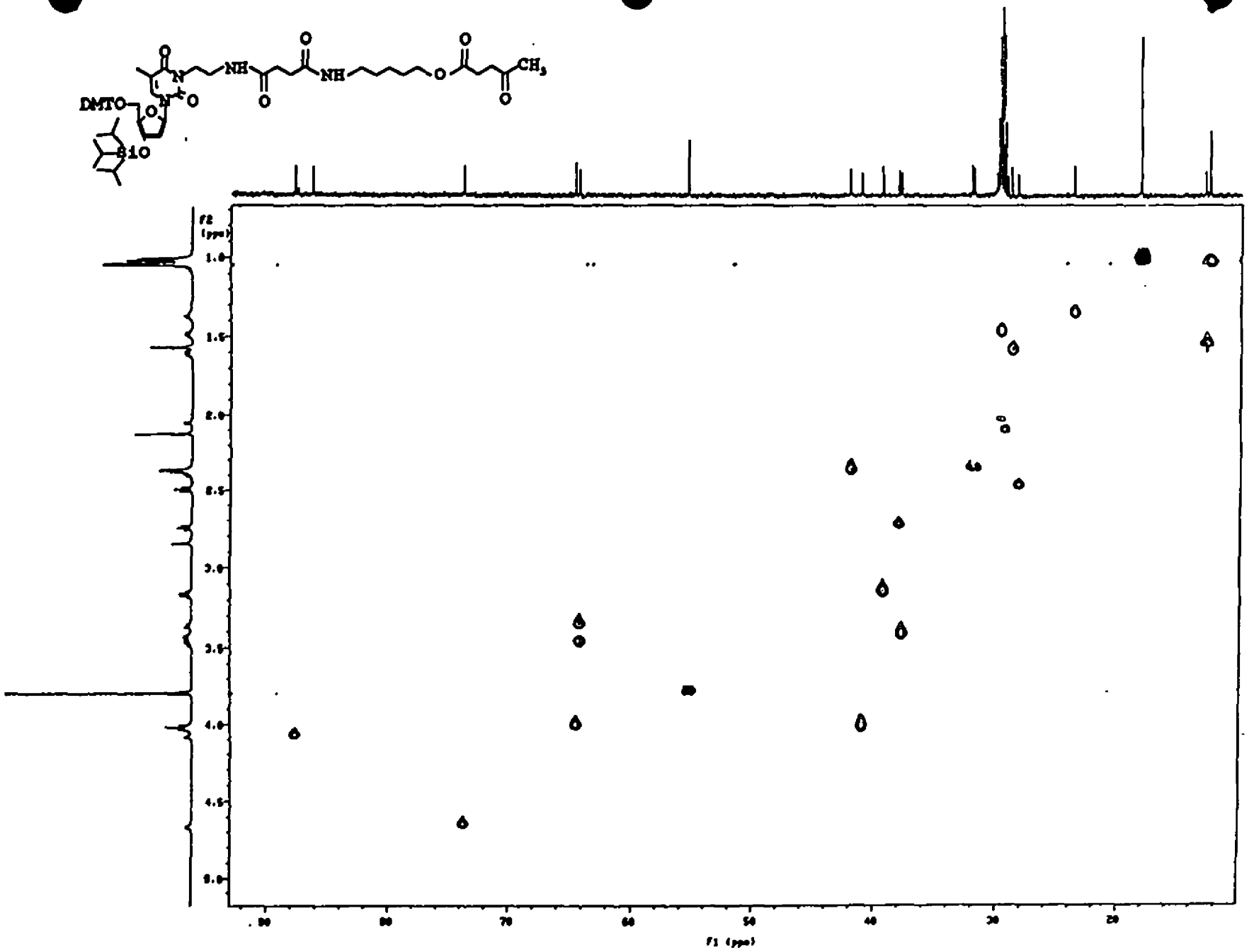

Figure A5 The 500 MHz HMQC spectrum of levulinic ester 33 in acetone-d_6

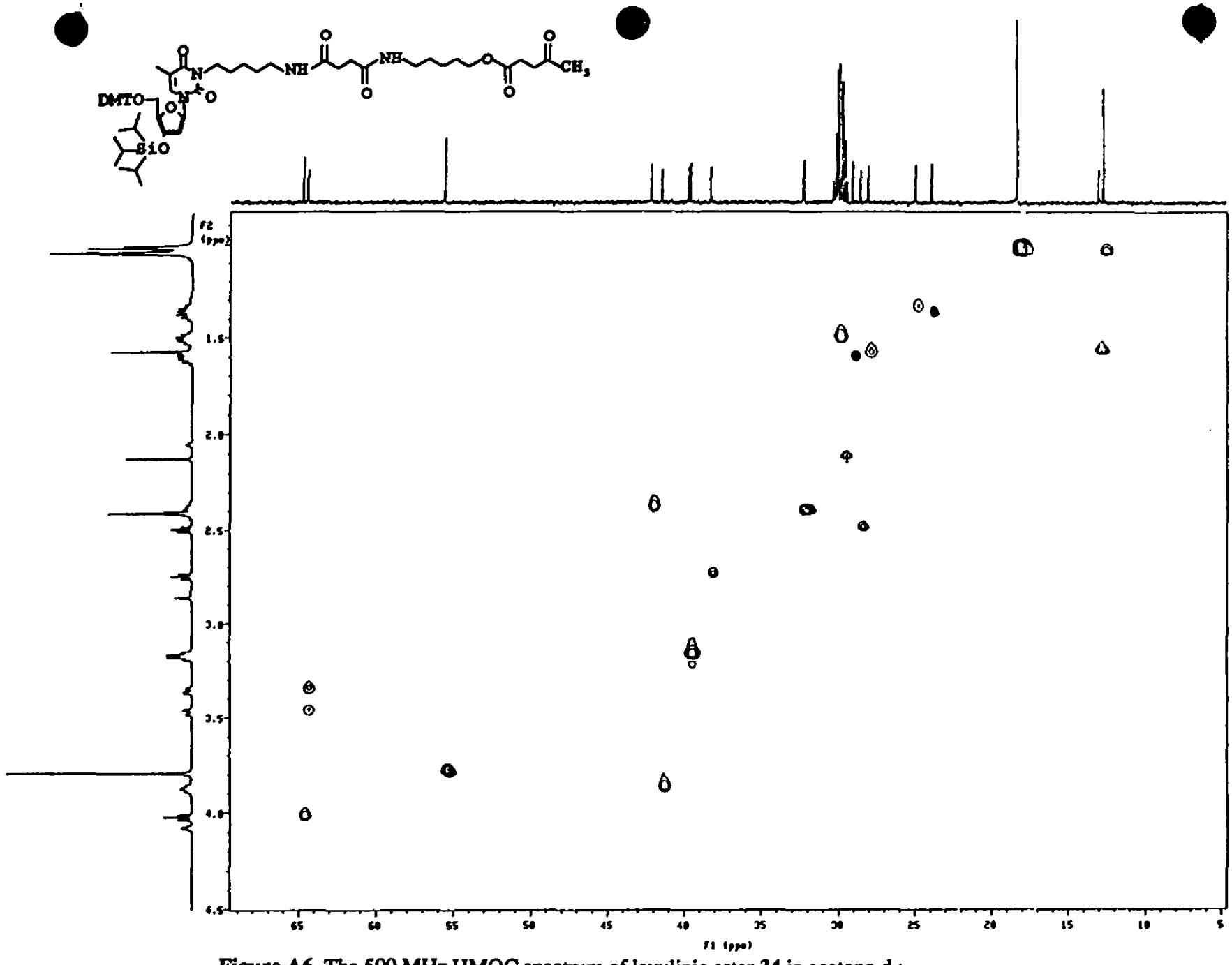

Figure A6 The 500 MHz HMQC spectrum of levulinic ester 34 in acetone-d_6